Effect of Roux-en-Y Gastric Bypass on Lipid and Glucose Metabolism in Male ApoE*3Leiden.CETP Mice

Dissertation

zur

Erlangung der naturwissenschaftlichen Doktorwürde
(Dr. sc. nat.)

vorgelegt der

Mathematisch-naturwissenschaftlichen Fakultät

der

Universität Zürich

von

Erika Tarasco

aus

Italien

Promotionskommission

Prof. Dr. Thomas A. Lutz (Vorsitz)

Prof. Dr. Max Gasmann

Prof. Dr. Thorsten Hornemann

Prof. Dr. Christian Wolfrum

Zürich, 2018

Table of contents

1 Summary

Obesity is one of the major healthcare problems worldwide and it is expected to increase in the next decades. It leads to and drives hypertension, hyperlipidaemia, and hyperglycaemia. These factors are components of the metabolic syndrome (MetS), which plays a major role in obesity-related comorbidities like type 2-diabetes mellitus (T2DM), cardiovascular disease (CAD) and non-alcoholic fatty acid liver disease (NAFLD).

Roux-en-Y gastric bypass (RYGB), among different bariatric surgery techniques, is considered the “golden standard” procedure and the most effective therapy to achieve sustained and long-term weight loss and to improve obesity-related comorbidities. Improvements of glycaemic control, endothelial function and the lipid profile seem to be independent and to occur before changes in body weight.

ApoE*3Leiden.human Cholesterol Ester Transfer Protein (ApoE3L.CETP) mice have a humanized-lipoprotein metabolism: they have high low-density lipoprotein cholesterol (LDL-C) and low high-density lipoprotein cholesterol (HDL-C). When fed a western-type diet, they show typical features of the MetS such as increased body weight, hyperlipidaemia and hyperglycaemia. Even more, they show a heterogenic response to the MetS as is a typical situation in human patients; hence, they are one of the best animal model available to study the MetS.

In the first main study of my work, we investigated the causes of this heterogeneity in terms of lipid and glucose metabolism, identifying two different phenotypes, so-called responder mice (R) that develop dyslipidaemia and non-responder (NR) mice that do not develop the full dysmetabolic phenotype because of a compromised liver function. Second, we investigated the effect of RYGB in responder ApoE3L.CETP mice on lipid and glucose metabolism. To discriminate between surgical effect and body weight effects, we used Sham operated mice body weight-matched to the RYGB mice.

We showed that glucose metabolism and lipid profile improved within body weight loss, especially total cholesterol, non HDL-C and ceramide were greatly reduced in RYGB mice, indicating a body weight loss independent effect.

Our results highlighted the usefulness of RYGB in defeating the MetS, underlining which effects are surgery related and which effects are body weight loss related and hence probably can also achieved with other methods. We believe that our data provide an important proof-of-concept to the advantage of using the ApoEL.CETP mouse model after RYGB in deciphering the metabolic improvements after bariatric surgery to treat the MetS.

2 Zusammenfassung

Übergewicht ist eine der grössten Herausforderungen der Gesundheitssysteme weltweit, und die Häufigkeit und das Ausmass von Übergewicht werden in den kommenden Jahrzehnten wahrscheinlich weiter ansteigen. Übergewicht führt zu Bluthochdruck, Hyperlipidämie und Hyperglykämie, d.h. den wichtigsten Faktoren, die das metabolische Syndrom (MetS) darstellen. Das MetS seinerseits steht in direktem Zusammenhang mit Übergewicht-assoziierten Erkrankungen wie dem Typ 2 Diabetes mellitus (T2DM), Herz-Kreislauf-Erkrankungen (CAD) und Lebererkrankungen, wie der Fettlebererkrankungen, die nicht spezifisch durch Alkohol ausgelöst werden (NAFLD).

Der Roux-en-Y Magenbypass (RYGB) gilt unter allen Methoden der bariatrischen Chirurgie als der sog. Goldstandard. Er stellt bislang die effizienteste Therapie dar, die zu einem deutlichen und anhaltenden Gewichtsverlust führt, und durch den auch die genannten Begleiterkrankungen verbessert werden. So kommt es z.B. bereits vor einem markanten Gewichtsverlust zu einer Verbesserung des Glucose- und Fettstoffwechsels und der Endothelfunktion in Blutgefässen.

Die sog. ApoE*3Leiden.human Cholesterol Ester Transfer Protein (ApoE3L.CETP) Mäuse weisen einen Lipoprotein-Stoffwechsel auf, der gut demjenigen des Menschen entspricht; diese Mäuse haben z.B. hohes Low-density lipoprotein Cholesterol (LDL-C) und niedriges High-density lipoprotein Cholesterol (HDL-C). Wenn sie mit einer sog. Western-type Diät gefüttert werden, zeigen sie ausserdem die typischen Charakteristika des MetS, wie erhöhtes Körpergewicht, Hyperlipidämie und Hyperglykämie. Ebenso von Bedeutung ist die relativ heterogene Symptomatik des MetS unter diesen Bedingungen, was der typischen Situation bei Patienten entspricht. Momentan gelten diese Mäuse als das beste Nagermodell, um das MetS umfassend zu untersuchen.

Im ersten Teil meines Projekts untersuchten wir die möglichen Ursachen dieser Heterogenität hinsichtlich Fett- und Glucosestoffwechsel, und wir charakterisierten zwei verschiedene Phänotypen dieser Mäuse. Einerseits die sog. Responder Mäuse (R), die eine

charakteristische Dyslipidämie entwickeln, und die sog. Non-responder (NR) Mäuse, bei denen der metabolische Phänotyp weniger stark ausgeprägt ist. Interessanterweise scheint dies allerdings darauf zu beruhen, dass die Leberfunktion dieser Mäuse hochgradig eingeschränkt ist.

Im zweiten Teil meines Projekts untersuchten wir den Einfluss einer RYGB-Operation auf den Stoffwechsel der Responder ApoE3L.CETP Mäuse. Wir unterschieden dabei RYGB-spezifische Effekte von solchen, die rein durch die Körpergewichtsreduktion erklärt werden können. Wir konnten zeigen, dass der Glucose- und Fettstoffwechsel sich gewichtsabhängig verbesserte, dass aber z.B. die Reduktion des Gesamt-Cholesterols, des nicht an HDL gebundenen Cholesterols und von Ceramid nur bei RYGB reduziert waren, d.h. auf einem Operations-spezifischen Effekt beruhen.

Unsere Resultate unterstreichen, dass RYGB zurecht auch als sog. "metabolische Chirurgie" angesehen wird, da durch RYGB erstens das MetS positiv beeinflusst wurde, und da dieser Effekt z.T. gewichtsunabhängig war. Wir sind davon überzeugt, dass unsere Ergebnisse einen wichtigen Beitrag zur Untersuchung des MetS und dessen Behandlung liefern. Ausserdem glauben wir, dass die ApoEL.CETP Maus ein geeignetes Modell zur Untersuchung dieser Aspekte des MetS darstellt.

3 Introduction

3.1 Obesity

Obesity epidemics counted more than 650 million obese adults (390 million women and 281 million men) [1] and 1.9 billion overweight adults in 2016 worldwide. The World Health Organization (WHO) defines as overweight an adult with BMI greater or equal to 25 kg/m^2 and as obese an adult with a BMI greater or equal to 30 kg/m^2. Also childhood obesity and overweight increased dramatically in the past 40 years (47%) in both developed and developing countries [2].

Obesity per se results from an imbalance between calories consumed and calories expended; this creates a positive energy balance and results in excess body weight [3]. The aetiology of obesity has its roots in a complexity of genetics, environmental and cultural factors. Several studies with different populations [4] and with twins [5] proved that a genetic predisposition to gain weight exits: especially, some specific polymorphisms have been associated with an increased risk of obesity [6, 7]. This genetic predisposition, however, is believed to contribute to less than 1.5% of the entire obesity aetiology [8], and part of this genetically susceptibility has been shown to be overwhelmed by physically active lifestyle [9]. Nevertheless, life style choices and sedentary life contribute to obesity as well [3, 10].

3.2 Obesity and related co-morbidities

Adulthood and childhood obesity are associated with other health problems as sleep, respiratory, gastrointestinal, endocrine, cardiovascular and psychiatric disorders [11] that, if developing during childhood, often persist in adulthood, lowering life style expectations by 6-14 years [12, 13]. Visceral obesity is one of the main factors that contributes to and drives hypertension, elevated plasma insulin concentrations and insulin resistance (IR), and, eventually, type 2 diabetes mellitus (T2DM), hypertriglyceridaemia and low levels of high-density lipoprotein cholesterol (HDL-C). The mentioned factors are components of the metabolic syndrome (or MetS) [14, 15]. In other words, the MetS describes a cohort of obesity-

related comorbidities such as T2DM, non-alcoholic fatty liver disease (NAFLD) and cardiovascular diseases (CAD). Data collected in the United States between 2003-2012 showed increased MetS epidemics in adults over 60 years, with a generally higher prevalence in women compared to men and a highest prevalence in Hispanics white compared to other ethnicities [16].

Even though some pathophysiological mechanisms of the MetS are understood today, many factors are still unknown and it is important to investigate them to find possible treatments and to ameliorate the quality of life for these patients.

3.3 Animal models for MetS

It is difficult to combine all the aspect of the MetS in one single animal model. MetS has been defined as obesity combined with at least one other disorder as dyslipidaemia, or impaired glucose in different mice model [17]. It is quite common in models of obesity to have IR, as commonly seen in humans where increased abdominal fat correlates with increased IR. Commonly used mice models to describe these two features of the MetS are: leptin-deficient ($Lep^{ob/ob}$) [18], leptin receptor-deficient ($LepR^{db/db}$) [19] and yellow agouti A^{y}/a [20]. They have spontaneous genetic modifications that make them become obese, insulin intolerant, and hyperglycaemic, so that they eventually develop diabetes mellitus. As a consequence of a leptin receptor defect, the $LepR^{db/db}$ mice have high leptin circulating levels that are related to their adiposity levels, while $Lep^{ob/ob}$ are leptin deficient. Aguti A^{y}/a mice particularly displayed delayed obesity onset and intact leptin signalling.

Even though these mice are severely obese and develop obesity related IR, the limiting factor of these mouse models is that they do not develop hypertension or modifications in their lipid profile, hence they hardly develop atherosclerosis on a high-fat diet. In fact, mice' lipoprotein profile consists primarily of HDL-C, while in human low density lipoprotein cholesterol (LDL-C) are the main lipoproteins present [17].

Because in people IR and obesity correlate with the development of dyslipidaemia [21], other

mice models were considered, such as LDL-C receptor knock-out mice ($LDLR^{-/-}$) mice, apoE-deficient mice, and ApoE*3Leiden.human Cholesterol ester transfer protein (ApoE3L.CETP) mice.

$LDLR^{-/-}$ mice [22] and apoE-deficient mice [23] develop hypercholesterolaemia on chow and on a HFHC (high fat high cholesterol) diet, and eventually atherosclerosis [24-26]. Data on obesity and IR developed in $ApoE^{-/-}$ mice are controversial: some studies indicated that apoE-/- mice do not develop obesity and IR [27, 28], while other studies indicated the opposite [29]. Overall apoE-/- mice are considered a good model for the MetS under HFHC diet conditions and the breeding of $Lep^{ob/ob}$ or $LepR^{db/db}$ on the apoE-/- background allowed to have a model of obesity, IR and hyperlipidaemia [17].

Up to know, ApoE3L.CETP mice seem to be the best available model to study the MetS since they present a humanized lipoprotein metabolism, develop atherosclerosis when HFHC diet fed, and display a human-like response when treated with statins [30, 31]. Compared to wildtype mice, they have higher concentrations of very low density lipoprotein (VLDL) and LDL-C, and relatively low concentrations of HDL-C when fed the HFHC diet. The presence of the ApoE3Leiden transgene hampers the uptake of VLDL remnants by the liver leading to increased VLDL/LDL-C levels in plasma, similar to humans [32]. Further, the introduction of the human glycoprotein CETP is responsible for the transport of cholesterol ester from HDL-C to apolipoprotein-B (apo-B) containing lipoproteins in exchange of triglycerides, leading to decreased HDL-C [32]. For these reasons, we used these mice in the experiments performed for my dissertation.

The last aspect not always described or mentioned as a key feature of the MetS is hypertension. Hypertension, indeed, is not always present in all MetS patients, even if it has been shown to correlate in some of them with increased atherosclerosis [33]. Most of the *in vivo* studies concerning obesity and hypertension were mainly performed in rats and only a few in mice investigating the effects of blood pressure and diet-induced obesity, or focusing on the renin-angiotensin system (RAS) summarising alterations in adipokines, leptin and adiponectin [17, 34]. For example, Gupte et al [34] showed that blockade of the angiotensin II

type 1 receptor abolished hypertension; similarly, Kouyama et al [35] demonstrated that deficiency in the same receptor decreased diet-induced body weight gain, improves IR as well as hypertension. Despite these data, scientists are still debating on the inconsistency of the animal models in showing hypertension on one hand due to difficulties in reproducing the same blood pressure measurements with telemetry or with the tail cuff method [34, 36, 37], and on the other hand due to differences in the animals' background strain, age, gender and way to induce obesity [17]. For example, $Lep^{ob/ob}$ mice (on the C57BL/6J background) were found to be hypotensive [38] while some $LepR^{db/db}$ mice were reported to be either hypotensive or hypertensive [39].

In humans, instead, the role of RAS in the MetS is well demonstrated and clinical data showed that pharmacological inhibition or blockade of enzymes in the RAS system (as e.g. angiotensin converting enzyme inhibitors or angiotensin receptor blockers [40, 41]) are not only the first line treatment for hypertension in obese patients, but also they can improve insulin sensitivity highlighting their applicability in treating MetS patients [17].

Nevertheless, clinical and animal studies proved the importance of RAS in some aspects of the MetS, confirming a connection between obesity and hypertension and the importance in investigating also this aspect.

3.3.1 ApoE3L-CETP mice: our model used to describe the MetS; differences between responder (R) mice and non-responder (NR) mice

ApoE3L.CETP mice, commercially available at TNO (TNO innovation for life, Leiden, The Netherlands) exhibit a dyslipidemic phenotype combined with obesity, IR, and atherosclerosis when administered HFHC diet [42-45]. Responses of ApoE3L.CETP mice to the HFHC diet were reported to be highly variable [46] and therefore an attempt was made to clarify the causes of the observed heterogeneity inherent to this model; hence, the ApoE3L.CETP mice can be clustered into two different phenotypes within the same genetic background in ApoE3L.CETP mice: responder (R) mice and non-responder (NR) mice.

Mice that do not fully display the expected MetS phenotype, i.e., increased body weight and increased triglycerides and total cholesterol levels after HFHC diet exposure, are classified as NR and represent approximately 20% of the total ApoE3L.CETP mice population at TNO (TNO innovation for life, Leiden, The Netherlands, personal communication). In fact, NR mice and R mice can already be differentiated at young age when chow fed, based on their prevailing triglyceride and cholesterol plasma levels. Hence, chow fed mice at 6-7 weeks of age with triglycerides levels lower than 2 mmol/L (i.e. 177 mg/dL) are considered as NR mice, while those with triglycerides levels above this arbitrary threshold are classified as R mice.

3.4 HDL metabolism and obesity

HDL-C plays a very important role in MetS. HDL-C is involved in cholesterol homeostasis because it mediates the transfer of cholesterol from extra-hepatic tissues to the liver; excess cholesterol is removed from peripheral tissues, preventing its accumulation and atherosclerotic plaque formation (Fig 1). Hence, HDL-C has a protective and anti-atherogenic action that is determined not only by its concentration, but even more importantly by its properties [47].

HDL-C forms are a heterogeneous class of lipoproteins divided in several subclasses defined by density, size, shape and by their lipid and protein composition [48]. HDL-C subclass distribution was firstly described in early 1950s by De Lalla et al [49] by ultracentrifugation and HDL_2-C and HDL_3-C were defined. Particularly, HDL_2-C are less dense (1.063-1.125 g/mL) are relative rich in lipids while HDL_3-C are more dense (1.125-1.21 g/mL) and relative rich in proteins. Considering their gel electrophoresis mobility, based on their particle size, Nichols et al [50] fractioned HDL_2-C and HDL_3-C in: HDL_{3c} -C (7.2-7.8 nm diameter), HDL_{3b} -C (7.8-8.2nm), HDL_{3a} -C (8.2-8.8 nm), HDL_{2a} -C (8.8-9.7 nm) and HDL_{2b} -C (9.7-12.0 nm).

HDL-C formation starts in the hepatocytes or in the enterocytes. Apo A-I secreted by the intestine and the liver interacts functionally with ABCA1 allowing the transfer of phospholipids and cholesterol to lipid-poor apo A-I. Lipidated apo A-I are converted first in discoidal particles

enriched in un-esterified cholesterol, and second in spherical HDL particles [51, 52] (Fig 2). Apo E and apo A-IV are also involved in the biogenesis of HDL-C [53, 54]. These lipid-free apolipoproteins or lipid-poor particles are in continuous evolution and allow hepatic and non-hepatic cells to acquire and exchange phospholipids and un-esterified cholesterol [55]. CETP mediates the transfer of triglycerides from VLDL and chylomicrons that are rich in triglycerides to HDL particles. The increase in circulating VLDL promotes triglycerides transfer to HDL-C particles, mainly HDL_2-C increasing HDL uptake [56].

The strong inverse relationship between the plasma concentration of HDL-C and the increased risk of developing coronary artery disease in the context of the MetS raised interest in better understanding the mechanisms underneath [57]. It had been shown that genetic, lifestyle and environmental factors contribute differently in lowering HDL-C plasma levels [58-60].

In obese subjects, HDL-C levels are decreased, HDL-C becomes dysfunctional, and together this increases the risk of cardiovascular disease and related comorbidities [61]. In particular, dysfunctional HDL-C loses its anti-oxidant function, has lower endothelial protective activity [62] and a reduced capacity of promoting cholesterol efflux [63]. Hence, obesity particularly lowers HDL_2-C [64] and increases free fatty acids release from adipose tissue into the circulation providing a substrate for the formation of more VLDL particles by the liver [65]. This increases CETP activity lowering HDL_2-C and increasing VLDL.

Pharmacological inhibition of CETP activity with CETP inhibitors has been proposed as a therapeutic strategy in increasing HDL-C levels, but they failed in phase III of clinical trials, because of increased cardiovascular morbidity and mortality [66].

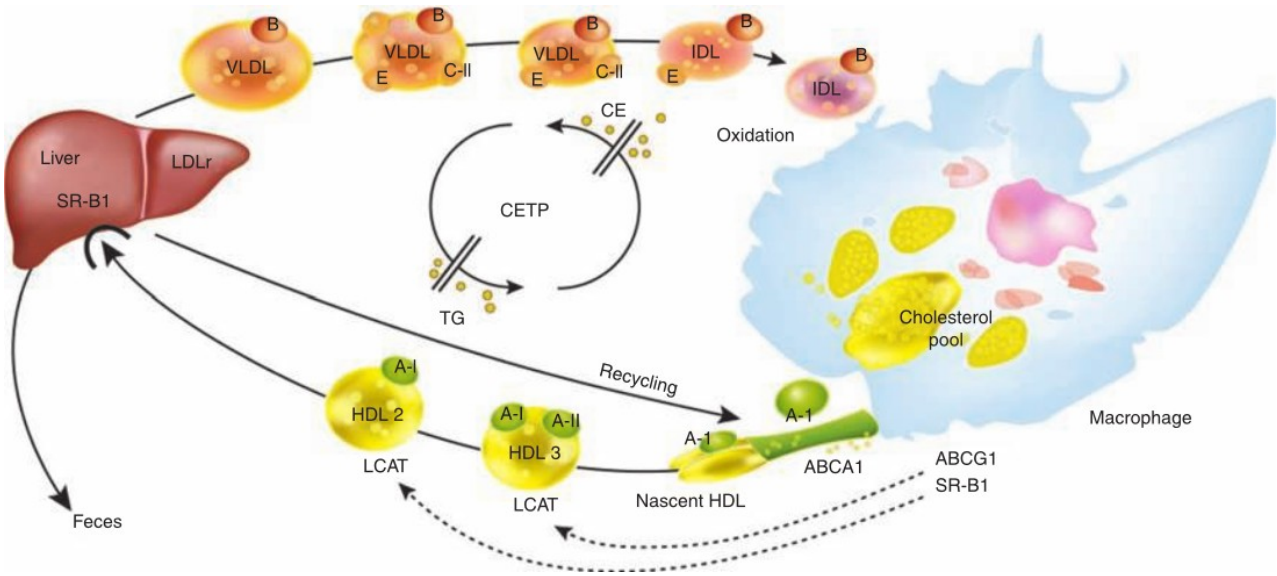

Fig. 1: Cholesterol homeostasis.
Cholesteryl ester transfer protein (CETP) mediates the exchange between triglycerides (TG) and lipoproteins of cholesterol ester (CE). CE are transferred into apolipoprotein B-containing low density lipoprotein (LDL-C) to form very low density lipoprotein (VLDL) to more atherogenic, readily oxidized LDL particles, that cojntribute to macrophage foam cell formation. ATP-binding cassette transporter A1/G1 (ABC-A1/ABC-G1) and Scavenger Receptor class B member 1 (SR-B1) mediate cholesterol efflux out of the peripheral macrophage to nascent, pre β-HDL-C, that matures to larger HDL via lecithin/cholesterol acyltransferase action [67] [68].

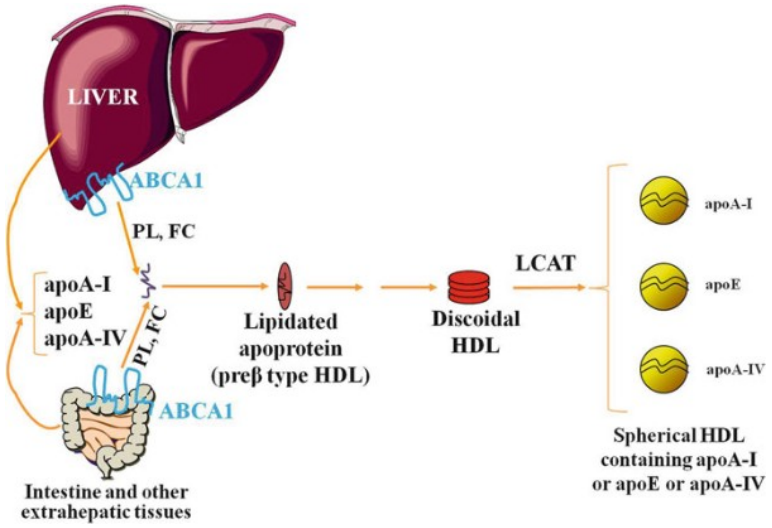

Fig 2: Representation of the biogenesis of HDL containing apo A-I, apo E or apo A-IV.
The interaction between secreted apo A-I and ATP- binding cassette transport 1 (ABC-A1) allows phospholipids (PL) and free cholesterol (FC) to be transferred to lipid-poor apo A-I. These lipidated apoproteins (pre β-HDL-C) are converted into discoidal particles enriched in unesterified cholesterol. The enzyme lecithin/cholesterol acyltransferase [67] converts discoidal HDL into spherical HDL particles [51].

3.5 Glucose metabolism and obesity

Overweight and obesity are two conditions that induce alterations in glucose metabolism: according to Colditz et al. [69], an increase of body weight by 1 kg is related to an increased risk for developing T2DM of 9%.

Glucose metabolic alterations include IR that precedes the development of T2DM, and it is usually associated with hypersulinaemia as a compensatory mechanism to maintain normoglycaemia [70]. It has also been proposed by several research groups that IR and hyperinsulinemia are associated with increased VLDL-C/triglycerides levels, low HDL-C levels and hypertension, and all of these factors may directly contribute to the progression of T2DM [71] and cardiovascular dysfunction [72]. In fact, IR increases lipolysis and reduces adipocytes' glucose uptake leading to hyperlipidaemia and fatty organs, in other words adipocytes lose in part their ability to convert carbohydrate in lipid to store [73].

Even if a strong correlation between a metabolic abnormality (e.g. overweight, obesity, hypertension, hyperlipidaemia) and the risk of developing T2DM had been demonstrated by Janghorbani et al [74], research to identify new biomarkers or criteria to predict T2DM or CAD onset at early stages is still ongoing. Townsend et al [75] particularly highlighted the problem of healthy adults undiagnosed for IR or hyperinsulinaemia prior to the disease development. Up to now measuring dysglycaemia in fasted or postprandial states, as well as fasting insulin or insulin during oral glucose tolerance test (OGTT) have been proposed to try to predict early onset of T2DM [75].

3.6 Treatment for the MetS

The main goal for obese patients with the MetS is to improve their quality of life and to prolong their life expectancies, reducing atherosclerosis and diabetes and other comorbidities. Caloric restriction is always recommended and it is beneficial in the reduction of the MetS complications, along with adjustments of physical activity, but this is not sufficient on a population levels [76, 77]. In clinical studies, weight loss of 5-10% due to lifestyle intervention,

as diet or exercise, can already improve insulin resistance and lipid levels [77] and is so-called first-line MetS treatment [78]. According to the National Institutes of Health [79] guidelines for the treatment of obesity pharmacological intervention, also so-called second-line treatment, is necessary when patients have a BMI > 30 or > 27 kg/m^2 with comorbidities [80]. At present, new pharmacological approaches are being developed for the long-term treatment and aim to induce body-weight loss, weight maintenance, and reduced fat mass in combination with reduction in lipids or glucose levels [78, 81]. Bariatric devices and bariatric surgery are considered third- and fourth-line treatments for the MetS even if to date success of surgical interventions largely outweighs the success of diet or pharmacotherapy.

3.7 Bariatric surgery

Bariatric surgery is considered a gold-standard treatment for MetS that leads to improvement and remission of diabetes, reduction of CAD risk, sustained and maintained body weight loss and improvement of the quality of live and prolonged survival [82, 83]. It is recommended for patients with a BMI ≥ 35 kg/m^2 with at least one comorbidity (particularly T2DM) or a BMI ≥ 40 kg/m^2 without such comorbidities [84].

Nowadays gastric banding (GB), sleeve gastrectomy (SG), Roux-en-Y gastric bypass (RYGB), biliopancreatic diversion with duodenal switch (BPD-DS) and mini gastric bypass (MGBP) are the most effective therapies for obesity and its comorbidities (Fig 3-4). 97% of all bariatric surgery performed in the USA are done laparoscopically, allowing a quicker recovery period, reduction of post-operative pain and wound-related complications if compared to standard open surgery procedures [85, 86]. Hence, mortality associated with bariatric surgery had been reported to be lower than 0.1-0.3% [87, 88] thanks to the introduction of the laparoscopic approach [89].

Surgical capacity, and surgical post-operative care costs are still the main limiting factors that allows only <1% of the USA and worldwide population who would be eligible for bariatric surgery to be actually operated; nevertheless, in the past 2 decades in USA, the number of

surgery cases increased from 158’000 in 2001 to 193’000 in 2014 [90]. While in the USA the most common procedure is SG, worldwide RYGB (45%) and SG (37%) are the most common bariatric procedure performed [91].

Bariatric surgery per se was proposed for the first time in the mid-1960s by Edward Mason as the most effective procedure to achieve weight loss [92]. Particularly a single loop anastomosis was described as the first gastric bypass, later modified into the current RYGB [82]. In the early 1980's, other bariatric surgery procedures started to being developed taking into consideration different ways of portioning the stomach and of reconstructing the small intestine, so-called biliopancreatic diversion and with the addition of the duodenal switch [93]. Even if SG had been initially proposed as the initial step of a two-stage approach in RYGB or MGBP [94], given its success as a bariatric operation in the late 2000s it has been established by the FDA (U.S. Food and Drug Administration) as one of the bariatric surgery procedures available [82].

Alternative and less invasive approaches have been proposed in the past couples of years to induce body weight. For example, in 2015, FDA approved vagal nerve blockade devices to treat severe obese patients (BMI 35-45 kg/m^2) since it has been shown that blockage of the vagal nerve may induce body weight loss [82, 95].

Different endoscopic bariatric surgeries and new devices are currently in development and close to being approved by the FDA. The main actions are related to restriction or manipulation of the stomach or to neuro-hormonal alterations or a combination of the two. For example, the single and the integrated dual intra-gastric balloons were approved by FDA in 2015 to treat obese patients with a BMI of 30-40 kg/m^2 [96]. Only 6% of patients up to now developed complications as abdominal pain, gastro-esophageal reflux or gastric ulcers that could lead to balloon removal. Long-term and severe complications results are not yet available due to the novelty of the technique [82].

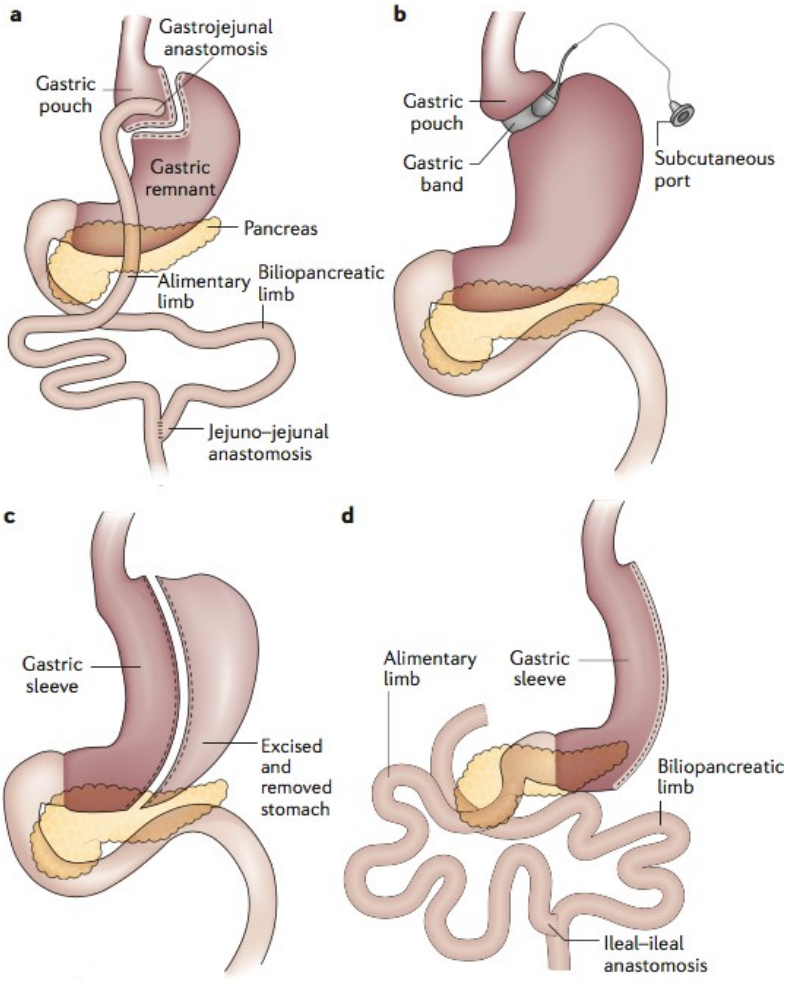

Fig 3: Gastrointestinal anatomy after different bariatric surgery procedures:
(a) Roux-en-Y gastric bypass (RYGB), (b) Gastric banding (GB), (c) Sleeve gastrectomy (SG) and (d) Biliopancreatic diversion with duodenal switch (BPD-DS) [82].
(b)

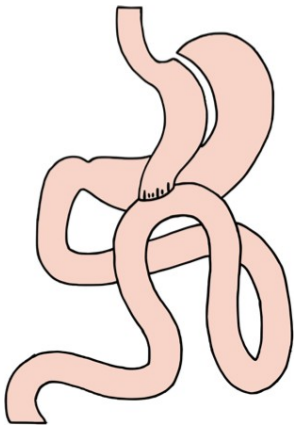

Fig 4: Schematic representation of mini gastric bypass [97]

3.7.1 Gastric Banding

Gastric banding (GB) (Fig 3b) was commonly used in last 20 years, but it has been gradually substituted by SG and RYGB due to the demand for revision or conversion to other bariatric surgery procedures in one in five patients, and because more invasive procedures proved to be more efficient [98, 99]. During the GB surgery, an adjustable silicon band is placed around the stomach, just below the gastro-esophageal junction and securely fixed with proper sutures. Adding or removing saline through a subcutaneous port allows adjustment of the size of the silicon banding, hence controlling/limiting food intake [100]. For the first 6 week post-surgery, patients normally receive a liquid or semi liquid diet, then a normal diet.

After GB patients progressively lost weight, had reduced HbA1c levels (33% patients who underwent GB reached HbA1c below 6.5% after 1 year) [101], reduced diastolic and systolic blood pressure, and showed a modest improvement in total cholesterol and triglycerides. Nonetheless, changes in body weight could not always predict changes in any of the metabolic parameters mentioned above.

The main complications described are band slippage or prolapse (with an incidence of 22%) [98], band infection, tube disconnection and band erosion (incidence of 11%) [102]. Compared to other bariatric surgery techniques it is safer, less invasive with a shorter operating time, shorter hospitality stay and fewer short-term complications [100] and with a mortality risk almost close to zero [101]. Since, it has also been shown that some patients reached diabetes remission after 2 years with a combined multidisciplinary team care [103], GB is still considered a valid treatment for MetS [101].

3.7.2 Sleeve Gastrectomy

Sleeve Gastrectomy (SG) (Fig 3c) is today one of the most commonly used procedures to achieve long term body weight loss in the United States, and it consists of an excision of the greater curvature of the stomach (80%), leaving a tubular stomach or sleeve [98, 104, 105]. It is relatively simple compared to other bariatric surgery techniques since no bypass

anastomosis is needed and the rest of the gastrointestinal tract is left intact [106], and it is generally offered to super-obese patients with a BMI > 60 kg/m^2 [107]. SG induced reduction of daily caloric intake [108], and improvements in glucose and lipid metabolism [109], even if with lower effects compared to RYGB. Although glucose homeostasis improved after SG, with levels of HbAc1 <6%, to maintain normal glycaemia SG patients still needs drugs [110] and T2DM is not always remitted [111, 112] .

Complications to SG are related to leakage along the staple line and to strictures. Leakage (incidence of 3% for primary procedures and 10% for revisional procedures) can induce peritonitis and sepsis; strictures, as kinking or twisting of the tubular pouch, can induce inability to tolerate oral intake; dysphagia, reflux [113]; post-surgery haemorrhage (3.57%) [107].

3.7.3 Biliopancreatic diversion with duodenal switch

Biliopancreatic diversion with duodenal switch (BPD-DS) (Fig 3d) consists of two different components. Initially a vertical gastrectomy is performed, similarly to a SG, to create a tubular gastric pouch, then a large portion of the small intestine (50%) is bypassed creating malabsorption [82]. At approximately 250 cm to the ileocaecal valve a segment of the distal ileum is divided and anastomosed to the duodenum. Then a second anastomosis is created at 100 cm approximately to the ileocaecal valve. Since most the small intestine is bypassed, decreased absorption of protein, fat, nutrients and vitamins occurs [82], but also improvement in glucose metabolism [114]. Hence, it is considered the most effective treatment for severe obesity and T2DM when compared to the other bariatric surgery procedures [115]. Short-term complications (e.g. leakage or obstructions) and long-term complications as nutritional deficiencies limited a wider use of this technique [93, 116]; only about 1% of all bariatric surgery performed in the USA consist of BDP-DS [90] and it is used for patients with a BMI > 50kg/m^2 or with weight regain after other bariatric operations [82].

3.7.4 Mini Gastric Bypass

The laparoscopic mini gastric bypass (Fig 4) firstly reported by Rutledge et al [117] recently gained popularity since it allows to achieve similar results as RYGB and since its procedure is technically less demanding with shorter hospitalization and fewer post-operative complications [97].

Initially, the stomach is divided between the body and the antrum of the stomach, without modifying the gastric vessels. Then a small intestinal segment, about 200 cm distal to the ligament of Treitz, is selected and anastomosed to the stomach [118] (Fig 4).

Mini-gastric bypass induced substantial body weight loss and improvements in glucose metabolism, hence it is a promising technique compared to RYGB given the safer and easier procedure [97]. Clinical data collections around this procedure are still ongoing to better understand the underlying mechanisms around changes in lipoprotein profile and bile acids and to have a complete long-term follow up [97].

3.8 Roux-en-Y Gastric Bypass

The Roux-en-Y gastric bypass (RYGB) (Fig 3a) is considered the “gold standard” weight-loss procedure worldwide [119]. It divides the stomach into an upper pouch sized of 15-30 mL and a gastric remnant. The gastric pouch is anastomosed to the mid-jejunum through a gastro-jejunal anastomosis. The rest of the stomach and the duodenum are viable, bypassed and reconnected to the distal jejunum. This procedure creates a Y-shape structure in the intestine where almost undigested food goes through the gastric pouch and the so-called alimentary (or Roux) limb, while pancreatic, gastric juices and bile acids pass through the bypassed duodenum, also called biliopancreatic limb. These two limbs reconnect together in the so-called common channel, that is the last part of the small intestine. This change in the gastro-intestinal tract physiology may induce fat malabsorption at least when diets high in fat content are fed, and to some degree, it decreased micronutrient absorption, leading to for examples to iron and calcium deficiency, making lifelong supplementation a necessity [120, 121]. Since

this is the surgical technique performed for the purposes of the experiments described in my dissertation, specification about the effects of RYGB surgery on lipid and glucose metabolism will be extensively discussed in paragraphs 3.8.2 and 3.8.3; a general overview of the beneficial effects of RYGB is schematised in Fig 5.

Also for Roux en-Y gastric bypass (RYGB) one of the major complications that occur is related to staple line leakage, reported at present in less than 2% and with a higher frequency in the gastro-jejunal anastomosis [122]. In some cases, also bowel obstruction and internal hernia were reported with an incidence between 1-16% [98, 123, 124]; it can occur at time while marginal ulceration has an incidence of 1-16% in open RYGB and 7% after laparoscopic RYGB [98, 125].

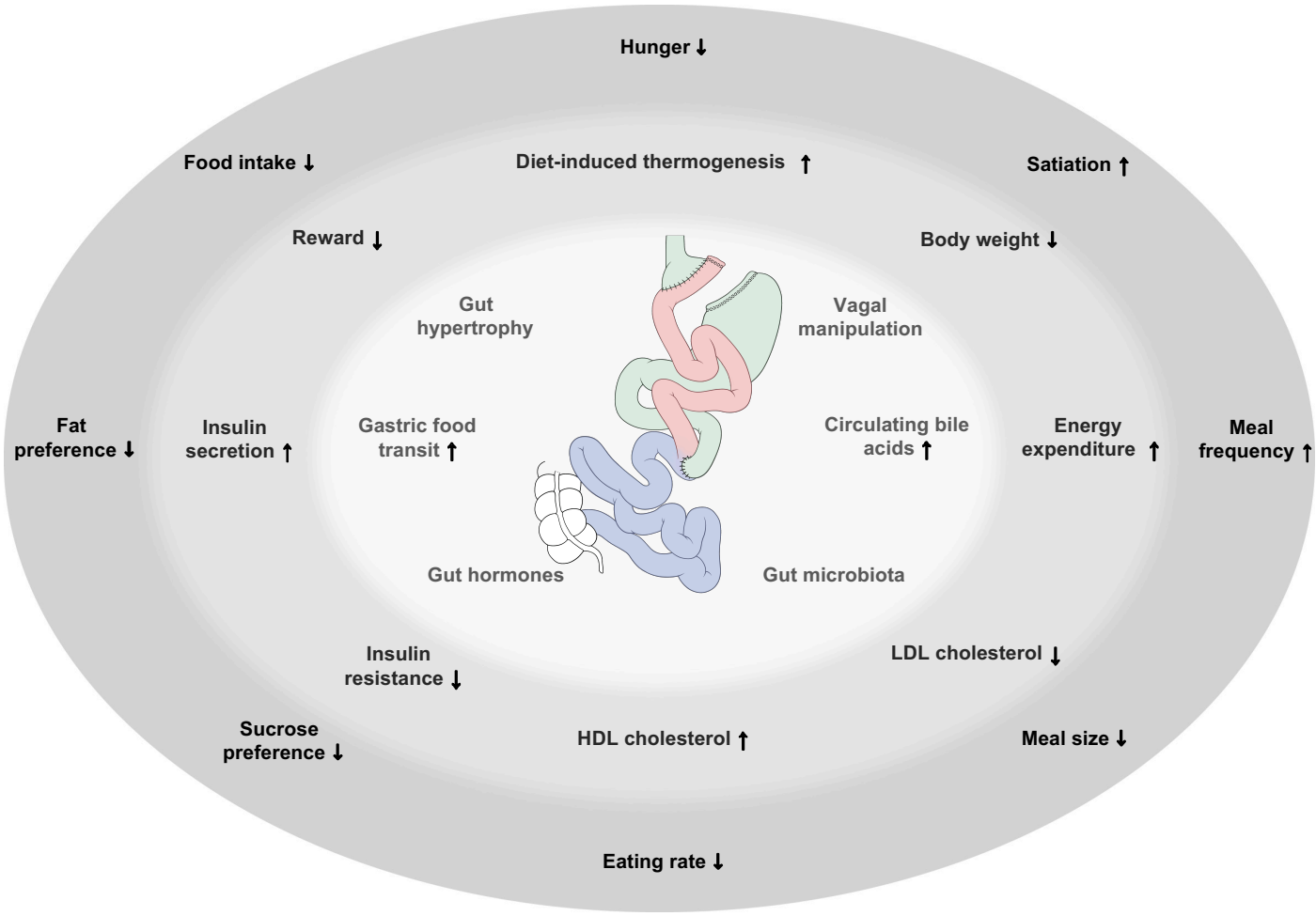

Fig 5: Schematic illustration of the physiological mechanisms after RYGB surgery. These mechanisms involve gastrointestinal effects (inner circle), systemic effects (middle circle) and behavioural effects (outer circle). Image adapted from Lutz et al, 2014 [126].

3.8.1 RYGB and mechanisms involved in body weight loss

RYGB procedure induces rapid and sustained body weight loss mainly due reduction in eating and mainly increased energy expenditure in rodents [126]. One of the key point that indicate body weight loss, is the loss of excessive fat mass because the body rearrange its body weight control "setting" [126, 127]. Body weight loss after RYGB is dependent from patient to patient; typically, T2DM patients lose on average 20% of their total body weight, while heavier patients lose much more [128, 129].

RYGB reduces eating in part by reducing meal size [130] and hunger sensation [131], and changes in food preferences [130].

Even though mice studies showed increased energy expenditure after RYGB [132, 133], data in humans are controversial. Some studies showed that energy expenditure decreased in patients with a normal preoperative metabolic rate [134], but it tended to increase in patients that were hypo-metabolic before surgery [133]. It is believed that discrepancies in the data might be due to different methodology in measuring energy expenditure [130].

3.8.2 RYGB and lipid metabolism

All bariatric surgery procedures reduced total cholesterol and triglycerides at different levels. Perhaps different from other surgical procedures, Osto et al. [135] demonstrated that RYGB induces improvements in hyperlipidaemia independently and prior to any substantial body weight loss. As a matter of fact, total cholesterol, triglycerides and LDL-C levels decreased after already 1 month after RYGB surgery, indicating a direct surgical effect per se because the same had not been seen in sham-operated weight matched controls [136].

Several hypotheses have been proposed to explain how RYGB reduces directly lipid levels. The so-called exogenous hypothesis refers to changes in exogenous lipids sources, reduction in food intake and loss of appetite [137]. In fact, RYGB causes a delay in food mixing and digestion. It further induces reduced preference for high-fat food [138, 139], changes in lipid absorption [140], and modification in the gut microbiota [141]. In fact, it has been reported a

reduction of intestinal cholesterol and increased faecal fat levels after RYGB surgery [142, 143], and that alterations in the intra-luminal viscosity of the gut might reduce lipid absorption [144].

The second hypothesis, or endogenous hypothesis, takes into account modifications in gut hormones, for example GLP-1 [145] and insulin which impacts lipolysis [146]. In other words, this theory stated that the delivery of not completely digested food or nutrients to the distal gut increased the secretion of insulinotropic and appetite-controlling gut hormones, inducing increased body weight loss and improved glucose and lipid metabolism [136]. Particularly, it has been shown that due to reduced energy intake post-surgery insulin levels decrease and inhibition of lipolysis is reduced [147].

Moreover, several studies reported greater improvement in HDL-C levels after 1, 2 and 10 years of follow up after RYGB surgery with respect to a general improvement in total cholesterol and triglycerides levels [110, 148, 149]. Nonetheless, body weight loss and body weight maintenance per se might help in the process of increasing HDL-C plasma levels [150]. Indeed, HDL-C levels after RYGB surgery not only increased in respect to their concentration, but a shift towards remodelling into more mature particles [151, 152] with a higher anti-oxidative potential [152] and higher content of the anti-atherogenic apolipoprotein apo A-1 was also shown. The main reasons why apolipoproteins increased after RYGB find their explanations in enhanced intestinal secretion, increased hepatic synthesis and reduced catabolism [153, 154].

In the last decades, the role of sphingolipids and phospholipids as regulators of lipid metabolism and biomarkers for atherosclerosis raised its attention [155]. Notably, already 3 and 6 months after RYGB surgery, ceramide levels decreased within body weight loss, and nicely correlated with improvements in CAD risk, in insulin sensitivity and glucose homeostasis

3.8.3 RYGB abd glucose metabolism

75-85% of obese diabetic patients who underwent RYGB surgery had resolution of T2DM, normal blood glucose and glycated haemoglobin levels with discontinuation of diabetes-related medications [148]. These improvements occur within few days after surgery and even before weight loss occurs [156]. The main mechanisms around glycaemic metabolism improvement are not completely understood, and several hypotheses were advanced. The first one takes in consideration the hypocaloric intake diet after surgery [157], followed by decreased liver fat that reduces hepatic insulin resistance. Second, improved B-cell function occurs as a consequence of the increased sensitivity to glucose and increase in GLP-1 secretion [158].

Another approach addresses the improvements in glucose metabolism after RYGB with the so-called hindgut versus foregut hypothesis. The hindgut hypothesis considers the accelerated delivery of chyme into the distal intestine to improve GLP-1 secretion that consecutively improves glucose metabolism [159]. Hence, GLP-1 is believed to affect directly the proliferation and anti-apoptosis of pancreatic B-cells [160]. In the foregut hypothesis, improvements of glucose metabolism are believed to depend on the fact that the duodenum and the proximal jejunum are bypassed which would prevent the secretion of a signal that reduces insulin sensitivity and hence that promotes T2DM [161]. Up to now, evidences for both theories have been provided.

Further studies also focussed on the side effect of postprandial glycaemic peaks followed by hypoglycaemic symptoms in T2DM remitters after RYGB [162]. Data available during continuous glucose monitoring in patients after RYGB could not completely clarify the underlying cause of these abnormalities but only highlight the pharmacological implementation to minimize them [163]. Despite these problematics RYGB has been proposed as a treatment for diabetic and obese patients [83].

4 Hypothesis, aims and experimental design

4.1 Hypothesis

Several clinical findings showed that RYGB improves the pathophysiology of the MetS: body weight loss, reduced cardiovascular risk factors, T2DM remission, and reduced mortality. Based on these findings, we wanted to elucidate the long-term effects of RYGB surgery on the improvement of lipid and glucose metabolism in ApoE*3Leiden.CETP mice, a murine model for the MetS.

4.2 Aims and experimental design

Aim 1: Characterization of the effects of long-term access to a high fat high cholesterol diet in the ApoE*3Leiden.CETP mouse model on feeding behaviour, glucose and lipid metabolism: comparison between responder and non-responder mice

To investigate glucose and lipid metabolism, male ApoE*3Leiden.CETP responder and non-responder mice were chow fed for 2 weeks, followed by a high fat (60%) high cholesterol (0.25%) diet for 20 weeks. Mice were subjected to OGTT (oral glucose tolerant test) and IST (insulin sensitivity test) and to blood sampling to measure lipids profile. Baseline tests were performed when mice were chow fed, and then every month when they were fed the HFHC diet. A separate cohort of ApoE*3Leiden.CETP responder and non-responder mice were housed in an automated cage system to measure feeding behavior. Finally, extensive metabolic and histologic liver analysis of these two phenotypes were performed.

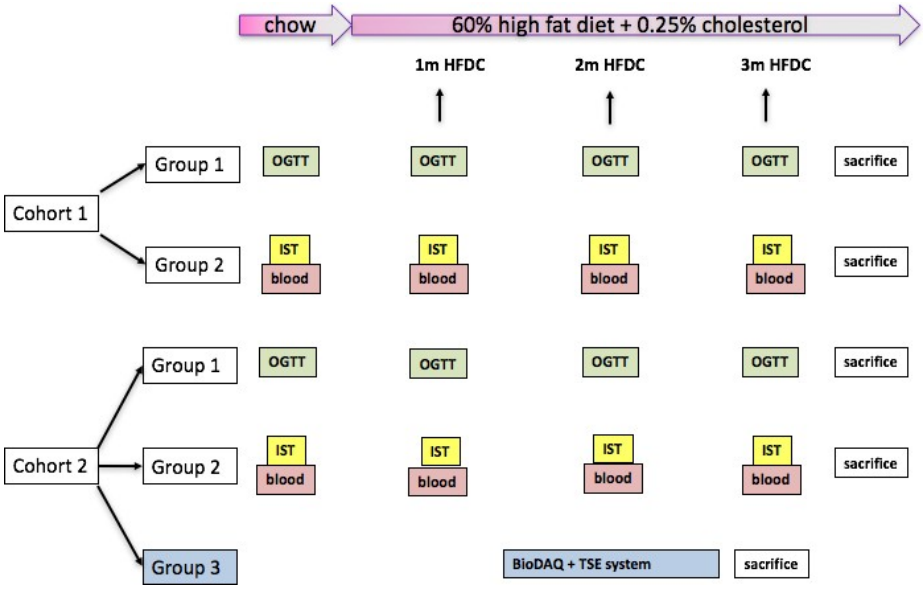

Fig 6: Design of the experiments under Aim 1
OGTT, oral glucose tolerance test; IST, insulin sensitivity test; blood, blood sampling; sacrifice, organ harvesting, terminal blood sampling

Aim 2: Effects of RYGB surgery in obese male ApoE*3Leiden.CETP mice on glucose and lipid metabolism: comparisons between RYGB and sham operated mice

To study the effects of RYGB surgery on glucose and lipid metabolism, male ApoE*3Leiden.CETP mice were fed HFHC diet for 8 weeks prior to perform RYGB or sham surgery.

Glucose metabolism was tested with OGTT and IST while lipid metabolism was analysed through blood sampling. Tests were performed before surgery, that is when mice were chow fed, and after 6 weeks of HFHC diet; and then about three weeks after surgery.

20 days after surgery mice were sacrificed and RYGB effects were assessed on liver and pancreas histology.

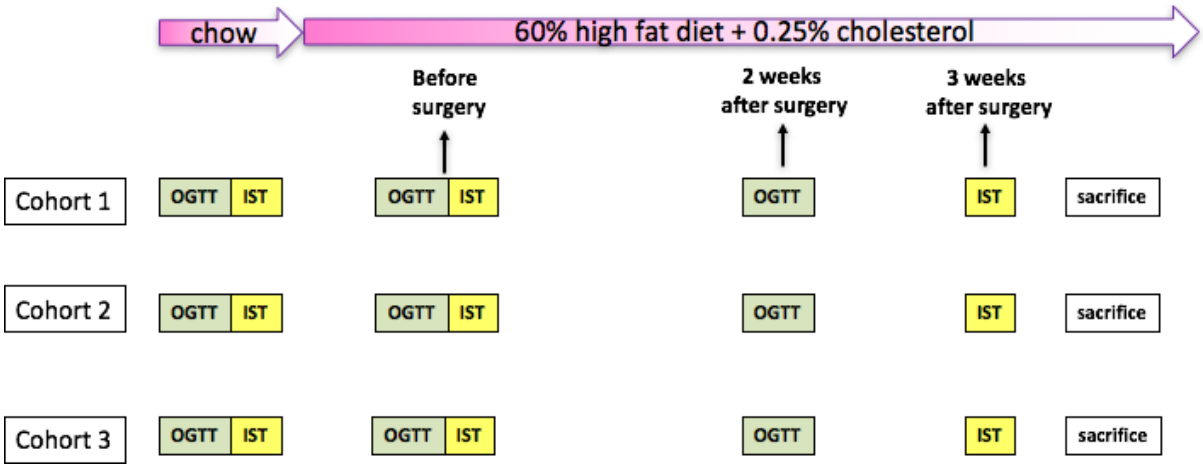

Fig 7: Design of the experiments under Aim 2
OGTT, oral glucose tolerance test; IST, insulin sensitivity test; blood, blood sampling; sacrifice, organ harvesting, terminal blood sampling

5 Results

5.1 Original research article: “Phenotypical heterogeneity in respodner (R) and non-responder (NR) male ApoE*3Leiden.CETP mice”

This section contains an original research article that was submitted to American Journal of Physiology - Gastrointestinal and Liver Physiology in March 2018 and it is currently in revision. It contains part of the studies performed for the completion of the present PhD thesis.

My contribution, as first author of this article, includes the study design, data acquisition, data analysis and interpretation, and writing and revising the manuscript

American Journal of Physiology

Phenotypical heterogeneity in responder (R) and non-responder (NR) male ApoE*3Leiden.CETP mice

Erika Tarasco[1,2]; Giovanni Pellegrini[3]; Lynda Whiting[4]; Thomas A. Lutz[1,2]

[1]*Institute of Veterinary Physiology, Vetsuisse Faculty University of Zurich, Winterthurerstrasse 260, 8057 Zurich, Switzerland;*

[2]*Zurich Center for Integrative Human Physiology (ZIHP), University of Zurich, 8057 Zurich, Switzerland;*

[3]*Laboratory for Animal Model Pathology (LAMP), Institute of Veterinary Pathology, Vetsuisse Faculty University of Zurich, Winterthurerstrasse 268, 8057 Zurich, Switzerland;*

[4] *Institute of "Drug and Discovery Biology", University of Monash, Victoria 3800, Australia*

Running title: Phenotypical characterization of ApoE*Leiden.CETP mice

Address for correspondence:

Prof. Thomas A. Lutz

Institute of Veterinary Physiology

University of Zurich

Winterthurerstrasse 260

CH 8057 Zurich

Switzerland

Ph +41 - 44 - 635 88 08

Mail tomlutz@vetphys.uzh.ch

Abbreviations:

MetS: Metabolic syndrome

R: responder

NR: non-responder

HFHC: high fat high cholesterol diet

Keywords: metabolic syndrome, heterogeneity and phenotype, liver functionality, inflammation

Abstracts max 250 words

The metabolic syndrome (MetS) is a major health issue worldwide and is associated with obesity, insulin resistance, and hypercholesterolemia. Several animal models have been used to describe the MetS, however many of them do not mimic well the MetS pathophysiology in humans. To overcome this limitation, ApoE*3Leiden.CETP mice with a humanised lipoprotein metabolism were developed ten years ago and they are still been used to describe the MetS. A heterogeneous response to Western type diet feeding has been reported in these mice: responder (R) mice show increased body weight, and cholesterol and triglycerides levels, while NR mice do not show this expected phenotype.

The aim of this study was to characterize the differences observed in the two cohorts, investigating in detail feeding behavior, body weight gain, glucose tolerance, and lipid parameters, along with liver histology.

Our data confirmed that only R mice resemble the pathological features of human MetS. NR mice develop instead a severe inflammatory hepatic condition, which affects liver function and prevents them to develop the expected metabolic features of the MetS.

We conclude that R mice and NR mice exhibit prominent metabolic and morphological differences. Hence, it is critical to properly separate them to decrease heterogeneity in the data. Clinical chemistry and histological analysis can be used successfully to identify the phenotype, and for retrospective classification of the animals. Moreover, we point out that NR mice may not be an appropriate control for studies involving ApoE*3Leiden.CETP R mice.

Introduction

Obesity in humans (defined as Body Mass Index, BMI>30 kg/m^2) is one of the major health problems worldwide and is expected to increase even more in the next decades [1]. Although genetics factors are known to be involved in the pathogenesis of obesity [2, 3], its onset in the majority of people is due to excessive energy intake combined with a lack of physical activity. Obesity is often associated with other comorbidities such as cardiovascular diseases (CAD) [4], type 2 diabetes mellitus (T2DM) [5], hypertriglyceridemia [6], and non-alcoholic fatty liver disease (NAFLD) [7]. Together these conditions form the metabolic syndrome (or MetS). Since obesity may induce insulin resistance or changes in lipoprotein metabolism, it may be considered the major driving force behind the MetS [9]. While not all the underlying pathophysiological mechanisms are completely understood, the number of MetS patients increases [10]. Thus, understanding and deciphering these mechanisms will hopefully provide new means to counteract the MetS epidemic.

Several animal models, such as the diet-induced obese (DIO) mouse [11], the leptin-receptor deficient *db/db* mouse [12] or the Zucker rat [13], have been used in the past decades to try to understand the consequences of a Western type diet on metabolism; however they typically do not develop all aspects of the MetS; in particular, the underlying genetic defects in the *db/db* mouse and the Zucker rat do not replicate the typical human pathophysiology. Moreover, there are animal models in which features of the MetS [14] develop spontaneously on chow diet as for example in the DahlS.*Z*-*Lepr*$^+$/*Lepr*$^+$ rat [15], the Nile grass rat [16] or ZDSD rat [17]. This does not occur in human patients, who rarely show sign of the MetS when fed a balanced low fat diet; usually, only when eating a Western type diet, the typical MetS symptoms develop. Taking this into account, in our studies, we used the double transgenic mouse model ApoE*3Leiden.human Cholesterol ester transfer protein (ApoE3L.CETP). The ApoE3Leiden mutation [18, 19] and the introduction of human CETP gene [19] make these mice' lipoprotein metabolism more similar to humans thus making them one of the best animal models available to assess lipid metabolism in response to a Western type diet (e.g. a 60%

high fat supplemented with 0.25% cholesterol (HFHC) diet) [18, 19]. Hence, these mice show a humanized lipoprotein metabolism, develop atherosclerosis when fed HFHC diet, and display a human-like response when treated with statins [20, 21]. Compared to wildtype mice, they have higher concentrations of very low density lipoprotein (VLDL) and low density lipoprotein cholesterol (LDL-C), and relatively low concentrations of high density lipoprotein cholesterol (HDL-C) when fed the HFHC diet. The presence of the ApoE3Leiden transgene hampers the uptake of VLDL remnants by the liver leading to increased VLDL/LDL-C levels in plasma, similar to humans [19]. Further, the introduction of the human glycoprotein CETP is responsible for the transport of cholesterol ester from HDL to apolipoprotein-B (apo-B) containing lipoproteins in exchange of triglycerides, leading to decreased HDL-C [19].

The major aim of this study was to characterize the effect of long-term access to the HFHC diet in the ApoE3L.CETP mice on feeding behavior, and glucose and lipid metabolism. Interestingly, responses of ApoE3L.CETP mice to the HFHC diet are highly variable and therefore an attempt was made to clarify the causes of the observed heterogeneity inherent to this model. Our study highlighted in detail the presence of two different phenotypes within the same genetic background in ApoE3L.CETP mice: responder (R) mice and non-responder (NR) mice.

We characterized the morphological, metabolic and functional aspects of these two phenotypes through an extensive metabolic and histologic liver analysis of this mouse model. Our data indicate that only R ApoE3L.CETP mice recapitulate adequately the salient pathological features of human MetS. NR mice develop instead a prominent inflammatory hepatic condition that has detrimental effects on liver function, and may prevent the development of the expected “MetS phenotype”. Hence, the results of this study indicate that the high heterogeneity observed in this model might affect study outcomes, without an accurate distinction being made between R and NR animals.

Material and Methods

Animals and husbandry

Male ApoE3L.CETP mice (TNO, Innovation for Life, The Hague, Netherlands) [19, 22] aged 7-19 weeks were used in all experiments. Prior to be delivered to our facility, 6-7 weeks old mice kept on a standard chow diet were tested by TNO for plasma total cholesterol and triglycerides levels; mice with triglycerides levels lower than 2 mmol/L (i.e. 177 mg/dL) were considered as NR mice, while those with triglycerides levels above this arbitrary threshold were classified as R mice. In the cohorts used in our experiments, particularly, NR mice had total cholesterol levels between 1.4 – 2.2 mmol/L (i.e. 54.1 - 84.9 mg/dL), and triglycerides between 0.6 - 1.9 mmol/L (i.e. 53.1 - 168.1 mg/dL), while R mice total cholesterol was higher than 1.9 mmol/L (i.e. 73.4 mg/dL) and triglycerides higher than 2.1 mmol/L (i.e. 185.8 mg/dL) at 6-7 weeks of age. For consistency, we will report henceforth our study data only in mg/dL units, and refer to both mmol/L and mg/dL only for data collected at TNO.

Two different cohort of R mice and NR mice were ordered from TNO. Upon arrival at our facility, per each cohort, mice were separated into R ApoE3L.CETP mice and NR ApoE3L.CETP mice, and group housed at a temperature of 21°C with a 12h light-dark cycle (light on 2:00 am, light off 2:00 pm). They were acclimated to the new housing and environmental conditions for 2 weeks prior to the start of the experiments. During the acclimation period and for the following 2 weeks, mice were fed chow diet (4.5% fat; #3436, Kliba Nafag, Kaiseraugst, Switzerland) after which they were switched to a high fat high cholesterol diet containing 60% kcal fat and 0.25% cholesterol (D14010701, HFHC diet, Research Diets, New Brunswick NJ, USA) until the end of the experiments. In table 1 it is summarized the experimental design. The Cantonal Veterinary Office of Zurich approved all the animal experiments (licence 122/2014).

Animal health

Mice imported from TNO were negative for endo- and ectoparasites, viruses and bacteria, as indicated by the latest FELASA-compliant health reports (results not shown). Sentinel mice at

our facility were tested quarterly and resulted negative for major etiologic agents. Additional testing was conducted to confirm the specific pathogen free health status for *Helicobacter spp*. using qPCR on pooled frozen liver samples obtained from R mice and NR mice used in this study (n=3). The qPCR analysis was conducted in a diagnostic laboratory (Idexx Bioresearch, Ludwigsburg, Germany) using *Helicobacter* genus and *Helicobacter* species-specific PCR primers.

Body weight and body composition

Body weight was measured weekly from arrival at the facility until the end of the experiments. After sacrifice, 7 mice from each group were subjected to CT scanning (LaTheta LCT-100A scanner, Hitachi-Aloka Medical Ltd., Tokyo, Japan) for body composition, and the proportion between lean and fat mass (subcutaneous and intra-abdominal adipose tissue) in the region between lumbar vertebrae L1-L5 was analysed using LaTheta software (version 2.10, Hitachi-Aloka Medical Ltd.) [23, 24].

Feeding behavior

After 6 weeks of HFHC diet feeding, R mice (n=8) and NR mice (n=8) were single-housed in BIODAQ cages (Research Diets, New Brunswick, NJ, USA) equipped with external food hoppers to measure food intake continuously. Meal size and meal pattern over 24h were then determined. Meal pattern data collected from each mouse were grouped into meals by clustering independent feeding bouts. A meal was defined as a minimum inter-meal interval (IMI) of 600 sec and minimum size of 0.02 g [25]. Mice were not disturbed during these measurements.

The same mice were then transferred to an open-circuit indirect calorimetric system (TSE Phenomaster, TSE Systems GmbH, Bad Homburg, Germany) to monitor metabolic rate and respiratory gas exchange. Two weeks of adaptation were given prior to measurements for each test.

Glucose metabolism: oral glucose tolerance test and insulin sensitivity test

Oral glucose tolerance (OGTT) and insulin sensitivity (IST) tests were carried out in separate groups of R mice and NR mice to avoid stress and excessive blood sampling.

OGTTs were performed in R mice and NR mice on chow diet and after 1, 2 and 3 months of HFHC diet feeding (n=28 each time-point per group). Mice were fasted for 6h prior to the test and were briefly anesthetized with isoflurane (3% isoflurane in the induction chamber, 0.8L/min) to collect blood in microvette EDTA microtubes (Sarstedt, Nümbrecht, Germany) by sublingual vein puncture to measure basal glucose and insulin levels. At T0, a baseline blood sample was collected and a bolus of glucose (2g/kg) was given by oral gavage, after which blood was sampled by tongue bleeding at time 15 and 30 min, and by tail bleeding at time 45, 60, 90 and 120 min for glucose measurements (Breeze 2, Bayer Glucose Meter, Basel, Switzerland). The area under the curve (AUC) was calculated above the lowest glucose value of each mouse during the OGTT. Blood was kept on ice and centrifuged at 4°C for 5 min at 11000 rpm. EDTA plasma was separated and stored at -80°C until assayed. Insulin levels at time-points 0, 15 and 30 min were measured with a specific Mouse Insulin ELISA (Mercodia AB, Uppsala, Sweden) (Data not shown).

ISTs were performed using different cohorts of R mice (n=19) and NR mice (n=15), which were fasted for 4h and bled at the same time-points (see above). After baseline blood sample measurements, insulin Humalog (0.5U/kg, 100U.I./mL, Lilly, Geneva, Switzerland) was injected intraperitoneally and blood glucose levels were measured at 15, 30, 45, 60, 90 and 120 min after injection in blood samples collected by tail bleeding. Mice that became hypoglycemic (i.e. reached glucose levels of 2.5 mmol/L or less) were immediately given a bolus of glucose (2g/kg) and were excluded from the test for all subsequent time-points. In our analysis particularly, 9/27 R mice and 8/23 NR mice were excluded. The AUC was calculated above the lowest level of glucose of each mouse during IST test.

Cytokines and Transaminase measurements

Cytokines were measured in plasma isolated from terminal blood samples with V-Plex Cytokine kit (Meso Scale Discovery, Gaithersburg, MD, USA) following the manufacturer's protocol.

Plasma alanine transaminase (ALT) was measured via UniCel® DxC 800 Synchron® Clinical System in plasma of R mice and NR mice at the time of sacrifice, according to manufacturer's instructions.

Liver and pancreas histology

All animals were deeply anesthetized by isoflurane and sacrificed via opening of the thoracic cavity and exsanguination by cardiac puncture. A complete necropsy, including a thorough external and internal gross *post mortem* examination was performed on each mouse. Mice were sacrificed at different time-points after 2, 3 and 4 months of HFHC diet feeding. Liver and pancreas were removed, weighed (liver) and appropriately sized samples were fixed in 10% neutral-buffered formalin (Formafix, Hittnau, Switzerland) or snap frozen. Formalin-fixed samples were trimmed according to guidelines [26], dehydrated through graded alcohols and routinely paraffin wax embedded. Consecutive sections (3–5 µm) were prepared, mounted on glass slides and routinely stained with hematoxylin eosin (HE) or subjected to immunohistochemical staining. Microscopic findings in the HE-stained livers slides were classified with standard pathological nomenclature and severities of findings were graded on a scale of 0 to 4 (no finding present (0), minimal (Melander, #475), mild (2), moderate (3), or severe (4)). Grades of severity for microscopic findings were subjective; minimal was the least extent discernible and severe was the greatest extent possible [27]. Lesions that were not graded were marked as present. Nomenclature of the microscopic observations in the liver was consistent with INHAND published guides [28]. A silver stain was performed on the formalin-fixed paraffin-embedded liver sections of selected mice according to routine procedures to exclude the presence of argyrophilic bacteria.

Immunohistochemistry was employed on liver sections from selected mice for the characterization of the inflammatory infiltrate and bile duct proliferation. Antibodies anti-CD3

(Clone SP7, Bioscience M3074, dilution 1:900), anti-CD45R/B220 (clone RA3-682, BD Pharmigen, dilution 1:800) and anti F4/80 (clone SP115, Invitrogen MA5-16363 dilution 1:150) were used for the characterization of T cells, B cells and macrophages, respectively. A pan cytokeratin antibody (clone PCK-26, Novus Biological, dilution 1:500) was employed for the identification of biliary duct epithelial cells.

Oil red O (ORO) staining was performed on snap-frozen cryomold-embedded livers. Sections were cut at 6 µm, mounted on glass slides and allowed to dry at room temperature. They were then rinsed briefly in 50% ethanol, incubated in a 60% aqueous ORO solution (375.0 mg Oil Red O (Merck KGaA, Darmstadt, Germany) in isopropanol) at room temperature for 20 min, rinsed again in 50% ethanol and counterstained with hematoxylin for 2 min. ORO stained slides were scanned using a digital slide scanner (NanoZoomer-XR C12000, Hamamatsu Photonics K.K., Japan) and the fat content was calculated in the digital slides using the Visiopharm Integrator System (VIS, version 4.5.1.324, Visiopharm, Hørsholm, Denmark). Briefly, a threshold classification allowed recognition of positive (red) hepatocellular cytoplasm and negative hepatic parenchyma, and the results were expressed as positive area versus total area in the whole liver section. Data are presented as average (± SEM) percentage of lipid-containing parenchyma in the group.

Triglycerides and non-esterified fatty acids in livers

Approx. 50 mg of snap frozen liver were homogenized with 1 mL 2:1 chloroform:methanol (v/v) solution to measure triglyceride content. The homogenate was centrifuged for 5 min at 2500 rpm and supernatant was collected and diluted with 0.9% NaCl. Samples were centrifuged for 5 min 2000 rpm, then resuspended in a 1:1 methanol:H_2O (v/v) solution. The upper phase was then discarded, samples were let to dry and resuspended in Dimethyl sulfoxide (DMSO). Triglycerides content was then measured with the Cobas Mira Roche-Autoanalyzer (F. Hoffmann-La Roche Ltd., Basel, Switzerland), according to the manufacturer's instructions. Non-esterified fatty acids (NEFA) were measured on approx. 10 mg frozen liver following manufacturers' procedure (Merck KGaA, Darmstadt, Germany).

Pancreatic islets isolation and glucose-stimulated insulin secretion

At time of sacrifice, pancreas was digested and pancreatic islets were isolated using the adapted islets isolation procedure from Nordmann et al [29]. Subsequently, isolated islets were let recover for 2h in a cell culture incubator (37°C, 20%O_2 and 5%CO_2) and 10 islets/well were gently picked and plated into a 24 well ECM plate (Novamed, Jerusalem, Israel). Media was changed on day 2 and on day 4 when the glucose-stimulated insulin secretion (GSIS) test was performed following a procedure adapted from Rütti [30].

Krebs-Ringer phosphate solution supplemented with 0.1% BSA and 1M Hepes was prepared (KRH). Islets were pre-incubated for 30 min in KRH supplemented with 2.8 mM glucose at 37°C to let islets adapt to KRH solution before collection of the supernatant to measure insulin secretion. To measure basal insulin release, islets were incubated for 1h with fresh KRH + 2.8 mM glucose followed by 1h with KRH + 13.7 mM glucose to measure stimulated insulin release. After each incubation, supernatant was collected, immediately frozen and later used to measure secreted insulin. To quantify insulin content after the two incubations, islets were lysed with 0.18M HCl in 70% EtOH at 4°C overnight. Insulin was measured with the Mouse Insulin ELISA (Mercodia AB, Uppsala, Sweden) and secreted insulin was calculated as percentage of total insulin content.

Lipid parameters

Plasma total cholesterol and triglycerides were measured at TNO when mice were 6-7 weeks old to discriminate between R mice and NR mice. For consistency, we converted the unit for total cholesterol and triglyceride received from the TNO facility from mmol/L to mg/dL because all the measurements performed in our institute used this unit system. For our own measurements, an aliquot of blood collected from mice undergoing the IST was collected in Microvette Lithium-heparin vacutainers (Sarstedt, Nümbrecht, Germany) and used to analyze lipid parameters. An additional blood sample was collected at sacrifice by cardiac puncture. Blood was immediately centrifuged at 11000 rpm at 4°C for 5 min and heparin plasma was

aliquoted and stored at -80°C until assayed. Triglycerides, HDL-C and total cholesterol levels were analysed via UniCel® DxC 800 Synchron® Clinical System according to manufacturer's instructions, measured in mg/dL. Non-esterified fatty acids (HR Series NEFA –HR, Wako, Virginia, USA) and beta-hydroxybutyrate (Randox D-3-Hydroxybutyrate, Randoy Laboratories Ltd., Crumlin, County Antrim, United Kingdom) were analysed in blood samples collected at sacrifice using a Cobas Mira Roche-Autoanalyzer (F. Hoffmann-La Roche Ltd., Basel, Switzerland), according to the manufacturer's instructions. CETP activity was measured in plasma collected at sacrifice with CETP activity assay (CETP activity assay kit, MAK106, Merck KGaA, Darmstadt, Germany) according to manufacturer's instructions.

Bile acids profile in plasma and feces

Samples were analysed by the Department of Laboratory Medicine, University of Groningen, using 25 µL of plasma and 50 mg of feces. For plasma samples, to each sample, 250 µL internal standard solution (0.1 µM D4-CA and DA-CDCA, 0.2 µM DA-TCA, DA-TCDCA, DA-GCA, D6-TDCA, D4-TUDCA, D4-Tβ-MCA and D4-GCDCA) was added and vortexed. Samples were then centrifuged at 11000 rpm and the supernatant transferred into a clean glass tube. The liquid phase was then evaporated under nitrogen at 40°C. Before measuring, samples were reconstituted in 200 µL 1:1 methanol:H_2O (v/v), vortexed for 60 sec and centrifuged for 3 min at 4000 rpm. The supernatant was transferred into a 0.2 µm spin-filter and centrifuged at 4200 rpm for 10 min. After filtering, the samples were analyzed (10 µL injection volume) by Nexera X2 Ultra High Performance Liquid Chromatography system (SHIMADZU, Kyoto, Japan), coupled to a SCIEX QTRAP 4500 MD triple quadrupole mass spectrometer (SCIEX, Framingham, MA, USA) (UHPLC-MS/MS) [22].

For feces samples, bile acid composition was determined by capillary gas chromatography on a Hewlett-Packard gas chromatograph (HP 6890) equipped with a FID and a CP Sil 19 capillary column; length 25 m, internal diameter 250 µm and a film thickness of 0.2 µm (Chrompack BV, Middelburg, The Netherlands). Bile acids were methylated with a mixture of

methanol and acetyl chloride and trimethylsilylated with a mixture of piridyne, N,O-Bis (trimethylsilyl) trifluoroacetamide and trimethylchlorosilane. Neutral sterols were trimethylsilylated with a mixture of piridyne, N,O-Bis (trimethylsilyl) trifluoroacetamide and trimethylchlorosilane and measured on the same gas chromatograph equipped with the same column.

Data Analysis and Statistics

All data are expressed as mean ± standard error of the mean. Student's T-test, 2 way-ANOVA followed by Tukey or Sidak post-hoc tests were used for comparison among the groups (NR mice vs R mice), as appropriate. For all statistical analysis, a p-value lower than 0.05 was considered significant. Data were analyzed using Prism GraphPad 8.0.

RESULTS

Body weight, food intake, indirect calorimetry and body composition in R and NR mice

Upon arrival in our facility on chow diet, R mice and NR mice did not show any differences in body weight. R mice gained significantly more body weight (initial body weight 31.2 ± 0.6 g and final body weight 49.7 ± 1.1 g) compared to NR mice (initial body weight 29.0 ± 0.4 g and final body weight 39.0 ± 0.9 g) after 16 weeks of HFHC diet feeding (Fig 1A). The difference in body weight was significant from the 2nd week of HFHC diet feeding.

Body composition analysis showed no significant difference in lean mass (Fig 1F) and total fat mass between R mice and NR mice; nevertheless, NR mice had a tendency for decreased subcutaneous and significantly less intra-abdominal fat compared to R mice (Fig 1G).

Ad libitum food intake over 24h (Fig 1B), number of meals per day (Fig 1C) and parameters of energy metabolism (respiratory exchange ratio (Fig 1D) and energy expenditure (Fig 1E)) revealed no difference between the two groups.

Glucose and insulin tolerance in R mice and NR mice

Oral glucose tolerance tests (OGTT) were performed at several time-points in mice on chow diet and after 1, 2 and 3 months of HFHC feeding diet, respectively (Fig 2A-D). Already when chow fed, R mice and NR mice displayed differences in their glucose metabolism (Fig 2A). Fasting (baseline) glucose levels were higher in R mice (10.4 ± 0.3 mmol/L) compared to NR mice (8.5 ± 0.3 mmol/L) and, with the exception of the 15 min time-point, this trend continued during the entire OGTT (Fig 2A). Although this difference at specific time-points, both groups were able to reach baseline values after 120 min of test, indicating similar glucose tolerance; even though AUC on chow diet of R mice was increased by 20% as compared to NR mice (Fig 2E), the difference did not reach significance.

The difference between R mice and NR mice became more pronounced when mice were HFHC diet fed. Notably, after 1 month of HFHC diet feeding, R mice became glucose intolerant with higher glucose levels as compared to NR mice during the entire OGTT (Fig 2B). This

effect was exacerbated after 2 and 3 months of HFHC diet feeding (Fig 2C-D). After 3 months of HFHC diet, NR mice also slightly increased their glucose levels probably due to aging and the consequences of HFHC diet feeding [31]. This was also reflected in the higher AUC (Fig 2E) compared to earlier time-points.

Insulin sensitivity tests (IST) were performed in different groups of mice at the same time-point as the OGTT (Fig 3A-D). R mice, as previously observed during the OGTT, displayed higher glucose level at times 0 and 15 compared to NR mice. Already on chow diet (Fig 3A), and after 1 month of HFHC diet feeding (Fig 3B), NR mice showed a better insulin sensitivity response compared to R mice (indicated by the higher AUC in NR mice; Fig 3E). Over time, the differences between the two groups decreased probably due to aging effect, without reaching significance in the AUC (Fig 3E). Thus, even though R mice display higher glucose values during the IST, which indicates reduced glucose tolerance, on HFHC diet, based on the AUC during the IST, their overall insulin sensitivity was similar to NR mice (Fig 3E).

Morphology and lipid profile in the liver of R mice and NR mice

There was no gross abnormality detected in livers of R mice euthanized at approximately 14-16 weeks of age and kept on the chow diet, whilst livers of NR mice under the same experimental conditions appeared firmer than normal and exhibited a rough granular surface with multiple minimal indentations. Livers of 20-34 weeks old R mice fed the HFHC diet for 2, 3 or 4 months, respectively, were mildly enlarged, with rounded borders, and exhibited a diffuse yellow-brown discoloration and a homogeneously smooth surface (Fig 4A). Age-matched NR mice receiving the HFHC diet presented small, firm livers, with an extremely irregular granular surface, along with rare (3/30 NR mice) multifocal nodular masses, 0.1-0.4 cm in diameter (Fig 4B).

In line with these macroscopic observations, there was a statistically significant decrease in mean absolute liver weights in 20-34 weeks old, HFHC diet fed NR mice when compared to R mice under the same experimental conditions (1.8 ± 0.2 vs 2.9 ± 0.3 g; $p < 0.01$) (Fig 4I).

The results of the histopathological analysis are presented in Table 2. Apart from the presence of variably sized, predominantly periportal cytoplasmic eosinophilic inclusions (up to 20 μm in diameter) within the hepatocytes, indicative of mutant Apo-E lipoprotein accumulation [32], no histological abnormality was observed in the liver of R mice (5/5) fed the chow diet (Fig 4C). In contrast, NR mice (5/5) exhibited a minimal inflammatory response, alongside a slightly increased severity of eosinophilic droplets (average severity 3.3 ± 0.3 in R mice vs 4.0 ± 0 in NR mice). Inflammation was characterized by scattered, predominantly periportal foci of lymphocytes, macrophages and neutrophils, associated with minimal bile duct proliferation (Fig 4D, Table 2).

After HFHC diet feeding, mice from both groups exhibited minimal to severe macro- and micro-vesicular lipidosis (Fig 4E-F, Table 2), which progressively increased in severity with time (Table 1S). Lipidosis was mainly microvesicular in R mice and occurred with a higher average severity (3.3 ± 0.2) compared to NR mice (1.8 ± 0.2), in which a macrovacuolar pattern was noted more often. Histomorphometrical analysis of lipid droplets in liver sections stained with ORO confirmed this result, with livers of R mice showing higher proportions of fat content vs total parenchyma (76.6%) compared to NR mice livers (53.1%) (Fig 4E-F inset). The higher grade of hepatic lipidosis correlated with increased triglycerides levels (1.5 ± 0.1 mg/dL/g vs 2.7 ± 0.1 mg/dL/g) and non-esterified fatty acids (45.5 ± 3.6 mmol/L/g vs 49.9 ± 5.1 mmol/L/g) in livers of R mice vs NR mice (Fig 4G-H).

Chronic inflammation occurred with higher incidence and severity in NR mice compared to R mice (Table 2, Fig 5A-L). In the latter, the inflammatory reaction consisted of scattered aggregates of lymphocytes and macrophages, clustering within or at the periphery of lipidotic areas, associated with minimal bile duct proliferation (Fig 5A and 5C-F). The liver of NR mice showed, instead, a prominent mixed inflammatory cell infiltration expanding and bridging portal areas, dominated by T and B cells and macrophages, along with fewer plasma cell and neutrophils (Fig 5B and 5G-I). Chronic inflammation was accompanied by minimal fibrosis and prominent bile duct hyperplasia (Fig 5B and 5G-J). A few (3/30) NR mice exhibited proliferative

preneoplastic lesions, such as eosinophilic and clear cell foci of hepatocellular alteration (1/30, Fig 5K) and hepatocellular adenomas (2/30, Fig 5L), which correlated with the nodular masses observed macroscopically. There was no evidence of hepatocellular proliferative lesions in R mice.

Cytoplasmic eosinophilic inclusions occurred with lower severity in mice fed with the HFHC diet, compared to mice given a chow diet. This might be due to aging or to the concurrent high degree of lipidosis, which somehow prevents the formation or detection of these structures. However, similarly to mice fed with the chow diet, eosinophilic inclusions were observed with increased severity in NR mice (2.0 ± 0.3) compared to R mice (0.8 ± 0.2).

Thus, we observed two distinct phenotypes under HFHC diet feeding conditions. R mice showed increased lipidosis (mainly microlipidosis) along with mild inflammation, while NR mice showed lower lipidosis levels (mainly macrolipidosis) but higher incidence and severity of chronic inflammation; in a few NR mice, we also found evidence of hepatocellular proliferative lesions.

Pancreas

To further understand the regulation of glucose metabolism in R mice versus NR mice, pancreas histological analysis was performed; no histological abnormalities were found in R mice and NR mice (data not shown). These results agree with our findings obtained following static glucose stimulation in isolated islets from R mice and NR mice. In fact, static high glucose stimulation (13.7 mM) induced a similar increase in insulin secretion in pancreatic islets isolated from R mice and NR mice (Fig 6).

Cytokines and Transaminase in circulating blood of R mice and NR mice

Plasma cytokines concentrations were similar between R mice and NR mice at time of sacrifice, i.e. after 3 months of HFHC feeding (Fig 7).

However, increased levels of alanine transaminase (ALT) were observed in NR mice after 3 months of HFHC diet compared to chow conditions and compared to R mice at the same time-point (Fig 4J). This confirms liver damage as shown from histology of NR mice.

Lipid metabolism in R mice and NR mice

At the age of 6-7 weeks old, at TNO mice were tested for total cholesterol and triglycerides plasma levels to discriminate between R mice and NR mice. As expected, R mice displayed higher plasma cholesterol (2.9 ± 0.1 mmol/L; i.e.113.2 ± 3.8 mg/dL) compared to NR mice (1.7 ± 0.0 mmol/L; i.e. 68.4 ± 1.9 mg/dL) (Fig 8A).

Plasma total cholesterol was measured again upon arrival at our facility on chow diet, and after 1, 2 and 3 months of HFHC diet. Particularly during the first 2 months on HFHC diet, R mice had significantly increased plasma total cholesterol whereas cholesterol levels in NR mice remained similar to the chow-feeding period (Fig 8B). However, after 3 months of HFHC diet, NR mice showed significantly higher values (81.6 ± 3.8 mg/dL) in total cholesterol compared to chow (34.4 ± 2.9 mg/dL) (Fig 8B).

Triglycerides plasma levels were higher in R mice (3.9 ± 0.2 mmol/L; i.e. 341.5 ± 13.7 mg/dL) vs NR mice (0.9 ± 0.0 mmol/L; i.e. 79.4 ± 2.4 mg/mL) at the age of 6-7 weeks old, when measured at TNO (Fig 8C). Similar to total cholesterol, HFHC diet feeding resulted in significantly higher triglycerides concentrations in R mice than in NR mice (Fig 8D). R mice fed the HFHC diet showed uniformly high HDL-cholesterol (HDL-C) level, regardless of the duration of HFHC feeding (Fig 8F).

Free fatty acids ($P<0.05$, Fig 8G) were also significantly increased after 3 months of HFHC diet. No difference was noticed in beta-hydroxybutyrate levels between NR mice and R mice (Fig 8H).

At time of sacrifice, CETP activity, the enzyme that facilitates the transport of cholesterol ester and triglycerides between lipoproteins, was slightly higher in NR mice compared to R mice

(4704 ± 324 pmol transferred vs 3488 ± 537 pmol transferred), but the difference was not significant (Fig 8E).

Together, these results demonstrate that the lipid profile in R mice is markedly altered compared to NR mice kept under a HFHC diet feeding regimen.

Bile acid profile in plasma and feces

Plasma levels of bile acids were investigated at time of sacrifice (Fig 9). Overall, R mice showed decreased total bile concentrations; particularly, among free bile acids, cholic acid (CA), deoxycholic acid (DCA), and β-muricholic acid (β-MCA) compared to NR mice (Fig 9). All taurine-conjugated bile acids were also lower in NR mice compared to R mice (Fig 9). Fecal coprostanol excretion was higher in R mice compared to NR mice (Fig 10A). No other differences were found in excreted bile acids between R mice and NR mice (Fig10 B-J).

Discussion

This study aimed to characterize the long-term effect of a 60% kcal fat diet supplemented with 0.25% cholesterol (HFHC) diet on various parameters linked to glucose and lipid metabolism in ApoE3L.CETP mice, a humanized mouse model for the metabolic syndrome (Speliotes, #1157) [20]. The mutation ApoE3Leiden [18, 19] and the human transgene CETP gene [19] enable these mice' lipid metabolism and profile to be more similar to humans, hence they are one of the best animal models available to assess alterations in lipid metabolism in response to HFHC diet [19, 20].

ApoE3L.CETP mice exhibit a dyslipidemic phenotype combined with obesity, insulin resistance and atherosclerosis when administered HFHC diet [33-36]. Interestingly, some degree of phenotypic heterogeneity has been reported among age-matched individuals kept under similar experimental conditions [22]. Mice that do not fully display the expected phenotype, i.e., increased body weight and increased triglycerides and total cholesterol levels after HFHC diet exposure, are classified as non-responders (NR) and represent approximately 20% of the total ApoE3L.CETP mice population at TNO (TNO innovation for life, Leiden, The Netherlands; personal communication), the facility that established this mouse model and supplied them for this current study. In fact, NR mice and R mice can already be differentiated at young age when chow fed, based on their prevailing triglyceride and cholesterol plasma levels.

To our knowledge, the reasons for these phenotypic differences between R mice and NR mice have never been addressed in detail and it is not clear why APOE3L.CETP mice sharing the same genetic background exhibit heterogeneous responses to HFHC diet. We therefore believe that deciphering the metabolic differences found between R mice and NR mice is important. In addition, in some previous published studies, it is not explicitly mentioned whether NR mice were included [20, 22, 37]. This warrants overall caution when evaluating

heterogeneous metabolic profiles and responses in ApoE3L.CETP mice that might be related to the dimorphic phenotype of R mice and NR mice [22].

To assess the heterogeneity of the ApoE3L.CETP mice responses and to test the suitability of these mice to study the MetS [22], we investigated in detail body weight gain, feeding behavior, glucose metabolism, lipid profile, liver histology and inflammation markers over time in several cohorts of mice, and compared mice that were classified as young animals as R mice to mice that were classified as NR mice.

In line with what has been previously observed [22], our results confirmed a sharp distinction between R mice and NR mice responses to a HFHC diet. Mice originally classified as R mice were more prone to display the features of the MetS, and exhibited increased body weight, increased subcutaneous and intra-abdominal adipose tissues, increased plasma total cholesterol, triglycerides and HDL-C [19, 20, 22, 37], and reduced glucose sensitivity [38, 39] compared to NR mice.

In line with lipid metabolism parameters, histological analysis showed that hepatocellular lipidosis in R mice administered HFHC diet for 2, 3 or 4 months occurred with a high severity progressing over time (average severity: 3.3 ± 0.2, corresponding to 76.6% lipid content in the ORO stained liver sections), whilst NR mice exhibited reduced levels of lipidosis (average severity: 1.8 ± 0.2, corresponding to 53.1% lipid content in the ORO stained liver sections). Surprisingly, however, NR mice showed prominent hepatic inflammatory and proliferative changes, characterized by severe diffuse chronic lymphohistiocytic infiltration, bile duct proliferation, occasional foci of hepatocellular alteration, and hepatic adenomas. R mice, in contrast, exhibited only minimal inflammation and bile duct proliferation, in the absence of preneoplastic or neoplastic lesions. On an individual basis, there was a clear inverse correlation between the severity of chronic inflammation, and hepatocellular lipidosis, with mice that had high inflammatory scores showing low accumulation of hepatic lipids and decreased body weights, and vice-versa. This indicates that the hepatic pathology seen in NR mice may have a detrimental effect on hepatic function, as indicated by decreased lipid

accumulation - which we interpret as an inability to properly metabolize fat - and increased levels of ALT.

Differences in liver histology between R mice and NR mice were prominent following 2-4 months of HFHC diet feeding, however minimal inflammatory changes were already observed in NR mice at an earlier age (12-16 weeks) while kept on chow diet. Age-matched R mice kept under the same experimental conditions had no histological abnormality in the liver.

High body weight, high cholesterol and triglycerides levels and a liver histology dominated by lipidosis accompanied by minimal inflammatory changes are therefore the salient features of a responsive R phenotype. Based on this definition, separation between R mice and NR mice at an early stage based on triglycerides levels (<2mmol/L, i.e., 177 mg/mL) seems to be generally predictive of the final phenotype. However, we noted a certain degree of heterogeneity also within NR and R mice, respectively, leading to a partial overlap between the two groups. There were indeed a few mice within each cohort that did not show the predicted phenotype. 2/32 R mice (6.2%) were considered as outliers, i.e. mice originally classified as responders which exhibited low body weight (28.3 g and 35 g), low lipidosis (mainly macrolipidosis: scored 2 or 3) and high levels of chronic inflammation (scored 4). In the NR cohort, 3/30 mice (10%) exhibited parameters consistent with a responder mouse, with higher body weight gain (40, 49 and 51 g), high lipidosis (mainly microlipidosis: scored 4) and low levels of chronic inflammation (scored 0 or 1).

We suggest, therefore, that the introduction of other parameters such as liver histology might be helpful for the final classification of mice. It is important to note that a heterogeneity in the response to HFHC diet is also observed in humans with dysregulated metabolism, and it had to be taken in to account when transferring knowledge from an animal model to humans [20, 40].

In our study, we maintained the arbitrary classification carried out based only on cholesterol and triglycerides, given that the pathophysiological mechanisms underlying the NR phenotype are unknown and might have a multifactorial origin. Lack of the expected response might be

related to the C57BL/6J strain background, as it has been previously shown by Burcelin et al [41] and Hull et al [42]. In these studies, it was reported that C57BL/6J mice do not respond uniformly to HFHC diet feeding. Indeed, some mice gained weight, developed obesity and glucose intolerance, while some others did not [38, 39, 43-45]. The reason for this different response usually remain unclear.

We originally hypothesized that the difference between R mice and NR mice might be due to different copy numbers of the CETP transgene or to altered transgene expression. While we did not directly measure copy numbers of the CETP transgene in NR mice and R mice, this seems to be unlikely based on our results, as the measured CETP activity did not differ between NR mice and R mice.

It has been previously reported that APOE3Leiden gene overexpressing strains exhibit typical round cytoplasmic eosinophilic droplets, predominantly in the periportal hepatocytes [32]. These characteristic inclusions are consistent with aggregates of ApoE3Leiden, however the mechanisms which lead to their accumulation are still poorly understood. We noted that NR mice fed with a chow diet had higher numbers of cytoplasmic inclusions compared to R mice. This difference appeared more evident following HFHC diet feeding. A possible explanation might be that excessive accumulation of ApoE3Leiden protein elicits some form of damage, followed by an inflammatory response; however considerably more work will need to be done to elucidate a possible link between the presence of ApoE3Leiden and a NR phenotype.

Chronic-active inflammation, associated with cholangitis, biliary hyperplasia and proliferative hepatocellular lesions has been described in the liver of mice following chronic infection by *Helicobacter hepaticus* [28, 46]. Whilst most animals that carry *Helicobacter spp*. are asymptomatic, susceptible strains and individual mice might manifest clinical signs and lesions and we questioned whether the NR mouse phenotype could be simply the expression of an environmental infection in a proportion of more susceptible mice. FELASA-accredited health

check analyses that were conducted at the originating facility, as well as at our premises, revealed that the cohorts of mice employed in the current study did not carry pathogenic etiologic agents. There was no evidence of bacterial organisms in the livers of selected NR mice subjected to a silver stain for the detection of argyrophilic bacteria such as *Helicobacter spp*. Absence of Helicobacter was further confirmed by a qPCR analysis conducted on a pooled liver specimen obtained from R mice and NR mice.

Since R mice and NR mice did not show any differences in daily food intake or in their feeding behavior, the fact that NR mice did not increase their body weight as much as R mice cannot be explained by a diet-related aspect or a decrease in food intake. Interestingly, energy expenditure also did not differ between R and NR mice but we did not quantify total caloric loss via the feces as a possible mechanism.

Moreover, glucose metabolism was different between R mice and NR mice, and the difference was more prominent on HFHC diet feeding condition. Particularly, when HFHC diet fed, R mice showed increased basal blood glucose compared to NR mice suggesting that HFHC diet alters the basal glucose metabolism in R mice, and to a lesser extent in NR mice; this is in line with previously published studies [47]. We noticed a tendency toward glucose intolerance in R mice similarly to what reported in previous studies conducted with C57BL/6J that also show an increase in basal blood glucose values after HFHC diet [38, 44, 45, 48, 49]. Even though NR mice showed better glucose tolerance and insulin sensitivity during OGTT and IST, their basal values also slightly increased over time as a potential consequence of HFHC diet and aging [50].

We did not find major histological abnormalities in the pancreas of R mice that might explain the difference in glucose tolerance. Moreover, insulin secretion after glucose stimulation in islets isolated from R mice and NR mice did not show any differences. This indicates that insulin sensitivity rather than insulin secretion may be more critical for the different glucose

tolerance observed in R mice compared to NR mice. We did not perform a hyperinsulinemic euglycemic clamp to investigate the animals' insulin sensitivity in detail.

Studies in humans [51] and animal models showed the increasing importance of bile acids in modulating body glucose, lipid metabolism and body weight [52]. Our findings are contrary from previous data employing the same mouse model [22]: surprisingly our results show decreased levels of most of the circulating bile acids (CA, DCA, TDCA, TCDCA, TUDCA, TA/TB-MCA) in R mice compared to NR mice. We hypothesized that these differences in bile acids between R mice and NR mice are due to a dysregulation of bile acids metabolism: in fact, because of the severe liver pathology affecting NR mice, NR mice might be unable to reabsorb and recycle bile acids via hepatic portal vein circulation, hence bile acids might tend to accumulate in the systemic circulation, potentially explaining higher bile acids values in NR mice compared to R mice [53].

Indeed, some studies using another mouse model had shown how increased levels of MCA, as seen in our NR mice, might protect against body weight gain, steatosis, hypercholesterolemia and insulin resistance [54]. Higher CA levels in NR coupled with lower hepatic TG levels confirmed also previous data [55]. Furthermore, different metabolism of bile acids by gut microbiota may also explain why R mice and NR mice might show differences in their bile acids profile [56] but this was not formally tested in our studies.

Another aspect to take into consideration is that obesity is often accompanied by an increase in the inflammatory status in mice [44] and humans [57-59]. Our data indicate that circulating cytokines did not differ between R mice and NR mice; hence, the inflammation observed in livers of NR mice appears to be organ specific rather than a systemic feature of NR mice compared to R mice [44].

In summary, our findings suggest that in the heterogeneity previously described for the ApoE3L.CETP mice, two different and distinct phenotypes need to be considered: R mice and

NR mice. Particularly, R mice showed the expected phenotype after HFHC diet feeding, confirming its use as a good mouse model to describe the MetS especially in relation to lipid metabolism.

With respect to the liver histological finding, the histological features recapitulate those seen in NAFLD and likely shares the same pathophysiological mechanisms seen in R mice. As shown by Lau et al [60] several mice models were used to investigate NAFLD as C57BL/6, *db/db* and *ob/ob* mice. Nevertheless, we would rather consider the use of C57BL/6 mice as more accurate model for NAFLD [61, 62], since ApoE3L.CETP mice showed other liver histological features (i.e. minimal bile duct proliferation) that can create confounding factors. On the other hand, NR mice do not show the expected phenotype after HFHC diet feeding, investigations into liver morphology and function indicated that NR mice rather than the R mice might suffer from a severely disturbed liver metabolism. The fact that NR mice do not "respond" to the HFHC diet may therefore indicate that these animals may not be protected from the development of diet-induced obesity (and its consequences) in the classical sense, but that the NR mice may in fact be unable to respond adequately to the HFHC diet because of compromised liver function. For this reason, the liver pathology in NR mice would rather be classified as nonalcoholic steatohepatitis (Smolen, #235), i.e. a more aggressive phenotype of NAFLD [63].

We therefore suggest using NR mice with caution; it may be safer to use only R mice in experimental settings and to compare them to appropriate controls within the R cohorts, rather than taking NR mice as control groups. It may also be advised to reclassify the mice based on the *post mortem* examination and clinical chemistry analysis, to confirm their R mice phenotype based on liver histology and function, respectively.

Acknowledgments

We acknowledge Arnold von Eckardstein and Thorsten Hornemann from the Institute of Clinical Chemistry of the University of Zurich for their fruitful and expert discussions. We also thank RESOLVE EU-FP7 for generous funding and the Center for Clinical Studies (Vetsuisse Faculty) for kindly letting us use their equipment. We also thank Christelle le Foll for a critical revision of the manuscript.

Funding Sources

This work was supported in part by the European Union (RESOLVE, FP7-HEALTH 305707; TAL) and by the University of Zürich Forschungskredit (ET).

Table 1: Experimental design

Mice experimental design																								
		TNO facility	Zürich facility																					
			adaptation																					
			chow diet		high fat high cholesterol diet																			
	weeks		-1	0	1	2	3	4	5	6	7	8	9	10	11	12	13	14	15	16	17	18	19	20
	mice age	6-7 wks	7-19 wks																					
1st cohort mice	group 1	TC/TG			OGTT				OGTT				OGTT				OGTT							sacrifice/islets
	group 2	TC/TG			IST blood				IST blood				IST blood				IST blood							sacrifice/islets
			8-14 wks																					
2nd cohort mice	group 1	TC/TG			OGTT				OGTT				OGTT				OGTT					sacrifice/islets		
	group 2	TC/TG			IST blood				IST blood				IST blood				IST blood		sacrifice/islets					
	group 3	TC/TG								BioDAQ			TSE system			sacrifice/histology								

TC: total cholesterol
TG: triglycerides
NEFA: non-esterified fatty acids
BHB: betahydroxybutyrate
OGTT: oral glucose tolerance test
IST: insulin sensitivity test
HDL-C: high.density lipoprotein
ALT: alanine aminotransferase

blood: TC, TG, HDL-C time-point measurements
sacrifice terminal blood collection, NEFA, BHB, cytokines, ALT

Table 2. Liver scores for NAFLD

	Chow diet		HFHC diet	
	R	NR	R	NR
Age mice (weeks)	12-16	12-16	28-34	28-34
Liver[a]	5	5	32	30
Hepatocellular Lipidosis[b]	0/5	0/5	32/32	30/30
Grade 0	5	5	0	0
Grade 1	0	0	4	9
Grade 2	0	0	1	15
Grade 3	0	0	8	5
Grade 4	0	0	19	1
Average severity[c]	0 ± 0	0 ± 0	3.3 ± 0.2	1.7 ± 0.2***
Chronic Inflammation[b]	0/5	5/5	14/32	28/30
Grade 0	5	0	18	2
Grade 1	0	5	13	0
Grade 2	0	0	1	3
Grade 3	0	0	0	12
Grade 4	0	0	0	13
Average severity[c]	0 ± 0	1± 0	0.5 ± 0.1	3.2 ± 0.4***
Hepatocellular Eosinophilic Cytoplasmic Inclusions[b]	5/5	5/5	19/32	28/30
Grade 0	0	0	13	2
Grade 1	0	0	12	5
Grade 2	1	0	7	14
Grade 3	3	0	0	9
Grade 4	1	5	0	0
Average severity[c]	3 ± 0.3	4 ± 0	0.8 ± 0.2	2.0 ± 0.3
Isolated Foci[b]	0/5	0/5	0/32	1/30
Adenomas[b]	0/5	0/5	0/32	2/30

[a]: number of liver samples analysed, [b]: incidence of the findings, [c]: Average severity calculated as sum of all the scores given divided by the total number of liver samples analysed
***: p<0.001, NR v R, resp., Unpaired Student's T test

Figures legend

Fig 1: (A) Body weight over a 16-weeks period on HFHC diet in responders (R mice, n=51) and non-responders (NR mice, n=52) ApoE3L.CETP male mice; R mice increased body weight more compared to NR mice with HFHC diet feeding. (B) average 24h food intake and (C) average number of meal bouts in 24h after 8 weeks on HFHC diet in R mice (n=8) and NR mice (n=8); mice displayed no differences between the two groups. (D) Respiratory Exchange Ratio and (E) Energy Expenditure in R mice (n=8) and NR mice (n= 8) mice after 10 weeks on HFHC diet; no significant differences were found. (F) Lean and fat mass did not differ between R mice (n=7) and NR mice (n=7). (G) Subcutaneous and intra-abdominal fat mass revealed increased intra-abdominal fat mass in R mice. Data are represented as mean ± SEM. *, *** P< 0.05 or 0.001, resp., NR vs. R, after post hoc Sidak adjustment significant intergroup differences were found by 2-way ANOVA multiple comparison (A, D, E) or unpaired Student's T test, (B, C, F, G).

Fig 2: Oral glucose tolerance test was performed in responder mice (R mice = 28) and non-responders (NR mice =28) mice on chow (A), and after 1 (B), 2 (C) and 3 (D) months of HFHC diet. R mice from 1 month of HFHC diet displayed glucose intolerance compared to NR mice. (E) Area under the curve (AUC) over 120 min was calculated during the OGTT, above the lowest glucose value of each respective animal. Data represented as mean ± SEM., *, **, *** P < 0.05, 0.01, or 0.001 NR vs. R, resp., after unpaired Student's T test (Veitenhansl, #514) or after post hoc Sidak adjustment significant intergroup differences were found by 2-way ANOVA multiple comparison (E); different letters indicate significant differences.

Fig 3: Insulin sensitivity test was performed in responder mice (R mice = 19) and non-responder mice (NR mice = 15) on chow (A), and after 1 (B), 2 (C) and 3 (D) months of HFHC diet. At each time-point R mice displayed lower insulin sensitivity compared to NR mice. (E) Area under the curve (AUC) over 120 min was calculated during IST above the lowest glucose

value during the test. Data represented as mean ± SEM., *, **, *** P< 0.05, 0.01 or 0.001 NR vs. R, resp., after unpaired Student's T test (Veitenhansl, #514) or after post hoc Sidak adjustment significant intergroup differences were found by 2-way ANOVA multiple comparison (E). Different letters indicate significant differences.

Fig 4: (A and B) microphotographs of livers from R mouse (A) and NR mouse (B) after 3 months-HFHC diet. (A) R mouse liver show diffuse light brown discoloration, consistent with mild lipidosis. (B) NR mouse liver show multifocal well demarcated nodular masses (arrows; hepatocellular adenoma). (C and D) HE-stained liver sections from NR and R mice on a chow diet, scale bars = 100 µm: (C) Presence of eosinophilic cytoplasmic droplets (arrowheads), in a R mouse, (D) Minimal chronic inflammation (arrow) in a NR mouse. Eosinophilic droplets are increased in number compared to C. (E-F) HE-stained liver sections from mice on a HFHC diet, scale bars = 100 µm. Insets: Oil red O (ORO) stained liver sections from the same mice, scale bars = 20 µm: (E) R mouse: severe, predominantly microvesicular lipidosis (*). Inset: a high proportion of the hepatocyte cytoplasm contains ORO-positive lipid droplets. (F) NR mouse: mild, predominantly macrovesicular lipidosis (*). Inset: ORO-positive lipid content within the hepatocytes is decreased compared to E. (G) triglycerides levels extracted from livers from NR mice (n=10) and R mice (n=10) after sacrifice and (H) liver non-esterified fatty acids in NR mice (n=17) and R mice (n=15). (I) Absolute liver weight in R and NR mice on 2, 3 and 4 months ofHFHC diet. (J) Alanine transaminase (ALT) plasma levels in R mice (n=7) and NR mice (n=9) chow fed and after 3 months of HFHC diet. Data are represented as mean ± SEM. *, *** P<0.05 or 0.001, NR vs. R, resp., after unpaired Student's T test (G-H) or after post hoc Sidak adjustment significant intergroup differences were found by 2-way ANOVA multiple comparison (I and J); different letters indicate significant differences.

Fig 5: (A - B) HE-stained liver sections from mice fed HFHC diet, scale bars = 100 µm. (A) R mouse. Minimal chronic inflammation, characterized by scattered inflammatory cells (green

arrowhead) and negligible bile duct proliferation (arrow). Moderate numbers of eosinophilic cytoplasmic droplets (black arrowhead) are detected. (B) NR mouse. Marked chronic inflammatory reaction, with mononuclear cell infiltration (black arrowhead) and prominent bile duct proliferation (green arrowhead). Eosinophilic droplets (black arrowheads) are increased in number compared to R mouse. (Stemberger-Papic, #159;Veitenhansl, #514) Liver sections from a R mouse (Stemberger-Papic, #159) and a NR mouse (Veitenhansl, #514) on a HFHC diet, subjected to immunohistochemistry against the CD3 (T lymphocytes, C/G), CD45R/B220 (B lymphocytes, D/H), F4/80 (macrophages, E/I) and cytokeratin (biliary ductal epithelial cells, F/J) antigens, scale bars = 50 µm. Microphotographs are taken from the same area depicted in A or B, respectivey, (K and L) HE-stained liver sections from NR mice on a high fat high cholesterol (HFHC) diet. (K) Focus of cellular alteration (arrowheads), scale bar = 500 µm. Insets: Higher magnification of the lesion, scale bar = 50 µm. (L) Hepatocellular adenoma (arrowheads), scale bar = 1 mm.

Fig 6: Insulin secretion expressed as a percentage of total insulin content after glucose stimulated insulin secretion test (GSIS) in islets isolated from NR mice and R mice and cultured for 4 days. Data are represented as mean ± SEM. *, P< 0.05, resp., NR vs. R, after post hoc Tukey adjustment significant intergroup differences were found by 2-way ANOVA multiple comparison.

Fig 7: Plasma cytokines in plasma from non-responder (NR mice, n=7) and responder (R mice, n=9) mice at the time of sacrifice: (A) Interferon- γ, IFN-γ. (B) Interleukin 10, IL-10. (C) Interleukin 12p70, IL-12p70. (D) Interleukin 1β, IL-1β. (E) Interleukin 2, IL-2. (F) Interleukin 4, IL-4. (G) Interleukin 5, IL-5. (H) Interleukin 6, IL-6. (I) Keratinocyte chemoattractant/growth-regulated oncogene, KC-GRO and (J) tumour necrosis factor α, TNF-α. No difference between the two groups was found. Data are represented as mean ± SEM. *, P< 0.05, NR vs. R, resp after unpaired Student's T test.

Fig 8: Plasma lipid profile in non-responder (NR mice, n=11) and responder (R mice, n=13) mice at different time points. Total cholesterol (A, B) and triglycerides (C, D) at aged 6-7 weeks, analysis performed from TNO when discrimination between R mice and NR mice took place (A, C) and at time 0 (chow fed upon arrival in our facility), and after 1, 2 and 3 months of HFHC diet (B, D). (E) CETP activity at time of sacrifice in NR mice (n=10) and R mice (n=8); no difference was found. (F) HDL cholesterol (HDL-C) on chow diet upon arrival, and after 1, 2 and 3 months of HFHC. (G) non-esterified fatty acids (NEFA) were higher in R mice vs NR mice, and (H) and beta-hydroxybutyrate (BHB) in NR mice (n=10) and R mice (n=10). Data are represented as mean ± SEM. *, *** P< 0.05 or 0.001, resp., NR vs. R, after post hoc Tukey adjustment significant intergroup differences were found by 2-way ANOVA multiple comparison (B, D, F) or unpaired Student's T test, (A, C, E, G, H). Different letters indicate significant differences

Fig 9: Total plasma bile acids profile in non-responder (NR) and responder (R) mice at time of sacrifice. (A) Total bile acids, total BA (n=17, 20). (B) cholic acid, CA (n=14, 15). (C) chenodeoxycholic acid, CDCA (n=14, 10). (D) deoxycholic acid, DCA (n=17, 15). (E) α-muricholic acid, α -MCA (n=13, 6). (F) β-muricholic acid, β-MCA (n=15, 14). (G) tauro cholic acids, TCA levels (n=15, 15). (H) taurodeoxycholic acid, TDCA (n=17, 15). (I) taurocheno deoxycholic acid, TCDCA (n=16,10), (J) tauroursodeoxycholic acid, TUDCA (n=17, 20), (K) tauro-α-muricholic acid, Tα-MCA (n=16, 14) and (L) tauro-β-muricholic acid, Tβ-MCA (n=17, 12). Data are represented as mean ± SEM. *, **, *** P< 0.05, 0.01 or 0.001, resp., NR vs. R, using unpaired Student's T test.

Fig 10: Total coprostanol, cholesterol, dihydrocholesterol and bile acids profile in non-responder (NR) and responder (R) mice feces at time of sacrifice. (A) Coprostanol, Copr (n=5, 2). (B) cholesterol, Chol (n=6, 5). (C) dihydrocholestero,l diHyChol (n=5, 5). (D) cholic acid,

CA (n=6, 5). (E) allo cholic acid, alloCA (n=6, 5). (F) deoxy cholic acid, DCA (n=6, 5). (G) α-muricholic acid, α-MCA (n=6, 5). (H) β-muricholic acid, β-MCA (n= 6, 5). (I) ω-muricholic acid, ω-MCA (n= 6, 5). (J) total bile acids, total BA (n= 6, 5). Data are represented as mean ± SEM. ** P<0.01 NR vs. R, resp. using Unpaired Student's T test.

References

1. Friedrich MJ: **Global Obesity Epidemic Worsening**. *JAMA* 2017, **318**(7):603.
2. Pigeyre M, Yazdi FT, Kaur Y, Meyre D: **Recent progress in genetics, epigenetics and metagenomics unveils the pathophysiology of human obesity**. *Clin Sci (Lond)* 2016, **130**(12):943-986.
3. Yazdi FT, Clee SM, Meyre D: **Obesity genetics in mouse and human: back and forth, and back again**. *PeerJ* 2015, **3**:e856.
4. Poirier P, Cornier MA, Mazzone T, Stiles S, Cummings S, Klein S, McCullough PA, Ren Fielding C, Franklin BA, American Heart Association Obesity Committee of the Council on Nutrition PA *et al*: **Bariatric surgery and cardiovascular risk factors: a scientific statement from the American Heart Association**. *Circulation* 2011, **123**(15):1683-1701.
5. Wali JA, Thomas HE, Sutherland AP: **Linking obesity with type 2 diabetes: the role of T-bet**. *Diabetes Metab Syndr Obes* 2014, **7**:331-340.
6. Bays HE, Toth PP, Kris-Etherton PM, Abate N, Aronne LJ, Brown WV, Gonzalez-Campoy JM, Jones SR, Kumar R, La Forge R *et al*: **Obesity, adiposity, and dyslipidemia: a consensus statement from the National Lipid Association**. *J Clin Lipidol* 2013, **7**(4):304-383.
7. Bellentani S: **The epidemiology of non-alcoholic fatty liver disease**. *Liver Int* 2017, **37 Suppl 1**:81-84.
8. Kopelman PG: **Obesity as a medical problem**. *Nature* 2000, **404**(6778):635-643.
9. Grundy SM: **Metabolic syndrome pandemic**. *Arterioscler Thromb Vasc Biol* 2008, **28**(4):629-636.
10. Flier JS: **Obesity wars: molecular progress confronts an expanding epidemic**. *Cell* 2004, **116**(2):337-350.
11. Wang CY, Liao JK: **A mouse model of diet-induced obesity and insulin resistance**. *Methods Mol Biol* 2012, **821**:421-433.

12. Kobayashi K, Forte TM, Taniguchi S, Ishida BY, Oka K, Chan L: **The db/db mouse, a model for diabetic dyslipidemia: molecular characterization and effects of Western diet feeding**. *Metabolism* 2000, **49**(1):22-31.

13. Yokoi N, Hoshino M, Hidaka S, Yoshida E, Beppu M, Hoshikawa R, Sudo K, Kawada A, Takagi S, Seino S: **A Novel Rat Model of Type 2 Diabetes: The Zucker Fatty Diabetes Mellitus ZFDM Rat**. *J Diabetes Res* 2013, **2013**:103731.

14. Kapourchali FR, Surendiran G, Chen L, Uitz E, Bahadori B, Moghadasian MH: **Animal models of atherosclerosis**. *World J Clin Cases* 2014, **2**(5):126-132.

15. Hattori T, Murase T, Ohtake M, Inoue T, Tsukamoto H, Takatsu M, Kato Y, Hashimoto K, Murohara T, Nagata K: **Characterization of a new animal model of metabolic syndrome: the DahlS.Z-Lepr(fa)/Lepr(fa) rat**. *Nutr Diabetes* 2011, **1**:e1.

16. Noda K, Melhorn MI, Zandi S, Frimmel S, Tayyari F, Hisatomi T, Almulki L, Pronczuk A, Hayes KC, Hafezi-Moghadam A: **An animal model of spontaneous metabolic syndrome: Nile grass rat**. *FASEB J* 2010, **24**(7):2443-2453.

17. Peterson RG, Jackson CV, Zimmerman K, de Winter W, Huebert N, Hansen MK: **Characterization of the ZDSD Rat: A Translational Model for the Study of Metabolic Syndrome and Type 2 Diabetes**. *J Diabetes Res* 2015, **2015**:487816.

18. Havekes L, de Wit E, Leuven JG, Klasen E, Utermann G, Weber W, Beisiegel U: **Apolipoprotein E3-Leiden. A new variant of human apolipoprotein E associated with familial type III hyperlipoproteinemia**. *Hum Genet* 1986, **73**(2):157-163.

19. Westerterp M, van der Hoogt CC, de Haan W, Offerman EH, Dallinga-Thie GM, Jukema JW, Havekes LM, Rensen PC: **Cholesteryl ester transfer protein decreases high-density lipoprotein and severely aggravates atherosclerosis in APOE*3-Leiden mice**. *Arterioscler Thromb Vasc Biol* 2006, **26**(11):2552-2559.

20. van den Hoek AM, van der Hoorn JW, Maas AC, van den Hoogen RM, van Nieuwkoop A, Droog S, Offerman EH, Pieterman EJ, Havekes LM, Princen HM:

APOE*3Leiden.CETP transgenic mice as model for pharmaceutical treatment of the metabolic syndrome. *Diabetes Obes Metab* 2014, **16**(6):537-544.

21. van der Hoorn JW, de Haan W, Berbee JF, Havekes LM, Jukema JW, Rensen PC, Princen HM: **Niacin increases HDL by reducing hepatic expression and plasma levels of cholesteryl ester transfer protein in APOE*3Leiden.CETP mice**. *Arterioscler Thromb Vasc Biol* 2008, **28**(11):2016-2022.

22. Paalvast Y, Gerding A, Wang Y, Bloks VW, van Dijk TH, Havinga R, Willems van Dijk K, Rensen PCN, Bakker BM, Kuivenhoven JA *et al*: **Male apoE*3-Leiden.CETP mice on high-fat high-cholesterol diet exhibit a biphasic dyslipidemic response, mimicking the changes in plasma lipids observed through life in men**. *Physiol Rep* 2017, **5**(19).

23. Hillebrand JJ, Langhans W, Geary N: **Validation of computed tomographic estimates of intra-abdominal and subcutaneous adipose tissue in rats and mice**. *Obesity (Silver Spring)* 2010, **18**(4):848-853.

24. Villars FO, Pietra C, Giuliano C, Lutz TA, Riediger T: **Oral Treatment with the Ghrelin Receptor Agonist HM01 Attenuates Cachexia in Mice Bearing Colon-26 (C26) Tumors**. *Int J Mol Sci* 2017, **18**(5).

25. Stengel A, Goebel M, Wang L, Rivier J, Kobelt P, Monnikes H, Tache Y: **Activation of brain somatostatin 2 receptors stimulates feeding in mice: analysis of food intake microstructure**. *Physiol Behav* 2010, **101**(5):614-622.

26. Ruehl-Fehlert C, Kittel B, Morawietz G, Deslex P, Keenan C, Mahrt CR, Nolte T, Robinson M, Stuart BP, Deschl U *et al*: **Revised guides for organ sampling and trimming in rats and mice--part 1**. *Exp Toxicol Pathol* 2003, **55**(2-3):91-106.

27. Shackelford C, Long G, Wolf J, Okerberg C, Herbert R: **Qualitative and quantitative analysis of nonneoplastic lesions in toxicology studies**. *Toxicol Pathol* 2002, **30**(1):93-96.

28. Thoolen B, Maronpot RR, Harada T, Nyska A, Rousseaux C, Nolte T, Malarkey DE, Kaufmann W, Kuttler K, Deschl U *et al*: **Proliferative and nonproliferative lesions of the rat and mouse hepatobiliary system**. *Toxicol Pathol* 2010, **38**(7 Suppl):5S-81S.

29. Nordmann TM, Dror E, Schulze F, Traub S, Berishvili E, Barbieux C, Boni-Schnetzler M, Donath MY: **The Role of Inflammation in beta-cell Dedifferentiation**. *Sci Rep* 2017, **7**(1):6285.

30. Rutti S, Ehses JA, Sibler RA, Prazak R, Rohrer L, Georgopoulos S, Meier DT, Niclauss N, Berney T, Donath MY *et al*: **Low- and high-density lipoproteins modulate function, apoptosis, and proliferation of primary human and murine pancreatic beta-cells**. *Endocrinology* 2009, **150**(10):4521-4530.

31. Nunes-Souza V, Cesar-Gomes CJ, Da Fonseca LJ, Guedes Gda S, Smaniotto S, Rabelo LA: **Aging Increases Susceptibility to High Fat Diet-Induced Metabolic Syndrome in C57BL/6 Mice: Improvement in Glycemic and Lipid Profile after Antioxidant Therapy**. *Oxid Med Cell Longev* 2016, **2016**:1987960.

32. Mensenkamp AR, van Luyn MJ, van Goor H, Bloks V, Apostel F, Greeve J, Hofker MH, Jong MC, van Vlijmen BJ, Havekes LM *et al*: **Hepatic lipid accumulation, altered very low density lipoprotein formation and apolipoprotein E deposition in apolipoprotein E3-Leiden transgenic mice**. *J Hepatol* 2000, **33**(2):189-198.

33. Delsing DJ, Offerman EH, van Duyvenvoorde W, van Der Boom H, de Wit EC, Gijbels MJ, van Der Laarse A, Jukema JW, Havekes LM, Princen HM: **Acyl-CoA:cholesterol acyltransferase inhibitor avasimibe reduces atherosclerosis in addition to its cholesterol-lowering effect in ApoE*3-Leiden mice**. *Circulation* 2001, **103**(13):1778-1786.

34. Kleemann R, Princen HM, Emeis JJ, Jukema JW, Fontijn RD, Horrevoets AJ, Kooistra T, Havekes LM: **Rosuvastatin reduces atherosclerosis development beyond and independent of its plasma cholesterol-lowering effect in APOE*3-**

Leiden transgenic mice: evidence for antiinflammatory effects of rosuvastatin. *Circulation* 2003, **108**(11):1368-1374.

35. Kooistra T, Verschuren L, de Vries-van der Weij J, Koenig W, Toet K, Princen HM, Kleemann R: **Fenofibrate reduces atherogenesis in ApoE*3Leiden mice: evidence for multiple antiatherogenic effects besides lowering plasma cholesterol**. *Arterioscler Thromb Vasc Biol* 2006, **26**(10):2322-2330.

36. van der Hoorn JW, Kleemann R, Havekes LM, Kooistra T, Princen HM, Jukema JW: **Olmesartan and pravastatin additively reduce development of atherosclerosis in APOE*3Leiden transgenic mice**. *J Hypertens* 2007, **25**(12):2454-2462.

37. Gierman LM, Kuhnast S, Koudijs A, Pieterman EJ, Kloppenburg M, van Osch GJ, Stojanovic-Susulic V, Huizinga TW, Princen HM, Zuurmond AM: **Osteoarthritis development is induced by increased dietary cholesterol and can be inhibited by atorvastatin in APOE*3Leiden.CETP mice--a translational model for atherosclerosis**. *Ann Rheum Dis* 2014, **73**(5):921-927.

38. Montgomery MK, Hallahan NL, Brown SH, Liu M, Mitchell TW, Cooney GJ, Turner N: **Mouse strain-dependent variation in obesity and glucose homeostasis in response to high-fat feeding**. *Diabetologia* 2013, **56**(5):1129-1139.

39. Yang Y, Smith DL, Jr., Keating KD, Allison DB, Nagy TR: **Variations in body weight, food intake and body composition after long-term high-fat diet feeding in C57BL/6J mice**. *Obesity (Silver Spring)* 2014, **22**(10):2147-2155.

40. Limberg JK, Morgan BJ, Schrage WG: **Peripheral Blood Flow Regulation in Human Obesity and Metabolic Syndrome**. *Exerc Sport Sci Rev* 2016, **44**(3):116-122.

41. Burcelin R, Crivelli V, Dacosta A, Roy-Tirelli A, Thorens B: **Heterogeneous metabolic adaptation of C57BL/6J mice to high-fat diet**. *Am J Physiol Endocrinol Metab* 2002, **282**(4):E834-842.

42. Hull RL, Willard JR, Struck MD, Barrow BM, Brar GS, Andrikopoulos S, Zraika S: **High fat feeding unmasks variable insulin responses in male C57BL/6mouse substrains**. *J Endocrinol* 2017, **233**(1):53-64.

43. Williams LM, Campbell FM, Drew JE, Koch C, Hoggard N, Rees WD, Kamolrat T, Thi Ngo H, Steffensen IL, Gray SR *et al*: **The development of diet-induced obesity and glucose intolerance in C57BL/6 mice on a high-fat diet consists of distinct phases**. *PLoS One* 2014, **9**(8):e106159.

44. van der Heijden RA, Sheedfar F, Morrison MC, Hommelberg PP, Kor D, Kloosterhuis NJ, Gruben N, Youssef SA, de Bruin A, Hofker MH *et al*: **High-fat diet induced obesity primes inflammation in adipose tissue prior to liver in C57BL/6j mice**. *Aging (Albany NY)* 2015, **7**(4):256-268.

45. Surwit RS, Feinglos MN, Rodin J, Sutherland A, Petro AE, Opara EC, Kuhn CM, Rebuffe-Scrive M: **Differential effects of fat and sucrose on the development of obesity and diabetes in C57BL/6J and A/J mice**. *Metabolism* 1995, **44**(5):645-651.

46. Huang Y, Tian XF, Fan XG, Fu CY, Zhu C: **The pathological effect of Helicobacter pylori infection on liver tissues in mice**. *Clin Microbiol Infect* 2009, **15**(9):843-849.

47. Liang W, Verschuren L, Mulder P, van der Hoorn JW, Verheij J, van Dam AD, Boon MR, Princen HM, Havekes LM, Kleemann R *et al*: **Salsalate attenuates diet induced non-alcoholic steatohepatitis in mice by decreasing lipogenic and inflammatory processes**. *Br J Pharmacol* 2015, **172**(22):5293-5305.

48. Winzell MS, Ahren B: **The high-fat diet-fed mouse: a model for studying mechanisms and treatment of impaired glucose tolerance and type 2 diabetes**. *Diabetes* 2004, **53 Suppl 3**:S215-219.

49. Andrikopoulos S, Blair AR, Deluca N, Fam BC, Proietto J: **Evaluating the glucose tolerance test in mice**. *Am J Physiol Endocrinol Metab* 2008, **295**(6):E1323-1332.

50. Kleemann R, van Erk M, Verschuren L, van den Hoek AM, Koek M, Wielinga PY, Jie A, Pellis L, Bobeldijk-Pastorova I, Kelder T *et al*: **Time-resolved and tissue-specific**

systems analysis of the pathogenesis of insulin resistance. *PLoS One* 2010, **5**(1):e8817.

51. Prinz P, Hofmann T, Ahnis A, Elbelt U, Goebel-Stengel M, Klapp BF, Rose M, Stengel A: **Plasma bile acids show a positive correlation with body mass index and are negatively associated with cognitive restraint of eating in obese patients**. *Front Neurosci* 2015, **9**:199.

52. Ma H, Patti ME: **Bile acids, obesity, and the metabolic syndrome**. *Best Pract Res Clin Gastroenterol* 2014, **28**(4):573-583.

53. Chiang JYL: **Bile acid metabolism and signaling in liver disease and therapy**. *Liver Res* 2017, **1**(1):3-9.

54. Bonde Y, Eggertsen G, Rudling M: **Mice Abundant in Muricholic Bile Acids Show Resistance to Dietary Induced Steatosis, Weight Gain, and to Impaired Glucose Metabolism**. *PLoS One* 2016, **11**(1):e0147772.

55. Watanabe M, Houten SM, Wang L, Moschetta A, Mangelsdorf DJ, Heyman RA, Moore DD, Auwerx J: **Bile acids lower triglyceride levels via a pathway involving FXR, SHP, and SREBP-1c**. *J Clin Invest* 2004, **113**(10):1408-1418.

56. Sayin SI, Wahlstrom A, Felin J, Jantti S, Marschall HU, Bamberg K, Angelin B, Hyotylainen T, Oresic M, Backhed F: **Gut microbiota regulates bile acid metabolism by reducing the levels of tauro-beta-muricholic acid, a naturally occurring FXR antagonist**. *Cell Metab* 2013, **17**(2):225-235.

57. Hotamisligil GS: **Inflammation and metabolic disorders**. *Nature* 2006, **444**(7121):860-867.

58. Romeo GR, Lee J, Shoelson SE: **Metabolic syndrome, insulin resistance, and roles of inflammation--mechanisms and therapeutic targets**. *Arterioscler Thromb Vasc Biol* 2012, **32**(8):1771-1776.

59. Nehete P, Magden ER, Nehete B, Hanley PW, Abee CR: **Obesity related alterations in plasma cytokines and metabolic hormones in chimpanzees**. *IntJ Inflam* 2014, **2014**:856749.

60. Lau JK, Zhang X, Yu J: **Animal models of non-alcoholic fatty liver disease: current perspectives and recent advances**. *J Pathol* 2017, **241**(1):36-44.

61. Fengler VH, Macheiner T, Kessler SM, Czepukojc B, Gemperlein K, Muller R, Kiemer AK, Magnes C, Haybaeck J, Lackner C *et al*: **Susceptibility of Different Mouse Wild Type Strains to Develop Diet-Induced NAFLD/AFLD-Associated Liver Disease**. *PLoS One* 2016, **11**(5):e0155163.

62. Ryu JE, Jo W, Choi HJ, Jang S, Lee HJ, Woo DC, Kim JK, Kim KW, Yu ES, Son WC: **Evaluation of Nonalcoholic Fatty Liver Disease in C57BL/6J Mice by Using MRI and Histopathologic Analyses**. *Comp Med* 2015, **65**(5):409-415.

63. Oseini AM, Cole BK, Issa D, Feaver RE, Sanyal AJ: **Translating scientific discovery: the need for preclinical models of nonalcoholic steatohepatitis**. *Hepatol Int* 2018, **12**(1):6-16.

Figure 1

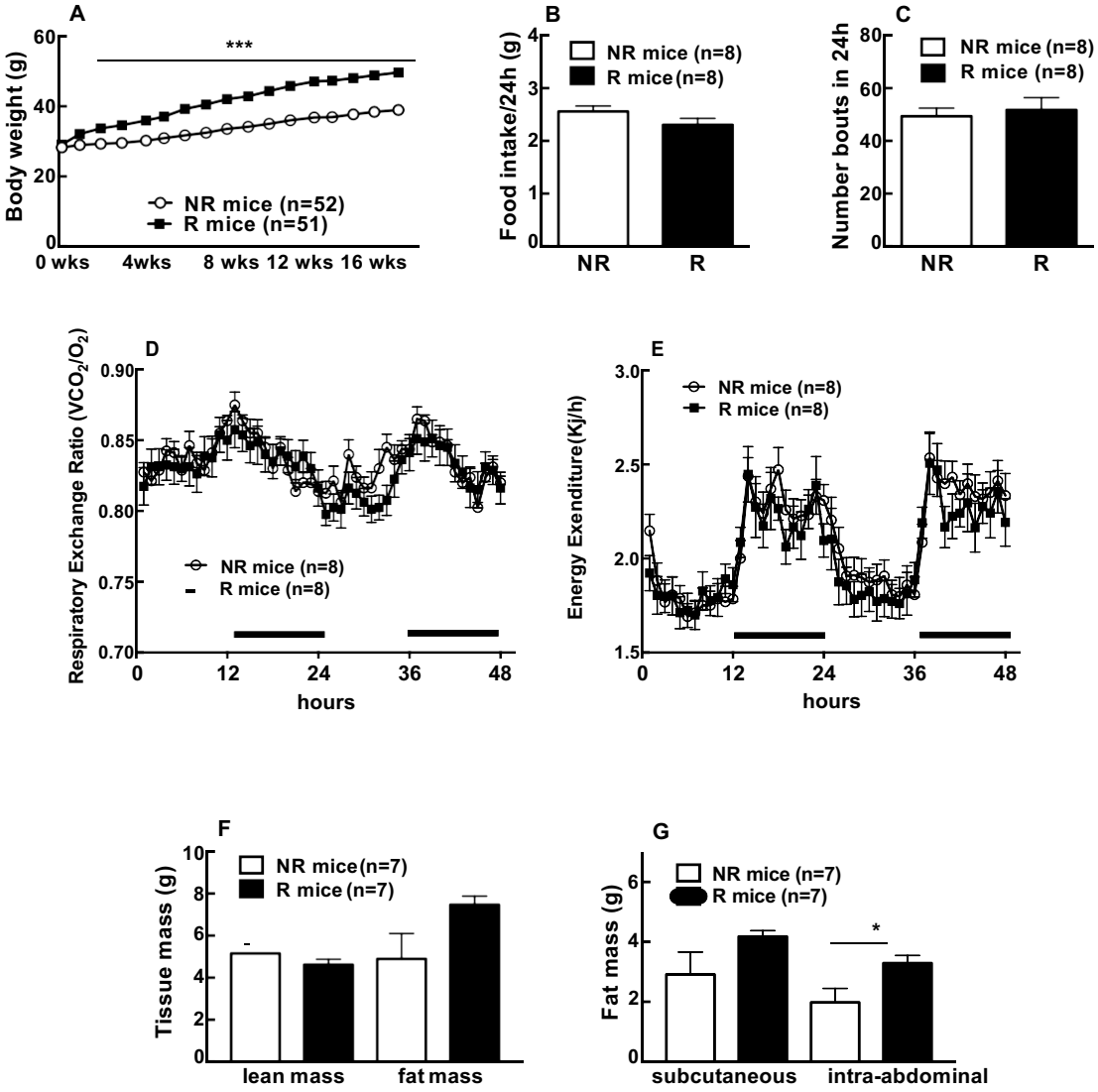
A
Body weight (g)
***
NR mice (n=52)
R mice (n=51)
0 wks
4wks
8 wks
12 wks
16 wks
B
Food intake/24h (g)
NR mice (n=8)
R mice (n=8)
NR
R
C
Number bouts in 24h
NR mice (n=8)
R mice (n=8)
NR
R
D
Respiratory Exchange Ratio (VCO2/O2)
NR mice (n=8)
R mice (n=8)
hours
E
Energy Exenditure(Kj/h)
NR mice (n=8)
R mice (n=8)
hours
F
Tissue mass (g)
NR mice(n=7)
R mice (n=7)
lean mass
fat mass
G
Fat mass (g)
NR mice (n=7)
R mice (n=7)
*
subcutaneous
intra-abdominal

Figure 2

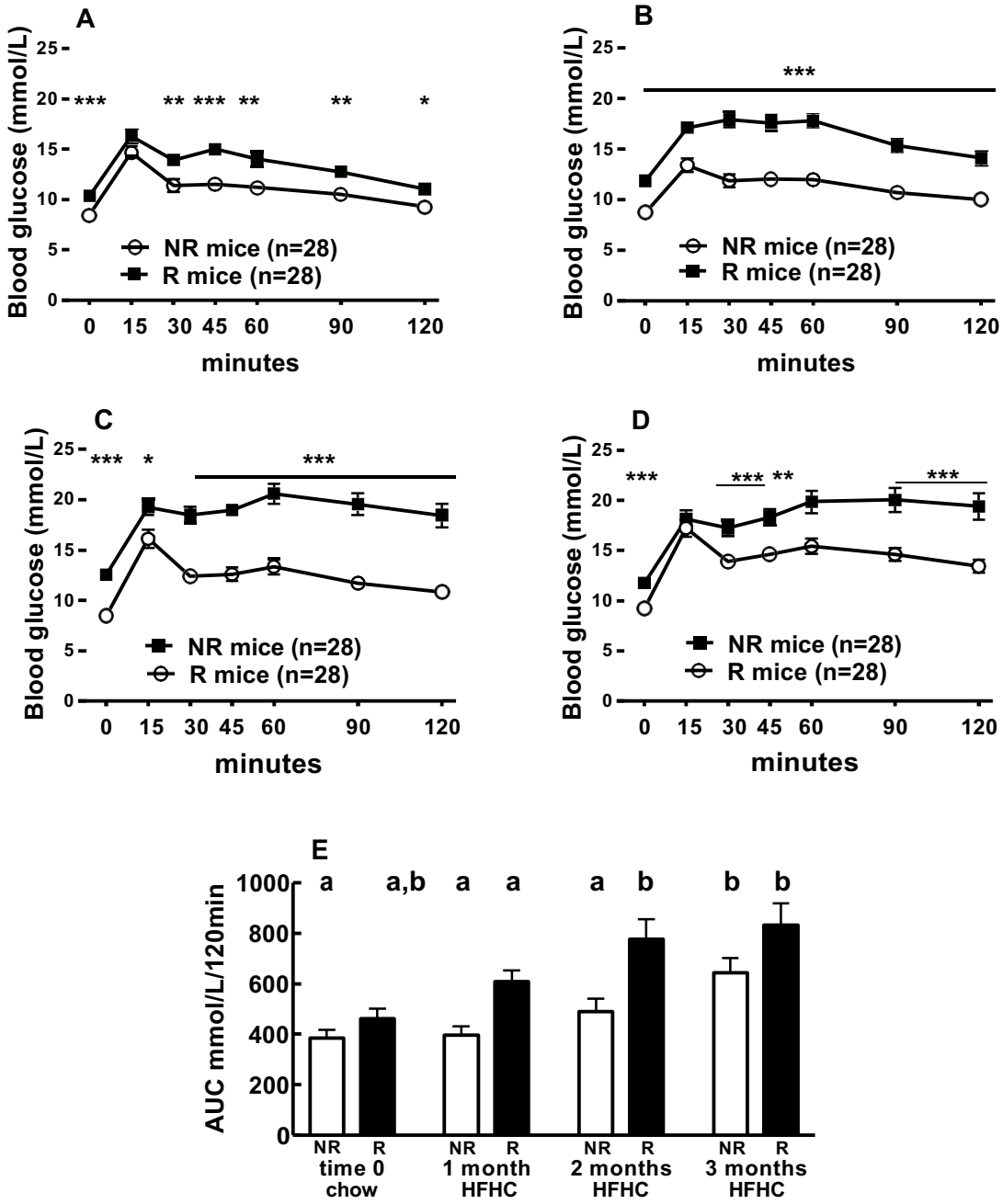
A
Blood glucose (mmol/L)
25
20
15
10
5
0
*** ** *** ** ** *
NR mice (n=28)
R mice (n=28)
0 15 30 45 60 90 120
minutes
B
Blood glucose (mmol/L)
***
NR mice (n=28)
R mice (n=28)
0 15 30 45 60 90 120
minutes
C
Blood glucose (mmol/L)
*** * ***
NR mice (n=28)
R mice (n=28)
0 15 30 45 60 90 120
minutes
D
Blood glucose (mmol/L)
*** *** ** ***
NR mice (n=28)
R mice (n=28)
0 15 30 45 60 90 120
minutes
E
AUC mmol/L/120min
1000
800
600
400
200
0
a a,b a a a b b b
NR R NR R NR R NR R
time 0 chow
1 month HFHC
2 months HFHC
3 months HFHC

Figure 3

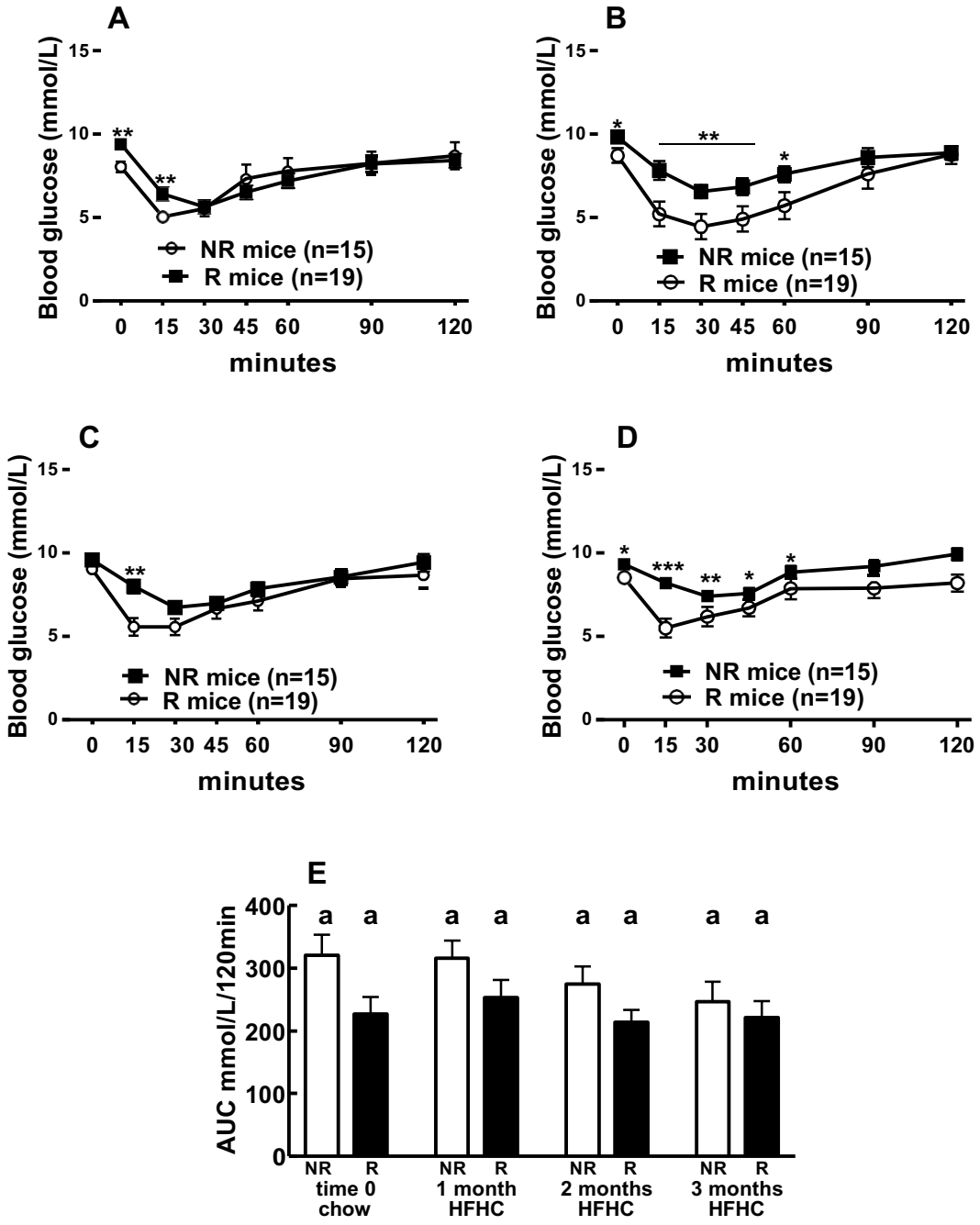
A
Blood glucose (mmol/L)
15
10
5
0
**
**
NR mice (n=15)
R mice (n=19)
0 15 30 45 60 90 120
minutes
B
Blood glucose (mmol/L)
*
**
*
NR mice (n=15)
R mice (n=19)
0 15 30 45 60 90 120
minutes
C
Blood glucose (mmol/L)
**
NR mice (n=15)
R mice (n=19)
0 15 30 45 60 90 120
minutes
D
Blood glucose (mmol/L)
*
***
**
*
*
NR mice (n=15)
R mice (n=19)
0 15 30 60 90 120
minutes
E
AUC mmol/L/120min
400
300
200
100
0
a a a a a a a a
NR R
time 0
chow
NR R
1 month
HFHC
NR R
2 months
HFHC
NR R
3 months
HFHC

Figure 4

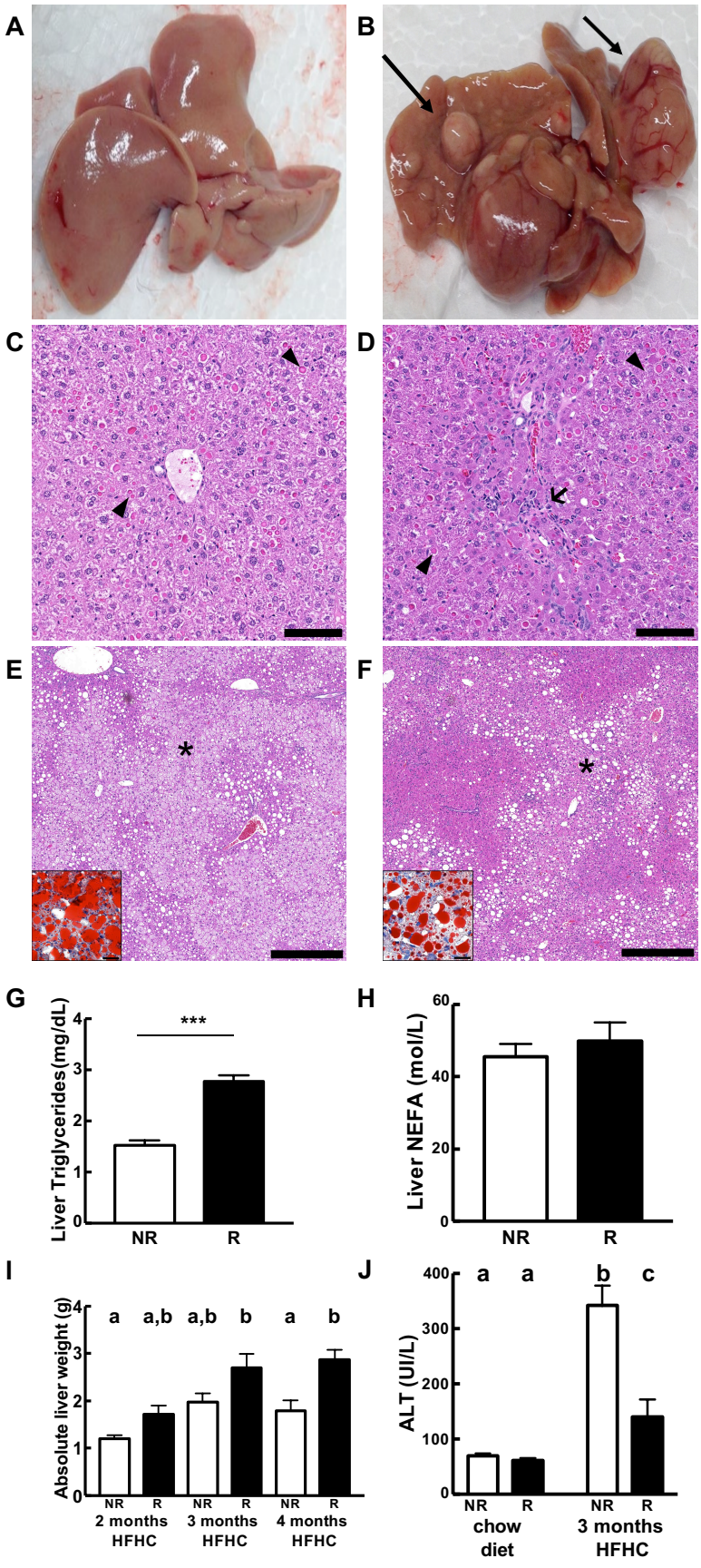
A
B
C
D
E
F
G
Liver Triglycerides (mg/dL)
***
NR
R
H
Liver NEFA (mol/L)
NR
R
I
Absolute liver weight (g)
a
a,b
a,b
b
a
b
NR
R
2 months HFHC
3 months HFHC
4 months HFHC
J
ALT (UI/L)
a
a
b
c
NR
R
chow diet
3 months HFHC

Figure 5

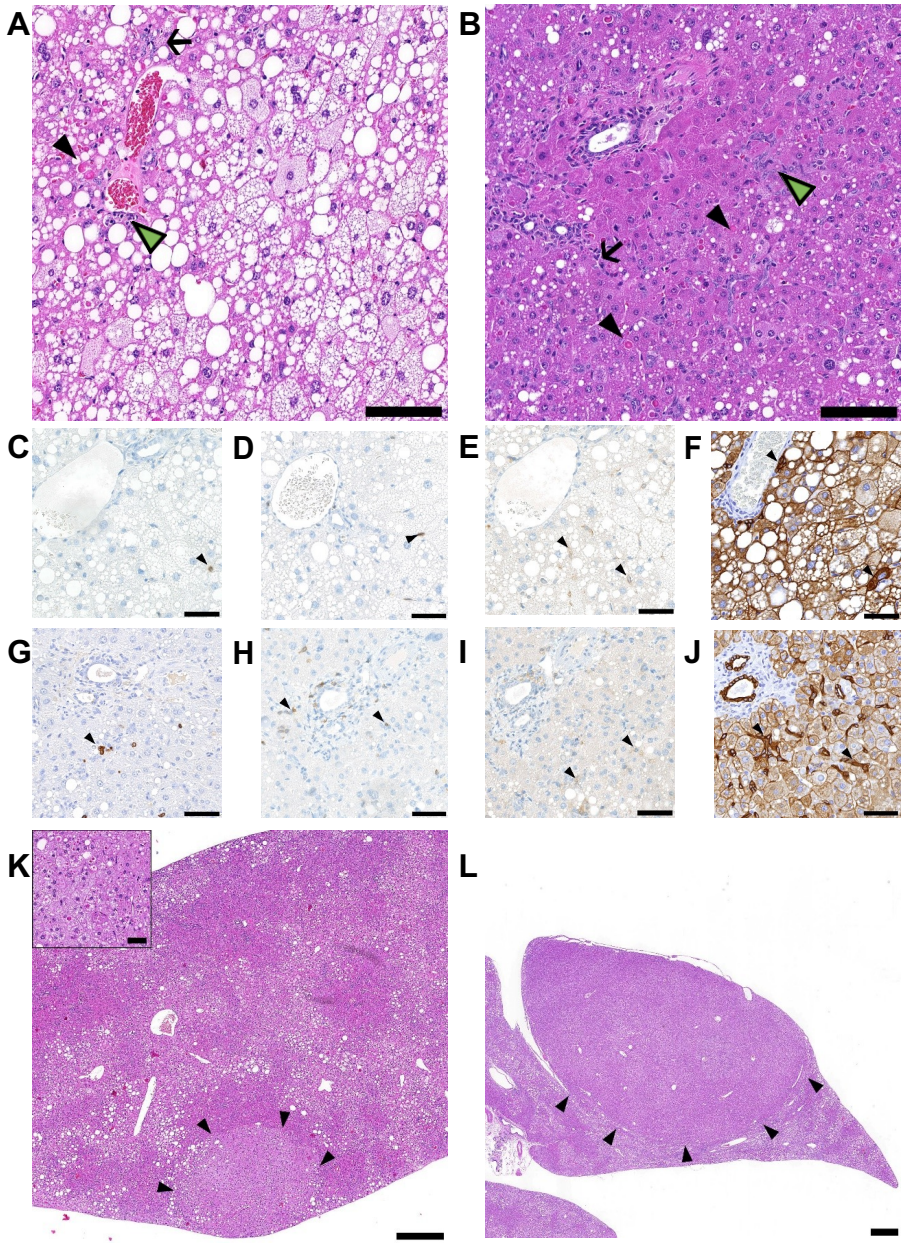

Figure 6

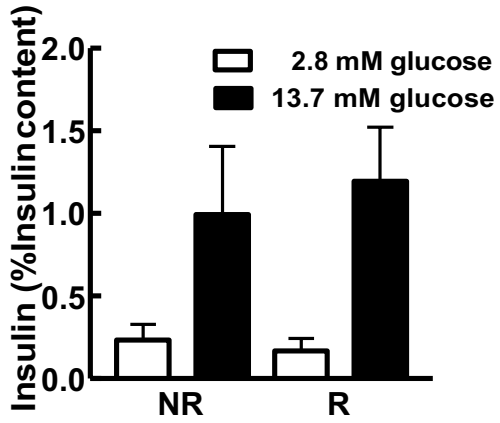
Insulin (%Insulin content)
2.0
1.5
1.0
0.5
0.0
2.8 mM glucose
13.7 mM glucose
NR
R

Figure 7

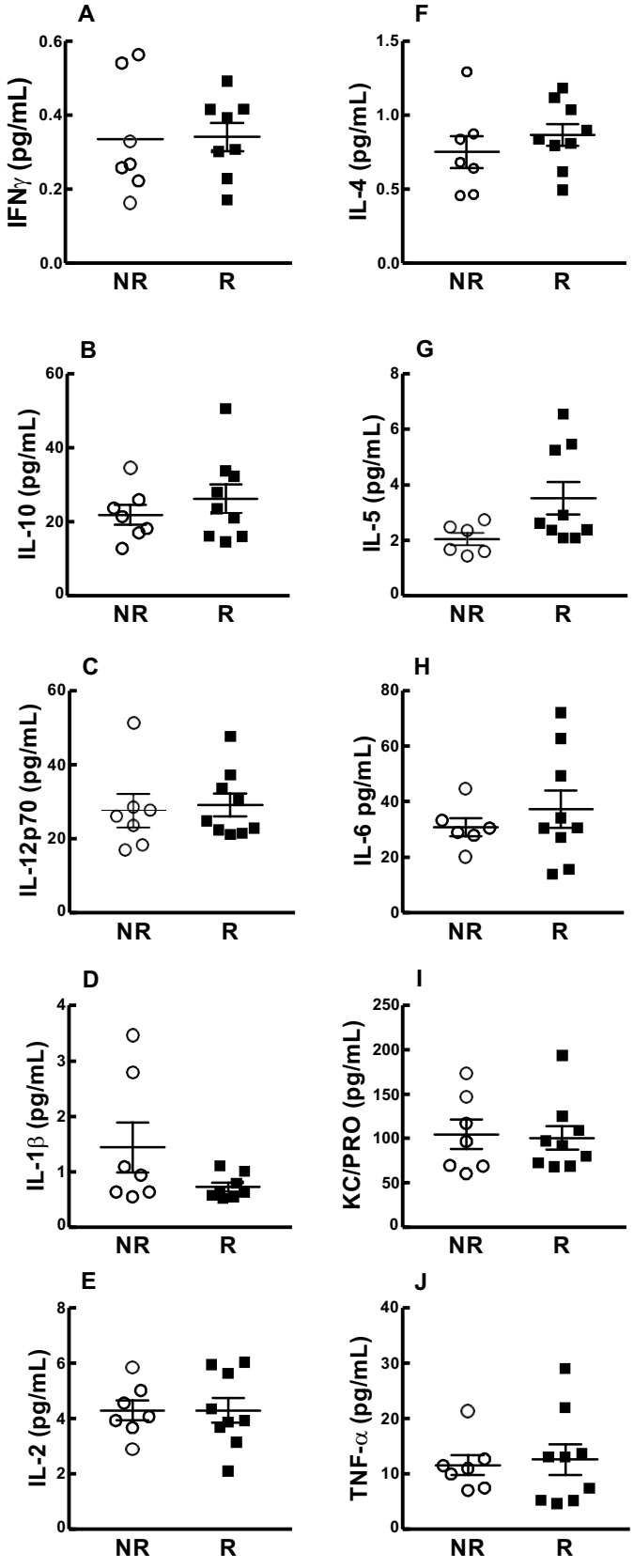
A
IFNγ (pg/mL)
0.6
0.4
0.2
0.0
NR
R
F
IL-4 (pg/mL)
1.5
1.0
0.5
0.0
NR
R
B
IL-10 (pg/mL)
60
40
20
0
NR
R
G
IL-5 (pg/mL)
8
6
4
2
0
NR
R
C
IL-12p70 (pg/mL)
60
40
20
0
NR
R
H
IL-6 pg/mL)
80
60
40
20
0
NR
R
D
IL-1β (pg/mL)
4
3
2
1
0
NR
R
I
KC/PRO (pg/mL)
250
200
150
100
50
0
NR
R
E
IL-2 (pg/mL)
8
6
4
2
0
NR
R
J
TNF-α (pg/mL)
40
30
20
10
0
NR
R

Figure 8

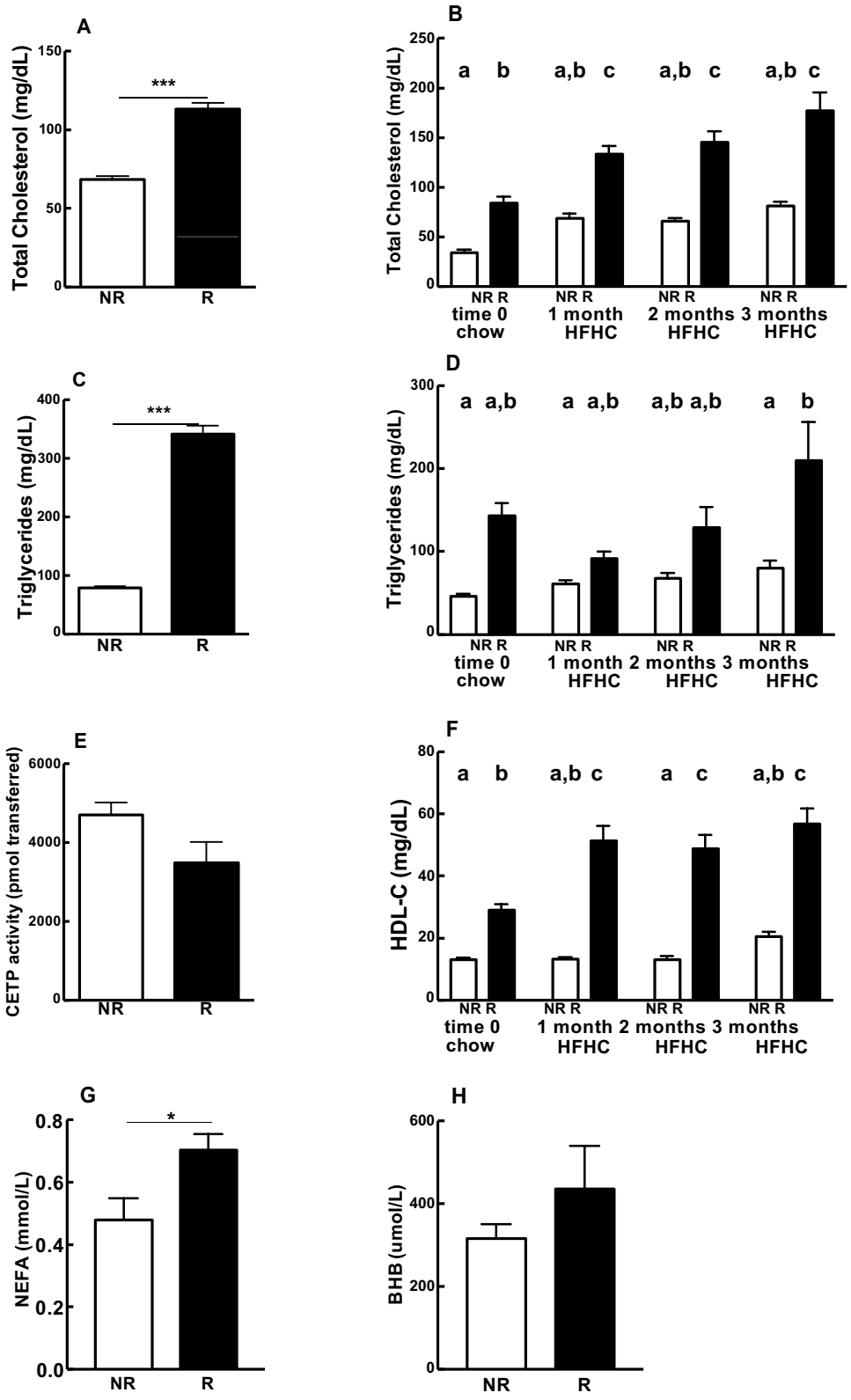
A
Total Cholesterol (mg/dL)
150
100
50
0
***
NR
R
B
Total Cholesterol (mg/dL)
250
200
150
100
50
0
a b a,b c a,b c a,b c
NR R NR R NR R NR R
time 0 chow
1 month HFHC
2 months HFHC
3 months HFHC
C
Triglycerides (mg/dL)
400
300
200
100
0
***
NR
R
D
Triglycerides (mg/dL)
300
200
100
0
a a,b a a,b a,b a,b a b
NR R NR R NR R NR R
time 0 chow
1 month HFHC
2 months HFHC
3 months HFHC
E
CETP activity (pmol transferred)
6000
4000
2000
0
NR
R
F
HDL-C (mg/dL)
80
60
40
20
0
a b a,b c a c a,b c
NR R NR R NR R NR R
time 0 chow
1 month HFHC
2 months HFHC
3 months HFHC
G
NEFA (mmol/L)
0.8
0.6
0.4
0.2
0.0
*
NR
R
H
BHB (umol/L)
600
400
200
0
NR
R

Figure 9

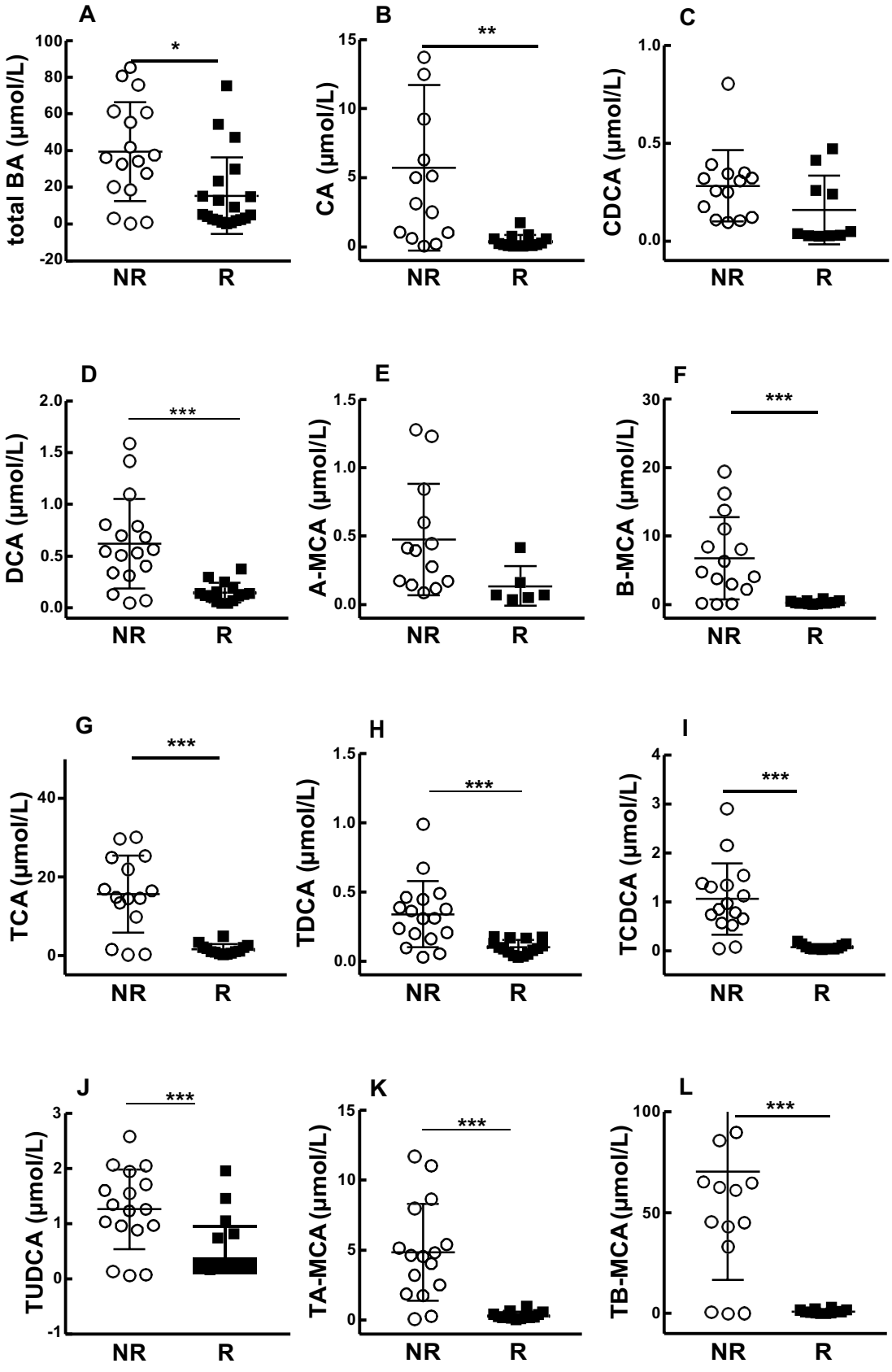
A
total BA (μmol/L)
100
80
60
40
20
0
-20
*
NR
R
B
CA (μmol/L)
15
10
5
0
**
NR
R
C
CDCA (μmol/L)
1.0
0.5
0.0
NR
R
D
DCA (μmol/L)
2.0
1.5
1.0
0.5
0.0
***
NR
R
E
A-MCA (μmol/L)
1.5
1.0
0.5
0.0
NR
R
F
B-MCA (μmol/L)
30
20
10
0
***
NR
R
G
TCA (μmol/L)
40
20
0
***
NR
R
H
TDCA (μmol/L)
1.5
1.0
0.5
0.0
***
NR
R
I
TCDCA (μmol/L)
4
3
2
1
0
***
NR
R
J
TUDCA (μmol/L)
3
2
1
0
-1
***
NR
R
K
TA-MCA (μmol/L)
15
10
5
0
***
NR
R
L
TB-MCA (μmol/L)
100
50
0
***
NR
R

Figure

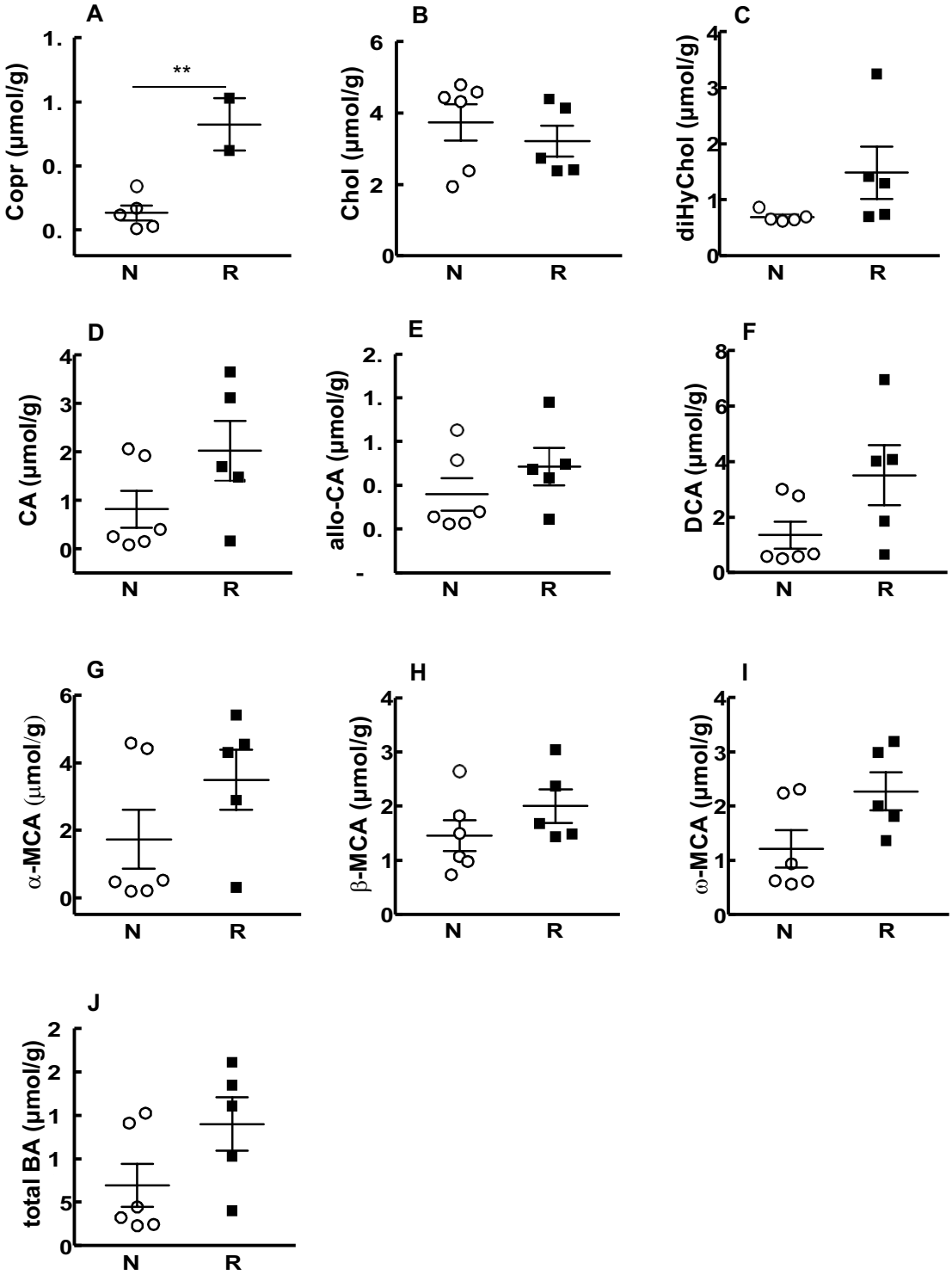
A
Copr (µmol/g)
**
N
R
B
Chol (µmol/g)
C
diHyChol (µmol/g)
D
CA (µmol/g)
E
allo-CA (µmol/g)
F
DCA (µmol/g)
G
α-MCA (µmol/g)
H
β-MCA (µmol/g)
I
ω-MCA (µmol/g)
J
total BA (µmol/g)

5.2 Original research article: ""Body weight-dependent and –independent improvements in lipid metabolism after Roux-en-Y gastric bypass in a humanized murine model for the metabolic syndrome"

This section contains an original research article that will be submitted to *International Journal of Obesity* in June 2018 and contains part of the studies performed for the completion of the present PhD thesis.

My contribution, as first author of this article, includes the study design, data acquisition, data analysis and interpretation, and writing and revising the manuscript.

International Journal of Obesity

Body weight-dependent and -independent improvements in lipid metabolism after Roux-en-Y gastric bypass in a humanized murine model for the metabolic syndrome

Erika Tarasco[1,2], Christina N. Boyle[1], Giovanni Pellegrini[3], Myrtha Arnold[4], Regula Steiner[5], Thorsten Hornemann[2,5], Dimitris Nasias[6], Dimitris Kardassis[6], Lynda Whiting[7], Thomas A. Lutz[1,2]

[1]*Institute of Veterinary Physiology, Vetsuisse Faculty University of Zurich, Zurich, Switzerland;*

[2]*Zurich Center for Integrative Human Physiology (ZIHP), University of Zurich, Zurich, Switzerland;*

[3]*Laboratory for Animal Model Pathology (LAMP), Institute of Veterinary Pathology, Vetsuisse Faculty University of Zurich, Winterthurerstrasse 268, Zurich, Switzerland;*

[4] *Physiology and Behaviour Laboratory, ETH Zurich, Schwerzenbach, Switzerland,*

[5] *Institute of Clinical Chemistry, University and University Hospital of Zurich, Zurich, Switzerland*

[6] *Department of Basic Medical Sciences, University of Crete Medical School and Institute of Molecular Biology and Biotechnology, Foundation for Research and Technology of Hellas Crete. Greece*

[7] *Institute of "Drug and Discovery Biology", University of Monash, Victoria, Australia*

Running title: RYGB effect in ApoE*3Leiden.CETP *mice*

Address for correspondence:

Prof. Thomas A. Lutz
Institute of Veterinary Physiology
University of Zurich
Winterthurerstrasse 260
CH 8057 Zurich
Switzerland
Ph +41 - 44 - 635 88 08
Mail tomlutz@vetphys.uzh.ch

Abstract

Background/Objectives: The incidence of the metabolic syndrome rapidly increases worldwide, and several biomarkers as increased total cholesterol and ceramide have been proposed to define the MetS risk. Roux-en-Y gastric bypass (RYGB) allows to achieve sustained and long-term weight loss and to improve comorbidities in the MetS. We elucidated whether improvements in lipid and glucose metabolism after RYGB surgery are body weight-dependent or not.

Subjects/Methods: Male ApoE*3Leiden.CETP (ApoE3L.CETP) mice fed Western type diet for 6 weeks underwent RYGB or Sham surgery. Sham groups were either fed *ad libitum* group or body weight-matched (BWm) to the RYGB mice, to discriminate and identify surgical effects from body weight loss associated effects. Plasma was collected to assess the metabolic profile before and after surgery, and glucose tolerance and insulin sensitivity was tested before and after surgery. 20 days after surgery, mice were sacrificed, liver was collected to assess metabolic, histological and transcriptomic changes after surgery.

Results: RYGB induced a greater reduction in body weight and total fat mass compared to BWm and Sham *ad libitum* mice (Sham AL). Total cholesterol, non high-density lipoprotein (non HDL-C) and ceramide were strongly reduced 20 days after surgery in RYGB compared to BWm mice. Glucose tolerance and insulin sensitivity improved 2 weeks after surgery in RYGB and BWm mice. Liver histology confirmed lipid reduction in RYGB and BWm mice while functional and transcriptomic data indicated modification in lipid metabolism.

Conclusions: RYGB surgery improves glucose metabolism and greatly ameliorates lipid metabolism in part in a body weight-dependent manner. Given that ApoE3L.CETP mice were extensively studied to describe the MetS, and given that RYGB improved ceramide after

surgery, our data confirmed the usefulness of ApoE3L.CETP mice after RYGB in deciphering the metabolic improvements to treat the MetS.

Introduction

Obesity (BMI >30 kg/m^2) is a major healthcare problem worldwide [1]. Obesity and its comorbidities such as type 2 diabetes mellitus (T2DM) [2], hypertension, non- alcoholic fatty liver disease (NAFLD) [3], hypertriglyceridemia [4] and cardiovascular disease (CAD) [5] are part of the metabolic syndrome (or MetS) [5].

Several rodent models of obesity have been used in the past decades trying to describe the consequences of a Western type diet on metabolism. However, animals like ob/ob mice [6], db/db mice [7] and Zucker rats [8] do not describe all aspects of the MetS and the underlying cause of their obesity differs from common obesity in people. The ApoE*3Leiden.human Cholesteryl Ester Transfer Protein (ApoE3L.CETP) mouse model better describes the physiology and pathophysiology of the MetS. Indeed, the ApoE3Leiden mutation [9, 10] and the introduction of the human CETP gene [10] allow these mice to have a humanized lipoprotein metabolism: hence they develop atherosclerosis when fed a high fat high cholesterol (HFHC) diet and show a human-like response when treated with statins [11, 12]. Moreover, ApoE3L.CETP mice, as humans, present low serum levels of high density lipoprotein cholesterol (HDL-C) and high serum levels of very low density lipoprotein (VLDL) and low density lipoprotein cholesterol (LDL-C) when fed a HFHC diet. Increased concentrations of VLDL/LDL-C are the result of the transgene ApoE3Leiden that impedes the uptake of VLDL remnants by the liver [9] while decreased HDL-C concentration is due to the introduction of the human CETP gene that is responsible for the transport of cholesterol ester from HDL to apolipoprotein-B (apo-B) containing lipoproteins in exchange of triglycerides (TG), leading to decreased HDL-C [10].

Bariatric surgery, and in particular Roux-en-Y gastric bypass (RYGB) is the most effective and available therapy in the treatment of obesity and MetS [13], in terms not only of long-term

maintenance of body weight loss [14, 15], but also in terms of improved glucose homeostasis [16], and reduced CAD and NAFLD [17-19]. Particularly relevant for us were the findings that several improvements after RYGB were achieved independently from changes in body weight [20, 21]. Among them was the reduction in sphingolipids [20]: indeed, it has been shown that changes in sphingolipids are involved in improvements in the pro-inflammatory state and insulin sensitivity [22].

The major aim of this study was to elucidate the effects of RYGB surgery on lipid and glucose metabolism in the ApoE3L.CETP mice. Our study emphasized the morphological and metabolic changes after RYGB surgery, in terms of blood parameters and extensive histology and metabolic liver analysis.

Material and Methods

Animals and housing conditions

All experiments were performed with male ApoE3L.CETP mice obtained from TNO (TNO, Innovation for Life, The Hague, The Netherlands) [10, 23]. Upon arrival at our facility, mice aged 17-20 weeks were group housed and kept at a room temperature of 21°C with a 12h light/dark cycle (light on 2:00am-2:00pm). Mice were given 2 weeks to acclimate to the new environmental and housing conditions, during which they were fed standard chow diet containing 4.5% fat (3436 Kliba Nafag, Kaiseraugst, Switzerland); after these two weeks, the mice were then switched to HFHC diet containing 60% fat and 0.25% cholesterol (D14010701, HFHC, Research Diets, New Brunswick NJ, USA). The HFHC diet was offered *ad libitum* for 6 weeks to induce obesity prior to surgery, and the same diet was offered after surgery until the end of the experiments. Three days prior to RYGB or Sham surgery and three days after surgery, mice were switched back to chow diet to avoid peri-surgical complications. After surgery, mice were single housed until the end of the experiments. The Cantonal Veterinary Office of Zurich approved all the animal experiments (licence 122/2014).

Bariatric surgery

Mice were allocated to RYGB or Sham surgery according to their body weight. To increase survival rate, we performed RYGB surgery on mice with a body weight of 32-48 g. Mice were fasted overnight before surgery, and received subcutaneous injections of antibiotics (Baytril 10mg/kg; Bayer, Lyssach, Switzerand) and analgesics (Metacam 2.5mg/kg, Boehringer, Ingelheim am Rhein, Germany) prior to surgery. Following anesthesia induction (3.5% isoflurane in room air at 0.8 L/min), mice were positioned in a supine position. Rectal temperature was monitored throughout and used to control the heating pad temperature (Heating Pad, Harvard Happaratus, Massachusetts, USA). Surgery was performed under continuous inhalation anesthesia (1.5% - 2% isoflurane in room air 0.8L/min) for the first and second cohort of animals and under injectable anesthesia for the third cohort (anesthesia

cocktail: 50 mg/kg Fentanyl, Fentanyl Sintetica, Sintetica SA, Switzerland; 5 mg/kg Midazolam, Roche, Switzerland; and 1.5 mg/kg Medetomidin,Virbac, Switzerland; all i.p.). Because there were no differences among the cohorts, data from all three cohorts were combined for further analysis.

Gastric bypass surgery was adapted from Bruinsma et al [24] and Hao et al [25]. Following a 1.5 to 2 cm midline laparotomy from the xyphoid, the stomach was carefully isolated to avoid damage of gastric arteries and the vagus nerve, and transected just distal to the cardiac antrum to create a small gastric pouch. The jejunum was transected 7 to 8 cm from the pylorus of the stomach. An end-to-side anastomosis of the proximal end of the transected jejunum to the distal small intestine, approximately 20 cm from the cecum, formed the respective biliopancreatic limb and common channel. The alimentary, or Roux, limb of 5 to 6 cm was formed by an end-to-end anastomosis of the distal transected jejunum to the gastric pouch. For Sham-operated mice, an anterior gastrostomy with subsequent closure was performed. Following completion of surgery, inhalation anesthesia was discontinued, or an antagonist cocktail supplement including a pain-killer was administered (0.2 mg/kg Temgesic, Schering-Plough, USA; 0.5 mg/kg Flumazenil, Labatec-Pharma, Swizerland; and 3.5 mg/kg Atipamezol, Graueb, Swizerland; all i.p.), respectively. Mice then received a second dose of Metacam (2.5 mg/kg i.p.) and 1 ml of warm saline, supplemented with 5% glucose.

Mice continued to receive subcutaneous injections of analgesics (dosing as above), and 0.9% saline supplemented with 5% glucose daily for the first 3 days after surgery, antibiotics were injected only 1 day post-surgery (dosing as above). Post-operatively, mice were fed chow for 3 days; starting from postoperative day 4, small amounts of HFHC diet were re-introduced to their diet. By post-operative day 8, mice were exclusively fed HFHC diet. RYGB and Sham *ad libitum* (Sham AL) had *ad libitum* access to food, while body weight matching (BWm) as part of the Sham operated mice, e.g. body weight-matched group (BWm) started on day 8 after surgery to allow mice to completely recover from the surgery beforehand.

Body weight and food intake

Mice were single housed after surgery. Body weight was measured weekly prior to surgery and daily after surgery. Daily food intake was measured manually, 4h prior to dark onset and expressed as grams/day consumed.

Body composition

Total lean mass and subcutaneous and intra-abdominal fat mass were measured by quantitative microcomputed tomography (LaTheta LCT-100A scanner, Hitachi-Aloka Medical Ltd., Tokyo, Japan) on the carcasses of mice after sacrifice. Analysis was performed by LaTheta software (version 2.10, Hitachi-Aloka Medical Ltd., Tokyo, Japan) in the lumbar region between vertebrae L1-L5 from 1 mm slices images, 250 x 250 pixel size [26, 27].

Lipid parameters

Blood was collected from all mice in microvette Lithium-heparin (Sarstedt, Nümbrecht, Germany) prior to surgery from the sublingual vein and 3 weeks after surgery by cardiac puncture in a terminal experiment to perform lipid analysis. Blood was immediately centrifuged at 11'000 rpm at 4°C for 5 min, and heparin plasma was aliquoted and stored at -80°C until assayed. Total cholesterol (TC), HDL-C and TG were analysed via UniCel® DxC 800 Synchron® Clinical System according to the manufacturer's instructions. Non-esterified fatty acids (NEFA) (HR Series NEFA –HR, Wako, Virginia, USA) and beta-hydroxybutyrate (BHB) (Randox D-3-Hydroxybutyrate, Randoy Laboratories Ltd., Crumlin, County Antrim, United Kingdom) were analysed with the Cobas Mira Roche-Autoanalyzer (F. Hoffmann-La Roche Ltd., Basel, Switzerland), according to the manufacturer's instructions.

Sphingolipids measurements

Analysis was performed via MS-LC system at the Institute of Clinical Chemistry, University of Zurich and University Hospital Zurich, Switzerland. A detailed description of the method is reported in the Supplementary Data.

Tissue histology

All animals were deeply anesthetized with isoflurane and sacrificed via opening of the thoracic cavity and exsanguination by cardiac puncture; a complete necropsy was performed on each mouse. Tissue of interest (liver and pancreas) were removed and fixed in 10% neutral-buffered formalin (Formafox, Hittmau, Switzerland) or snap-frozen. Formalin-fixed samples were trimmed according to guidelines [28], dehydrated through graded alcohols and routinely paraffin wax embedded. Consecutive sections (3-5 µm) were prepared, mounted on glass slides and routinely stained with hematoxylin eosin (HE).

Microscopic findings in the HE-stained livers slides were classified with standard pathological nomenclature and severities of findings were graded on a scale of 0 to 4 (no finding present 0, minimal 1, mild 2, moderate 3, or severe 4). Grades of severity for microscopic findings were subjective; minimal was the least extent discernible and severe was the greatest extent possible [29].

Oil red O (ORO) staining was performed on snap-frozen crymold-embedded livers (see supplementary data). Briefly, a threshold classification allowed recognition of positive (red) hepatocellular cytoplasm and negative hepatic parenchyma, and the results were expressed as positive area versus total area in the whole liver section.

Data are presented as average (± SEM) percentage of lipid-containing parenchyma in the group.

Please see Supplementary Data for the description of pancreas histology.

Triglycerides and non-esterified fatty acids in livers

To measure liver TG content, approximately 50 mg of tissue was homogenized with 1 mL 2:1 chloroform:methanol solution. The homogenate was centrifuged for 5 min at 2'500 rpm and the supernatant was collected and diluted with 0.9% NaCl. Samples were centrifuged for 5 min at 2'000 rpm, then resuspended in a 1:1 methanol-H_2O solution. The upper phase was discarded, then samples were dried and resuspended in dimethyl sulfoxide (DMSO). TG

content was measured with Cobas Mira Roche-Autoanalyzer (F. Hoffmann-La Roche Ltd., Basel, Switzerland), according to the manifacturer's protocol. Liver NEFA content was measured following manifacturer's indication with Free Fatty Acid Quantitation Kit (Merck KGaA, Darmstadt, Germany).

Liver transcriptomics

Analysis were performed at the Institute of Molecular Biology and Biotechnology, FORTH, University of Crete. A detailed description of the method is reported in the Supplementary Data.

Glucose metabolism: oral glucose tolerance test and insulin sensitivity test

Oral glucose tolerance (OGTT) and insulin sensitivity (IST) tests were performed in the same cohorts of mice at different time points prior to and after surgery. Before surgery, the tests were done when mice were chow fed (approx. 21 weeks of age) and after the switch to HFHC diet at 25-27 weeks of age, i.e. after approx. 6 weeks of HFHC exposure. OGTTs and ISTs were repeated 2 and 3 weeks after surgery, respectively, with one week of recovery in between.

For OGTT, mice were fasted for 6h and briefly anesthetized with isoflurane (3% isoflurane in the induction chamber, 0.8L/min). A bolus of glucose (2g/kg) was given by oral application (gavage). Blood was sampled in microvette EDTA tubes (Sarstedt, Nümbrecht, Germany) by tongue bleeding at time 0 (i.e., just before gavage), 15, 30 min, and at time 45, 60, 90 and 120 min by tail bleeding for glucose measurements (Breeze 2, Bayer Glucose Meter, Basel, Switzerland). For each mouse, the area under the curve (AUC) was calculated above its baseline. Blood was kept on ice and immediately centrifuged at 4°C for 5 min at 11'000 rpm. EDTA plasma was separated and stored at -80°C until assayed. For the OGTT test after surgery, mice were not anesthetized for tongue bleeding due to the high sensitivity of the RYGB mice to anesthesia.

ISTs were performed after 4h of fasting in the same cohort of mice. After a baseline blood sample from tail bleeding had been collected, Insulin Humalog (0.5U/kg, 100U.I./mL, Lilly, Genève, Switzerland) was injected intraperitoneally. After 15, 30, 45, 60, 90 and 120 min, blood glucose was measured by tail bleeding. Mice that became hypoglycemic (i.e. reached glucose values lower than 2.5 mmol/L) were immediately given a bolus of glucose (2g/kg) and were excluded from the current test. Since in our analysis mice became hypoglycemic only when chow fed, we excluded them only for this test but not when fed the HFHC diet. The AUC was calculated above each animal's individual baseline.

Cytokines measurements

At the time of sacrifice, i.e. 20 days after surgery, blood was collected by cardiac puncture in microvette EDTA (Sarstedt, Nümbrecht, Germany), immediately centrifuged at 11'000 rpm for 5 min at 4°C, aliquoted and stored at -80 °C prior to analysis. Cytokines were measured with V-Plex Cytokine kit (Meso Scale Discovery, Gaithersburg, MD, USA) following the manufacturer's protocol.

Data Analysis and Statistics

All data were expressed as mean ± standard error of the mean (SEM). One-way or 2 way-ANOVA followed by Bonferroni or Tukey post-hoc tests were used for comparison among the 3 groups (RYGB, BWm and Sham AL), as appropriate. For all statistical analysis, a p-value lower than 0.05 was considered significant. Data were analysed using Prism GraphPad 8.0.

RESULTS

RYGB mice have reduced body weight and food intake after surgery

RYGB induced a marked body weight loss (Fig 1A) compared to Sham AL mice, which was significant starting from day 8 after surgery.

Overall, RYGB-operated mice lost approx. 32% of their initial body weight 3 weeks after surgery, compared to a slight 9% weight loss in Sham AL mice. Weight loss in the BWm group (approx. 34%) was induced by food restriction (Fig 1B), to discriminate surgery-specific metabolic effects from effects induced by the body weight loss itself. Importantly, there was no difference in weight or weight loss in BWm compared to the RYGB mice at the time when metabolic testing was performed 2-3 weeks after surgery. The major body weight loss in RYGB mice was already seen during the first week after surgery (Fig 1A). The initial weight loss in the Sham AL group most likely was the result of the feeding regimen during the post-operative care period, which included 3 days of chow feeding. The lack of weight regain in Sham AL mice was probably due to post-surgical metabolic testing, including OGTT and IST; hence, in the second and third post-operative weeks, body weight was largely stable in the Sham AL group.

Food intake in the three groups of mice is highlighted in Fig 1B which shows that during the first post-operative week, RYGB mice ate on average approx. 1.3 ± 0.1 g of food per day, similar to BWm (1.3 ± 0.2 g) and Sham AL (1.3 ± 0.1 g). Further, during the following two weeks, no differences in average daily food intake were found between RYGB and Sham AL mice, respectively, while BWm mice had to be severely food restricted for the entire experiment to maintain the same body weight as a RYGB mice. This highlights that the sustained weight loss in RYGB mice is not due to a sustained reduction in eating, which is similar to previous studies [30] but different from RYGB operated rats [21].

RYGB surgery induced reduction in fat mass without changing in lean mass

Body composition analysis was performed 20 days after surgery, i.e. at the time when mice were sacrificed, and indicated that despite the lack of significant differences in lean mass among groups (Fig 1C), body fat was markedly reduced in RYGB mice (0.7 ± 0.1 g) compared to BWm (1.5 ± 0.3 g) and Sham AL mice (6.2 ± 0.2 g) (Fig 1D). The reduction in total fat mass in RYGB and BWm mice was due to a reduction in both subcutaneous and intra-abdominal fat depots (Fig 1D); despite a difference in total fat mass between RYGB mice and BWm mice, the relative reduction in the respective fat depots was similar.

Lipid profile improved after RYGB surgery

RYGB and BWm mice had significantly reduced plasma TC, non HDL-C, TG and NEFA 3 weeks after surgery (Table 1). The reduction in TC and non HDL-C was significantly stronger in RYGB than in BWm mice. No differences were found for plasma HDL-C and BHB among groups.

Among sphingolipds, RYGB surgery induced a reduction in ceramide, and deoxy-ceramide. Moreover, both RYGB and BWm mice showed a reduction in sphingomyelin, and also in dihydro-ceramide, sphingosin-1-phosphate and hexosylceramide but without reaching significance between BWm and Sham AL (Table 1). Deoxysphingoind base increased within body weight loss, without reaching significance in the comparison between BWm and Sham AL. No differences were found in dihydro deoxyceramide and sphingoid base among the three groups.

Although body weight loss per se was sufficient to induce a reduction the majority of these parameters, the additional reduction in TC, non HDL-C and ceramide in the RYGB mice were most likely a consequence of modification in fat absorption after RYGB surgery and hence surgery specific.

Liver histology and physiology

Livers from RYGB and BWm operated mice showed decreased lipidosis (0.3 ± 0.2 and 1.3 ± 0.4, resp.) compared to Sham AL livers (3.8 ± 0.1) (Table 3 and Fig 2A-C). Histomorphometrical analysis of lipid droplets in liver sections stained with ORO confirmed this result, with livers from Sham AL mice showing higher proportions of fat content vs total parenchyma (60%) compared to BWm and RYGB operated mice livers (41% and 24% resp.) (Fig 2A-C inset, 2E). The grade of hepatic lipidosis correlated with TG levels (Sham AL 1.7 ± 0.1 mg/dL/g, BWm 1.1 ± 0.2 mg/dL/g and RYGB 0.7 ± 0.1 mg/dL/g) and NEFA (Sham AL 52.4 ± 4.1 mol/L/g, BWm 43 ± 3.4 mol/L/g and RYGB 34.7 ± 3.3 mol/L/g) in livers of Sham AL, BWm and RYGB mice (Fig 2D, 2F). No differences were found in parameters of inflammation and hepatocellular eosinophilic cytoplasmic inclusions (Table 3).

Liver transcriptomics

Microarray analysis on liver samples revealed 1137 transcripts (656 upregulated, 481 downregulated) in the comparison between RYGB and BWm and 506 transcripts (300 upregulated, 206 downregulated) between RYGB and Sham AL. Ingenuity Pathway Analysis (IPA) indicated that the observed change in gene expression in the three different groups were mainly associated with lipid metabolism and energy production. Moreover, functional comparisons revealed that concentration of lipids, synthesis of lipids and steroid metabolism were the most affected biological aspects in the comparison between RYGB and Sham AL (Fig 3A). Cell movement and migration of cells appeared to be more active in RYGB compared to BWm (Fig 3B). Interestingly functions involved in “concentration of D-glucose” and “lean body mass” had a decreased z-score (≤ 2) implying a decreased activation state of these biological functions (Fig 3B) in RYGB mice compared to BWm and Sham AL.

Cytokines

Plasma cytokines were measured in all group before and after surgery (Table 2). Cytokine levels before surgery did not show any differences among groups. IL-4 and KC/GRO (keratinocyte chemoattractant/growth-regulated oncogene) did not show any differences among group or surgery related differences. After surgery, IFN-γ increased post-surgery in all groups; IL-10 and IL-5 increased in RYGB and BWm mice, while IL-12p70, IL-2 and IL-6 increased only in the RYGB group. TNF-α increased post-surgery only in Sham AL group.

RYGB mice improved glucose metabolism after surgery

Oral glucose tolerance tests (OGTT) and Insulin sensitivity tests (IST) were performed before surgery, i.e. in 19-21 weeks old mice when chow fed, and again in 25-27 weeks old mice after switching to HFHC diet (Fig 1E-J).

After 6 weeks of HFHC diet, mice showed impaired glucose tolerance ($P< 0.001$, Fig 1E) compared to chow fed mice. Already two weeks after surgery, glucose tolerance was improved in all groups (Fig 1F-G). Unexpectedly, glucose tolerance also improved in the Sham AL mice, despite the continued exposure to the HFHC diet (Fig 1E-F). This might have been due to the post-surgical feeding regimen because a marked reduction in caloric intake is known to improve glucose tolerance [31] or to the usage of isoflurane in the test before but not after surgery because it is known that isoflurane can induce increased in glucose levels [32].

Nonetheless, even though RYGB and Sham AL mice had similar baseline glucose levels, RYGB mice glucose levels peaked much higher 15 min after the glucose bolus than the other groups, probably reflecting the rapid transit of glucose through the stomach remnant into the small intestine. BWm mice displayed lower baseline glucose levels (6.7 ± 0.8 mmol/L), which may be due to the restrictive feeding conditions. Glycaemia in RYGB mice normalized faster than in the other two groups; in other words, during the OGTT, glucose levels in RYGB mice glucose presented a greater decrease (8.2 ± 0.9 mmol/L) at 30 min after glucose administration, as compared to Sham AL (11.4 ± 0.5 mmol/L) and BWm (10.1 ± 0.6 mmol/L)

(P<0.05). At 120 min, blood glucose levels in BWm mice were lower (7.1 ± 0.7 mmol/L) than in RYGB (8.3 ± 0.9 mmol/L) or in Sham AL mice (9.9 ± 0.4 mmol/L; P<0.05). The difference between RYGB and Sham AL mice was then no longer significant.

After 6 weeks of HFHC diet, mice showed reduced insulin sensitivity as compared to when they were chow fed (Fig 1H). 3 weeks after surgery, RYGB mice displayed improved insulin sensitivity as compared to Sham AL mice (P<0.05; Fig 1I-J). RYGB and Sham AL mice had slightly higher glucose baseline levels (8.8 ± 0.8 mmol/L and 8.5 ± 0.4 mmol/L) than BWm (6.8 ± 0.7 mmol/L), similarly to what has been shown in Fig 1F during the OGTT. Importantly, 15 min after the insulin injection, glucose levels dropped markedly in RYGB mice and were similar to BWm, but lower compared to Sham AL (P<0.05; 7.1 ± 0.4 mmol/L). RYGB mice maintained this lower glucose level until the end of the test (P<0.05; Fig 1I). BWm mice also maintained a lower glucose level which can be explained by the restrictive feeding condition throughout the post-operative period (Fig 1B, 1I). Thus, RYGB improved insulin sensitivity of mice fed HFHC diet fed compared to Sham AL mice, but the effect was similar in BWm mice which achieved the weight loss by food restriction.

Functional pancreas data

No major differences were found in pancreas histology and function. Please see Supplementary Data.

Discussion

This study aimed to test the effect of RYGB surgery on lipid and glucose metabolism in male ApoE3L.CETP mice, a humanized mouse model used to assess the development and the mechanisms behind the MetS [11]. We extensively investigated physiological changes in RYGB compared to BWm and Sham AL operated mice. The BWm group served as an additional control to discriminate the surgery-specific effects from body weight loss-induced effects.

Many of our findings indicated that changes in lipid and glucose metabolism were mainly body weight loss dependent; we showed that the marked body weight decrease in RYGB and in BWm mice was related to the reduction in lipid parameters and improvement in glucose metabolism. However, more interesting was the finding that RYGB surgery reduced total fat mass, TC, non HDL-C, ceramide, and deoxyceramide plasma levels more than in BWm mice, i.e. at least in part independent of the body weight loss. This indicates that physiological changes after RYGB surgery have a specific effect at least on some aspects of lipid metabolism.

Hence, our findings underline the importance of a caloric restriction to improve many aspects of lipid and glucose metabolism, but also reveal the specific effect of RYGB surgery in reducing the concentration of non HDL-C and several sphingolipids in plasma.

Although data in literature had shown improvements of lipid parameters independently from body weight loss after bariatric surgery [20, 21], other studies performed *in vivo* and in humans support our data that improved lipid and glucose parameters are to some extent a consequence of the caloric restriction in the post-surgical period and the resulting body weight loss [33, 34].

We showed that body weight loss in RYGB operated mice lasted for 16 days before reaching a plateau, and spontaneous food intake was reduced only in the first week post-surgery before

reaching similar food intake as in Sham AL group. BWm mice, instead, had to be strongly food restricted throughout the entire post-surgical period to achieve similar body weight to RYGB-operated mice. The body weight loss correlated in both RYGB and BWm groups with a significant reduction in total fat mass, but the effect for total fat mass was stronger in RYGB mice, even though the reductions in subcutaneous and intra-abdominal fat mass were not significantly larger than in BWm mice. Considering the similar food intake in RYGB and Sham AL mice, we believe that RYGB mice maintained lower body weight and fat mass mainly because of their increased energy expenditure, and perhaps in part increased faecal energy loss because of the use of the HFHC diet [30]. For experimental reasons, we could not assess energy expenditure in our experiment but data from Nestoridi et al [35] supports this hypothesis; they had suggested that the observed increased in energy expenditure directly contributes to the RYGB-induced body weight loss. They also showed that increases in thermogenesis and in resting energy expenditure are associated with increased food consumption and significant body weight loss in RYGB mice [35]. Furthermore, they also observed increased food intake and maintained body weight loss starting from the second week after surgery in the RYGB group [35], similar to what we also showed. Finally, our findings were also similar to the study reported by Hao et al [30] in terms of body weight loss, body composition and food intake among the corresponding experimental groups.

Even though body weight loss directly correlated with the decrease of some lipid parameters [21, 36-38], a further decrease in TC and non-HDL-C levels in RYGB mice compared to BWm mice already 20 days after surgery indicated the presence of a direct surgical effect [14]. Even if we could not prove the presence of a direct surgery specific mechanism to explain the differences found between RYGB and BWm, we hypothesized that changes in lipid absorption [39], mainly due to a reduction in cholesterol absorption and increased faecal levels after RYGB surgery [40, 41] could well explain the reduction seen in our lipid parameters.

We did not see an improvement in HDL-C levels in the time-frame of our studies, e.g. 20 days post-surgery, but other studies in rats had also reported changes in HDL-C only after 20 weeks post-surgery [42], and in humans 1 year after surgery [43].

An interesting effect of RYGB in our ApoE3L.CETP mice was the reduction in ceramide and deoxy-ceramide. Actually alterations in ceramide levels have been related with MetS [44]. Particularly, increased ceramide were found to correlated with in increased CAD risk [45] and atherosclerosis [46]. Moreover, a correlation between elevated ceramide and obese subjects with T2DM was demonstrated as well by Haus et al [47].
Our data are consistent with human studies that also showed reduced ceramide 1 month [20], and 3 and 6 months after RYGB [22, 44].

It is well established that the reduction in body weight and the improvement in lipid metabolism after RYGB directly impact liver histology and liver functionality [48, 49]. This was confirmed by our study because the histological liver findings at the time of sacrifice paralleled the improvement in metabolic parameters; hepatocellular lipidosis and liver TG levels were reduced in RYGB and BWm mice compared to Sham AL mice. A slight increase in inflammatory parameters was observed in RYGB mice which may have been associated to the rapid body weight loss [50, 51], but we did not observe any differences between BWm and RYGB regarding these parameters. Thus, most of these effects may be solely due to the body weight loss.

Overall, the functional analysis of liver metabolism was in line with the histological and physiological changes after RYGB.
Albeit systemic cytokines measurements showed no difference among groups before surgery, we saw a minor increase in some cytokines without any specificity group-related. We believe that a general pro-inflammatory state is one of a causative factors of the MetS in obesity [52]

and that a higher level of inflammation post-surgery could be a consequence of the surgical procedure and modification in the adipose tissue [53]. Importantly, metabolic parameters improved despite the slight increase in some inflammatory parameters.

Finally, we showed that already 2 weeks after surgery, RYGB-operated ApoE3L.CETP mice had significantly improved glucose tolerance and insulin sensitivity as it has been shown previously [33, 54, 55]. In addition, the major contribution to the improvement of glucose metabolism was due to the amelioration in insulin sensitivity in RYGB mice [56, 57]. Interestingly, caloric restriction after surgery may have been a major driver in these effects because the same was shown in BWm mice; this is consistent with previous studies that had also demonstrated that improved glucose metabolism is at least to some part due to reduced caloric intake in the immediate post-surgical period and the RYGB-induced weight loss [31].. According to the so-called foregut hypothesis, the bypass of duodenum and the proximal jejunum after RYGB surgery reduced insulin resistance, hence glucose metabolism improved [58].

In summary, our findings confirmed the importance of RYGB surgery to improve lipid and glucose metabolism in part in a body weight loss dependent and in part in a non -weight loss dependent manner. To our knowledge, these experiments demonstrate for the first time the effect of RYGB on the reduction in ceramide levels in a murine model for the MetS.

Since the ApoE3L.CETP mouse model is extensively studied to describe the MetS [11], particularly the atherosclerosis aspect [59] and since ceramides are considered a potential biomarker for atherosclerosis [44] we believe that our data provided an important proof-of-concept to the advantage of using the ApoEL.CETP mouse model after RYGB in deciphering the metabolic improvements after bariatric surgery to treat the MetS.

Acknowledgments

We acknowledge Arnold von Eckardstein from the Institute of Clinical Chemistry of the University of Zurich and his group for their fruitful and expert discussions. We also thank RESOLVE EU-FP7 for generous funding and the Center for Clinical Studies (Vetsuisse Faculty) for kindly letting us use their equipment. We also thank Christelle le Foll for a critical revision of the manuscript.

Funding Sources

This work was supported in part by the European Union (RESOLVE, FP7-HEALTH 305707; TAL and DK) and by the University of Zürich Forschungskredit (ET).

Disclosures

None.

Figure legend

Fig 1: (A) Body weight in Sham *ad libitum* (Sham AL, n=14), body weight-matched (BWm, n=11) and Roux-en-Y gastric bypass (RYGB, n=14) operated ApoE3L.CETP male mice. RYGB and BWm decreased body weight by more than 30% compared to the initial values. Imposed food restriction in BWm mice started on day 8 after surgery.

(B) Average daily food intake in Sham AL (n=14), BWm (n=11) and RYGB (n=14) groups in the first three post-operative weeks. BWm mice were food restricted in the 2^{nd} and 3^{rd} week post-surgery to maintain the same body weight as RYGB operated mice. Importantly, no difference in spontaneous average food intake was found between RYGB and Sham AL mice at any time after surgery.

(C-D) Body composition analysed by quantitative microcomputed tomography (LaTheta LCT-100A scanner, Hitachi-Aloka Medical Ltd., Tokyo, Japan). (C) Lean mass was similar in all groups, total fat mass was higher in Sham AL (n=12) compared to BWm (n=9) and RYGB (n=12) mice, and (D) the ratio of subcutaneous versus intra-abdominal fat was similar among the groups. (E-G) Oral glucose tolerance test (OGTT; 2 g/kg) performed when mice were chow fed (n=34) or after 2 months of high fed diet + 0.25% cholesterol (HFDC, n=34); (F), and 2 weeks after surgery (n=13, 10, 11); (G) area under the curve (AUC) over 120 min was calculated during the OGTT, above baseline of each respective animal. (H-J) Insulin sensitivity test (0.5U/kg i.p.) performed when mice were chow fed (n=27) or after 2 months of HFDC (n=32) (H), and (I) 3 weeks post-surgery (n= 12, 10, 8); area under the curve (AUC) over 120 min was calculated during the IST, above baseline of each respective animal (J).

Data are means +/- SEM. Parameters with differing superscripts differ from each other at the $P< 0.05$ levels by post hoc Bonferroni adjustment when significant intergroup differences were found by one-way ANOVA (B, C, D, G and J) and 2-way ANOVA (A, E, F, H, I). **, $P< 0.01$, ***, $P < 0.001$.

Fig 2: (A, C, E) HE-stained liver sections from (A) Sham AL, (C) BWm and (E) RYGB operated mice after 9 weeks of HFHC diet, scale bar = 100 µm. Insets: Oil red O (ORO) stained liver sections from the same mice; ORO-positive lipid content in the hepatocytes is decreased in C and E compared to A. (B) Triglyceride levels in liver extracts from Sham AL (n=13), BWm (n=9) and RYGB mice (n=11) after sacrifice; (D) quantification of the ORO staining in Sham AL (n=8), BWm (n=7) and RYGB (n=7) and (F) liver non-esterified fatty acids in Sham AL mice (n=13) and BWm mice (n=11) RYGB mice (n=11). Data are represented as mean ± SEM. Parameters with differing superscripts differ from each other at the $P< 0.05$ levels by post hoc Bonferroni adjustment when significant intergroup differences were found by one-way ANOVA (B, D, F).

Fig 3: Heatmaps of the p-value (purple) or heatmap of the z-score as predictive or the increased functional activity (orange) or decreased functionality (blue). Data represents comparisons between RYGB (n=6) vs BWm (n=5) or RYGB vs Sham AL (n=5).

References:

1. Gadde KM, Martin CK, Berthoud HR, Heymsfield SB. Obesity: Pathophysiology and Management. *J Am Coll Cardiol* 2018; **71**(1)**:** 69-84.

2. Wali JA, Thomas HE, Sutherland AP. Linking obesity with type 2 diabetes: the role of T-bet. *Diabetes Metab Syndr Obes* 2014; **7:** 331-40.

3. Bellentani S. The epidemiology of non-alcoholic fatty liver disease. *Liver Int* 2017; **37 Suppl 1:** 81-84.

4. Bays HE, Toth PP, Kris-Etherton PM, Abate N, Aronne LJ, Brown WV *et al.* Obesity, adiposity, and dyslipidemia: a consensus statement from the National Lipid Association. *J Clin Lipidol* 2013; **7**(4)**:** 304-83.

5. Poirier P, Cornier MA, Mazzone T, Stiles S, Cummings S, Klein S *et al.* Bariatric surgery and cardiovascular risk factors: a scientific statement from the American Heart Association. *Circulation* 2011; **123**(15)**:** 1683-701.

6. Wang CY, Liao JK. A mouse model of diet-induced obesity and insulin resistance. *Methods Mol Biol* 2012; **821:** 421-33.

7. Kobayashi K, Forte TM, Taniguchi S, Ishida BY, Oka K, Chan L. The db/db mouse, a model for diabetic dyslipidemia: molecular characterization and effects of Western diet feeding. *Metabolism* 2000; **49**(1)**:** 22-31.

8. Yokoi N, Hoshino M, Hidaka S, Yoshida E, Beppu M, Hoshikawa R *et al.* A Novel Rat Model of Type 2 Diabetes: The Zucker Fatty Diabetes Mellitus ZFDM Rat. *J Diabetes Res* 2013; **2013:** 103731.

9. Havekes L, de Wit E, Leuven JG, Klasen E, Utermann G, Weber W *et al.* Apolipoprotein E3-Leiden. A new variant of human apolipoprotein E associated with familial type III hyperlipoproteinemia. *Hum Genet* 1986; **73**(2)**:** 157-63.

10. Westerterp M, van der Hoogt CC, de Haan W, Offerman EH, Dallinga-Thie GM, Jukema JW *et al.* Cholesteryl ester transfer protein decreases high-density lipoprotein and severely aggravates atherosclerosis in APOE*3-Leiden mice. *Arterioscler Thromb Vasc Biol* 2006; **26**(11)**:** 2552-9.

11. van den Hoek AM, van der Hoorn JW, Maas AC, van den Hoogen RM, van Nieuwkoop A, Droog S *et al.* APOE*3Leiden.CETP transgenic mice as model for pharmaceutical treatment of the metabolic syndrome. *Diabetes Obes Metab* 2014; **16**(6)**:** 537-44.

12. van der Hoorn JW, de Haan W, Berbee JF, Havekes LM, Jukema JW, Rensen PC *et al.* Niacin increases HDL by reducing hepatic expression and plasma levels of cholesteryl ester transfer protein in APOE*3Leiden.CETP mice. *Arterioscler Thromb Vasc Biol* 2008; **28**(11)**:** 2016-22.

13. Simonson DC, Halperin F, Foster K, Vernon A, Goldfine AB. Clinical and Patient-Centered Outcomes in Obese Patients With Type 2 Diabetes 3 Years After Randomization to Roux-en-Y Gastric Bypass Surgery Versus Intensive Lifestyle Management: The SLIMM-T2D Study. *Diabetes Care* 2018; **41**(4)**:** 670-679.

14. Carswell KA, Belgaumkar AP, Amiel SA, Patel AG. A Systematic Review and Meta-analysis of the Effect of Gastric Bypass Surgery on Plasma Lipid Levels. *Obes Surg* 2016; **26**(4)**:** 843-55.

15. Kraljevic M, Delko T, Kostler T, Osto E, Lutz T, Thommen S *et al.* Laparoscopic Roux-en-Y gastric bypass versus laparoscopic mini gastric bypass in the treatment of obesity: study protocol for a randomized controlled trial. *Trials* 2017; **18**(1)**:** 226.

16. Mingrone G, Panunzi S, De Gaetano A, Guidone C, Iaconelli A, Leccesi L *et al.* Bariatric surgery versus conventional medical therapy for type 2 diabetes. *N Engl J Med* 2012; **366**(17)**:** 1577-85.

17. Bradley D, Magkos F, Klein S. Effects of bariatric surgery on glucose homeostasis and type 2 diabetes. *Gastroenterology* 2012; **143**(4)**:** 897-912.

18. Caiazzo R, Lassailly G, Leteurtre E, Baud G, Verkindt H, Raverdy V *et al.* Roux-en-Y gastric bypass versus adjustable gastric banding to reduce nonalcoholic fatty liver disease: a 5-year controlled longitudinal study. *Ann Surg* 2014; **260**(5)**:** 893-8; discussion 898-9.

19. Sjostrom L, Peltonen M, Jacobson P, Sjostrom CD, Karason K, Wedel H *et al.* Bariatric surgery and long-term cardiovascular events. *JAMA* 2012; **307**(1)**:** 56-65.

20. Kayser BD, Lhomme M, Dao MC, Ichou F, Bouillot JL, Prifti E *et al.* Serum lipidomics reveals early differential effects of gastric bypass compared with banding on phospholipids and sphingolipids independent of differences in weight loss. *Int J Obes (Lond)* 2017.

21. Osto E, Doytcheva P, Corteville C, Bueter M, Dorig C, Stivala S *et al.* Rapid and body weight-independent improvement of endothelial and high-density lipoprotein function after Roux-en-Y gastric bypass: role of glucagon-like peptide-1. *Circulation* 2015; **131**(10)**:** 871-81.

22. Huang H, Kasumov T, Gatmaitan P, Heneghan HM, Kashyap SR, Schauer PR *et al.* Gastric bypass surgery reduces plasma ceramide subspecies and improves insulin sensitivity in severely obese patients. *Obesity (Silver Spring)* 2011; **19**(11)**:** 2235-40.

23. Paalvast Y, Gerding A, Wang Y, Bloks VW, van Dijk TH, Havinga R *et al.* Male apoE*3-Leiden.CETP mice on high-fat high-cholesterol diet exhibit a biphasic dyslipidemic response, mimicking the changes in plasma lipids observed through life in men. *Physiol Rep* 2017; **5**(19).

24. Bruinsma BG, Uygun K, Yarmush ML, Saeidi N. Surgical models of Roux-en-Y gastric bypass surgery and sleeve gastrectomy in rats and mice. *Nat Protoc* 2015; **10**(3)**:** 495-507.

25. Hao Z, Zhao Z, Berthoud HR, Ye J. Development and verification of a mouse model for Roux-en-Y gastric bypass surgery with a small gastric pouch. *PLoS One* 2013; **8**(1)**:** e52922.

26. Hillebrand JJ, Langhans W, Geary N. Validation of computed tomographic estimates of intra-abdominal and subcutaneous adipose tissue in rats and mice. *Obesity (Silver Spring)* 2010; **18**(4)**:** 848-53.

27. Villars FO, Pietra C, Giuliano C, Lutz TA, Riediger T. Oral Treatment with the Ghrelin Receptor Agonist HM01 Attenuates Cachexia in Mice Bearing Colon-26 (C26) Tumors. *Int J Mol Sci* 2017; **18**(5).

28. Ruehl-Fehlert C, Kittel B, Morawietz G, Deslex P, Keenan C, Mahrt CR *et al.* Revised guides for organ sampling and trimming in rats and mice--part 1. *Exp Toxicol Pathol* 2003; **55**(2-3)**:** 91-106.

29. Shackelford C, Long G, Wolf J, Okerberg C, Herbert R. Qualitative and quantitative analysis of nonneoplastic lesions in toxicology studies. *Toxicol Pathol* 2002; **30**(1)**:** 93-6.

30. Hao Z, Mumphrey MB, Townsend RL, Morrison CD, Munzberg H, Ye J *et al.* Body Composition, Food Intake, and Energy Expenditure in a Murine Model of Roux-en-Y Gastric Bypass Surgery. *Obes Surg* 2016; **26**(9)**:** 2173-2182.

31. Isbell JM, Tamboli RA, Hansen EN, Saliba J, Dunn JP, Phillips SE *et al.* The importance of caloric restriction in the early improvements in insulin sensitivity after Roux-en-Y gastric bypass surgery. *Diabetes Care* 2010; **33**(7)**:** 1438-42.

32. Zuurbier CJ, Keijzers PJ, Koeman A, Van Wezel HB, Hollmann MW. Anesthesia's effects on plasma glucose and insulin and cardiac hexokinase at similar hemodynamics and without major surgical stress in fed rats. *Anesth Analg* 2008; **106**(1)**:** 135-42, table of contents.

33. Hao Z, Townsend RL, Mumphrey MB, Morrison CD, Munzberg H, Berthoud HR. RYGB Produces more Sustained Body Weight Loss and Improvement of Glycemic Control Compared with VSG in the Diet-Induced Obese Mouse Model. *Obes Surg* 2017; **27**(9)**:** 2424-2433.

34. Pop LM, Mari A, Zhao TJ, Mitchell L, Burgess S, Li X *et al.* Roux-en-Y gastric bypass compared with equivalent diet restriction: Mechanistic insights into diabetes remission. *Diabetes Obes Metab* 2018.

35. Nestoridi E, Kvas S, Kucharczyk J, Stylopoulos N. Resting energy expenditure and energetic cost of feeding are augmented after Roux-en-Y gastric bypass in obese mice. *Endocrinology* 2012; **153**(5)**:** 2234-44.

36. Benetti A, Del Puppo M, Crosignani A, Veronelli A, Masci E, Frige F *et al.* Cholesterol metabolism after bariatric surgery in grade 3 obesity: differences between malabsorptive and restrictive procedures. *Diabetes Care* 2013; **36**(6)**:** 1443-7.

37. Blanchard C, Moreau F, Ayer A, Toque L, Garcon D, Arnaud L *et al.* Roux-en-Y gastric bypass reduces plasma cholesterol in diet-induced obese mice by affecting trans-intestinal cholesterol excretion and intestinal cholesterol absorption. *Int J Obes (Lond)* 2018; **42**(3)**:** 552-560.

38. Heffron SP, Lin BX, Parikh M, Scolaro B, Adelman SJ, Collins HL *et al.* Changes in High-Density Lipoprotein Cholesterol Efflux Capacity After Bariatric Surgery Are Procedure Dependent. *Arterioscler Thromb Vasc Biol* 2018; **38**(1)**:** 245-254.

39. Pihlajamaki J, Gronlund S, Simonen M, Kakela P, Moilanen L, Paakkonen M *et al.* Cholesterol absorption decreases after Roux-en-Y gastric bypass but not after gastric banding. *Metabolism* 2010; **59**(6)**:** 866-72.

40. Carswell KA, Vincent RP, Belgaumkar AP, Sherwood RA, Amiel SA, Patel AG *et al.* The effect of bariatric surgery on intestinal absorption and transit time. *Obes Surg* 2014; **24**(5)**:** 796-805.

41. Kumar R, Lieske JC, Collazo-Clavell ML, Sarr MG, Olson ER, Vrtiska TJ *et al.* Fat malabsorption and increased intestinal oxalate absorption are common after Roux-en-Y gastric bypass surgery. *Surgery* 2011; **149**(5)**:** 654-61.

42. Mu S, Liu J, Guo W, Zhang S, Xiao X, Wang Z *et al.* Roux-en-Y Gastric Bypass Improves Hepatic Glucose Metabolism Involving Down-Regulation of Protein Tyrosine Phosphatase 1B in Obese Rats. *Obes Facts* 2017; **10**(3)**:** 191-206.

43. Schauer PR, Burguera B, Ikramuddin S, Cottam D, Gourash W, Hamad G *et al.* Effect of laparoscopic Roux-en Y gastric bypass on type 2 diabetes mellitus. *Ann Surg* 2003; **238**(4)**:** 467-84; discussion 84-5.

44. Heneghan HM, Huang H, Kashyap SR, Gornik HL, McCullough AJ, Schauer PR *et al.* Reduced cardiovascular risk after bariatric surgery is linked to plasma ceramides, apolipoprotein-B100, and ApoB100/A1 ratio. *Surg Obes Relat Dis* 2013; **9**(1)**:** 100-7.

45. Jiang XC, Paultre F, Pearson TA, Reed RG, Francis CK, Lin M *et al.* Plasma sphingomyelin level as a risk factor for coronary artery disease. *Arterioscler Thromb Vasc Biol* 2000; **20**(12)**:** 2614-8.

46. Holewijn S, den Heijer M, Swinkels DW, Stalenhoef AF, de Graaf J. Apolipoprotein B, non-HDL cholesterol and LDL cholesterol for identifying individuals at increased cardiovascular risk. *J Intern Med* 2010; **268**(6)**:** 567-77.

47. Haus JM, Kashyap SR, Kasumov T, Zhang R, Kelly KR, Defronzo RA *et al.* Plasma ceramides are elevated in obese subjects with type 2 diabetes and correlate with the severity of insulin resistance. *Diabetes* 2009; **58**(2)**:** 337-43.

48. Alli V, Rogers AM. Gastric Bypass and Influence on Improvement of NAFLD. *Curr Gastroenterol Rep* 2017; **19**(6)**:** 25.

49. Verbeek J, Lannoo M, Pirinen E, Ryu D, Spincemaille P, Vander Elst I *et al.* Roux-en-y gastric bypass attenuates hepatic mitochondrial dysfunction in mice with non-alcoholic steatohepatitis. *Gut* 2015; **64**(4)**:** 673-83.

50. Clark JM, Alkhuraishi AR, Solga SF, Alli P, Diehl AM, Magnuson TH. Roux-en-Y gastric bypass improves liver histology in patients with non-alcoholic fatty liver disease. *Obes Res* 2005; **13**(7)**:** 1180-6.

51. Hassanian M, Al-Mulhim A, Al-Sabhan A, Al-Amro S, Bamehriz F, Abdo A *et al.* The effect of bariatric surgeries on nonalcoholic fatty liver disease. *Saudi J Gastroenterol* 2014; **20**(5)**:** 270-8.

52. Balistreri CR, Caruso C, Candore G. The role of adipose tissue and adipokines in obesity-related inflammatory diseases. *Mediators Inflamm* 2010; **2010:** 802078.

53. Miller GD, Nicklas BJ, Fernandez A. Serial changes in inflammatory biomarkers after Roux-en-Y gastric bypass surgery. *Surg Obes Relat Dis* 2011; **7**(5)**:** 618-24.

54. Pournaras DJ, Nygren J, Hagstrom-Toft E, Arner P, le Roux CW, Thorell A. Improved glucose metabolism after gastric bypass: evolution of the paradigm. *Surg Obes Relat Dis* 2016; **12**(8)**:** 1457-1465.

55. Rubino F, Gagner M, Gentileschi P, Kini S, Fukuyama S, Feng J *et al.* The early effect of the Roux-en-Y gastric bypass on hormones involved in body weight regulation and glucose metabolism. *Ann Surg* 2004; **240**(2)**:** 236-42.

56. Hao Z, Munzberg H, Rezai-Zadeh K, Keenan M, Coulon D, Lu H *et al.* Leptin deficient ob/ob mice and diet-induced obese mice responded differently to Roux-en-Y bypass surgery. *Int J Obes (Lond)* 2015; **39**(5)**:** 798-805.

57. Jackness C, Karmally W, Febres G, Conwell IM, Ahmed L, Bessler M *et al.* Very low-calorie diet mimics the early beneficial effect of Roux-en-Y gastric bypass on insulin sensitivity and beta-cell Function in type 2 diabetic patients. *Diabetes* 2013; **62**(9)**:** 3027-32.

58. Pories WJ, Albrecht RJ. Etiology of type II diabetes mellitus: role of the foregut. *World J Surg* 2001; **25**(4)**:** 527-31.

59. Berbee JF, Wong MC, Wang Y, van der Hoorn JW, Khedoe PP, van Klinken JB *et al.* Resveratrol protects against atherosclerosis, but does not add to the antiatherogenic effect of atorvastatin, in APOE*3-Leiden.CETP mice. *J Nutr Biochem* 2013; **24**(8)**:** 1423-30.

60. Pellegrino RM, Di Veroli A, Valeri A, Goracci L, Cruciani G. LC/MS lipid profiling from human serum: a new method for global lipid extraction. *Anal Bioanal Chem* 2014; **406**(30)**:** 7937-48.

61. Basit A, Piomelli D, Armirotti A. Rapid evaluation of 25 key sphingolipids and phosphosphingolipids in human plasma by LC-MS/MS. *Anal Bioanal Chem* 2015; **407**(17)**:** 5189-98.

62. Nordmann TM, Dror E, Schulze F, Traub S, Berishvili E, Barbieux C *et al.* The Role of Inflammation in beta-cell Dedifferentiation. *Sci Rep* 2017; **7**(1)**:** 6285.

63. Rutti S, Ehses JA, Sibler RA, Prazak R, Rohrer L, Georgopoulos S *et al.* Low- and high-density lipoproteins modulate function, apoptosis, and proliferation of primary human and murine pancreatic beta-cells. *Endocrinology* 2009; **150**(10)**:** 4521-30.

Table 1. Lipid parameters post-surgery in Sham *ad libitum* (Sham AL=12), Body weight-matched (BWm=11) and Roux-en-Y gastric bypass (RYGB=11) operated ApoE*3Leiden.CETP male mice

	Sham AL	**BWm**	**RYGB**
TC (mg/dL)	261 ± 13 [a]	218 ± 10 [b]	109 ± 5 [c]
Non HDL-C (mg/dL)	216 ± 15 [a]	124 ± 13 [b]	70 ± 5 [c]
HDL-C (mg/dL)	45 ± 3 [a]	42 ± 5 [a]	38 ± 4 [a]
TG (mg/dL)	269 ± 34 [a]	114 ± 27 [b]	110 ± 17 [b]
NEFA (µmol/L)	1073 ± 52 [a]	764 ± 55 [b]	697 ± 78 [b]
BHB (mmol/L)	204 ± 64 [a]	246 ± 75 [a]	153 ± 27 [a]
Cer (µM)	3.9 ± 0.2 [a]	3.4 ± 0.3 [a]	2.4 ± 0.1 [b]
dhCer (nM)	445 ± 78 [a]	213 ± 70 [a,b]	166 ± 27 [b]
doxCer (nM)	687 ± 37 [a]	581 ± 50 [a]	405 ± 32 [b]
dh-doxCer (nM)	29.4 ± 3.5 [a]	22.5 ± 3.4 [a]	29.1 ± 5.1 [a]
hexCer (nM)	4.8 ± 0.6 [a]	3.7 ± 0.5 [a,b]	2.7 ± 0.1 [b]
SM (µM)	176 ± 7 [a]	134 ± 10 [b]	107 ± 6 [b]
S1P (nM)	599 ± 50 [a]	515 ± 41 [a,b]	409 ± 48 [b]
SB (nM)	208 ± 12 [a]	206 ± 20.3 [a]	159 ± 4 [a]
doxSB (nM)	13.5 ± 1.9 [a]	21.5 ± 3.2 [a,b]	23.9 ± 2.1 [b]

Total cholesterol (TC), High density lipoprotein cholesterol (HDL-C), non-esterified fatty acids (NEFA), beta-hydroxybutyrate (BHB), ceramide (Cer), dihydroceramide (dhCer), deoxyceramide (doxCer), dihydro deoxyceramide (dh-doxCer), hexosylceramide (hexCer), sphingomyelin (SM), sphingosin 1-phosphate (S1P), sphingoid base (SB), and deoxy sphingoid base (doxSB).

Data are presented as mean ± SEM. Parameters with differing superscript letters differ from each other at the $P < 0.05$ level by post hoc Bonferroni adjustment after significant intergroup differences were found by one-way ANOVA.

Table 2. Plasma cytokines levels (pg/mL) before (pre-op) and after (post-op) surgery in Sham *ad libitum* (Sham AL=8), Body weight-matched (BWm=7) and Roux-en-Y gastric bypass (RYGB=7) operated ApoE*3Leiden.CETP male mice.

	Sham AL		**BWm**		**RYGB**	
	Pre –op	**Post-op**	**Pre -op**	**Post-op**	**Pre -op**	**Post-op**
IFN-γ	0.25 ± 0.02 [a]	0.58 ± 0.04 [b]	0.25 ± 0.03 [a]	0.61 ± 0.06 [b]	0.25 ± 0.02 [a]	0.72 ± 0.06 [b]
IL-10	32.3 ± 3.2 [a,b]	38.9 ± 5.3 [a]	23.7 ± 2.0 [b]	33.6 ± 3.9 [a,b]	25.2 ± 1.9 [a,b]	38.4 ± 3.2 [a,b]
IL12p70	49.8 ± 4.3 [a,b]	57.9 ± 4.0 [a,b]	44.9 ± 6.3 [a,b]	56.6 ± 4 [a,b]	39.9 ± 5.2 [a]	65.1 ± 5.7 [b]
IL-1β	6.16 ± 1.75 [a,b]	1.49 ± 0.03 [a]	3.71 ± 0.81 [a,b]	2.25 ± 0.35 [a.b]	5.67 ± 1.53 [a,b]	9.91 ± 4.15 [b]
IL-2	6.81 ± 0.42 [a,b]	7.54 ± 0.65 [a,b]	6.24 ± 0.51 [a]	6.52 ± 0.30 [a,b]	6.05 ± 0.29 [a]	8.73 ± 0.62 [b]
IL-4	1.92 ± 0.17 [a]	1.97 ± 0.19 [a]	1.33 ± 0.16 [a]	1.87 ± 0.2 [a]	1.51 ± 0.36 [a]	1.81 ± 0.42 [a]
IL-5	3.76 ± 0.42 [a,b]	3.58 ± 0.47 [a.b]	2.49 ± 0.27 [a]	4.15 ± 0.74 [a.b]	3.78 ± 0.73 [a,b]	4.95 ± 0.68 [a.b]
IL-6	19.9 ± 1.5 [a]	35.7 ± 4.0 [a]	16.9 ± 2.1 [a]	32.5 ± 4.9 [a]	25.1 ± 5.2 [a]	57.2 ± 8.9 [b]
KG/GRO	146 ± 19 [a]	160 ± 23 [a]	140± 19 [a]	144 ± 31 [a]	118 ± 30 [a]	106 ± 18 [a]
TNF-α	16.7 ± 1.3 [a,b]	25.9 ± 4.1 [b]	14.4 ± 3.1 [a]	16.8 ± 1.9 [a,b]	14.4 ± 2.3 [a]	20.4 ± 2.6 [a,b]

Data are represented as mean ± SEM. Parameters with differing superscript letters differ from each other at the P< 0.05 level by post hoc Tukey adjustment after significant intergroup differences were found by multiple comparisons 2-way ANOVA.

Table 3. Liver histological scores [28, 29] in Sham *ad libitum* (Sham AL=12), Body weight-matched (BWm=11), and Roux-en-Y gastric bypass (RYGB=11) operated ApoE*3Leiden.CETP male mice.

	Sham AL	**BWm**	**RYGB**
Age mice (weeks)	17-20	17-20	17-20
Liver[n]	12	11	11
Hepatocellular lipidosis[§]	12/12	8/11	2/11
Grade 0	0	3	9
Grade 1	0	4	1
Grade 2	0	3	1
Grade 3	2	0	0
Grade 4	10	1	0
Average severity[$]	3.8 ± 0.1^{a}	1.3 ± 0.4^{b}	0.3 ± 0.2^{c}
Chronic Inflammation[§]	5/12	8/11	9/11
Grade 0	7	3	2
Grade 1	5	8	7
Grade 2	0	0	2
Grade 3	0	0	0
Grade 4	0	0	0
Average severity[$]	0.4 ± 0.1^{a}	$0.7 \pm 0.1^{a,b}$	1.0 ± 0.2^{b}
Hepatocellular Eosinophilic Cytoplasmic Inclusions[§]	11/12	10/11	9/11
Grade 0	1	1	2
Grade 1	11	9	8
Grade 2	0	1	1
Grade 3	0	0	0
Grade 4	0	0	0
Average severity[$]	0.9 ± 0.1^{a}	1.0 ± 0.1^{a}	0.9 ± 0.2^{a}

[n]: number of liver samples analysed, [§]: incidence of the findings, [$]: Average severity calculated as sum of all scores divided by the total number of liver samples analysed.

Data are represented as mean ± SEM. Parameters with differing superscript letters differ from each other at the $P < 0.05$ level by post hoc Bonferroni adjustment after significant intergroup differences were found by one-way ANOVA.

Figure 1

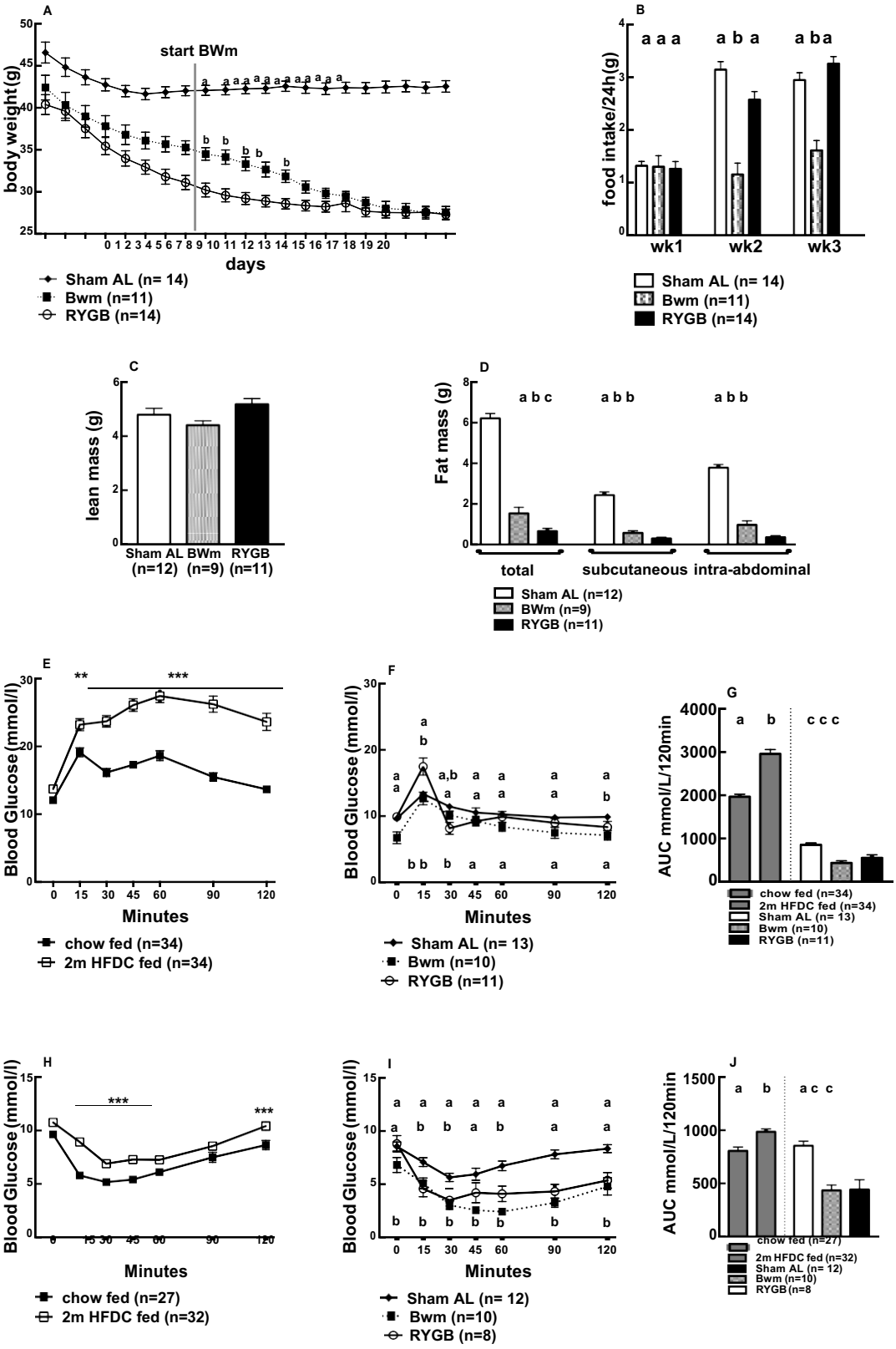
A
start BWm
body weight(g)
days
Sham AL (n= 14)
Bwm (n=11)
RYGB (n=14)
B
a a a
a b a
a ba
food intake/24h(g)
wk1
wk2
wk3
Sham AL (n= 14)
Bwm (n=11)
RYGB (n=14)
C
lean mass (g)
Sham AL (n=12)
BWm (n=9)
RYGB (n=11)
D
Fat mass (g)
a b c
a b b
a b b
total
subcutaneous
intra-abdominal
Sham AL (n=12)
BWm (n=9)
RYGB (n=11)
E
Blood Glucose (mmol/l)
Minutes
chow fed (n=34)
2m HFDC fed (n=34)
F
Blood Glucose (mmol/l)
Minutes
Sham AL (n= 13)
Bwm (n=10)
RYGB (n=11)
G
AUC mmol/L/120min
chow fed (n=34)
2m HFDC fed (n=34)
Sham AL (n= 13)
Bwm (n=10)
RYGB (n=11)
H
Blood Glucose (mmol/l)
Minutes
chow fed (n=27)
2m HFDC fed (n=32)
I
Blood Glucose (mmol/l)
Minutes
Sham AL (n= 12)
Bwm (n=10)
RYGB (n=8)
J
AUC mmol/L/120min
chow fed (n=27)
2m HFDC fed (n=32)
Sham AL (n= 12)
Bwm (n=10)
RYGB (n=8

Figure 2

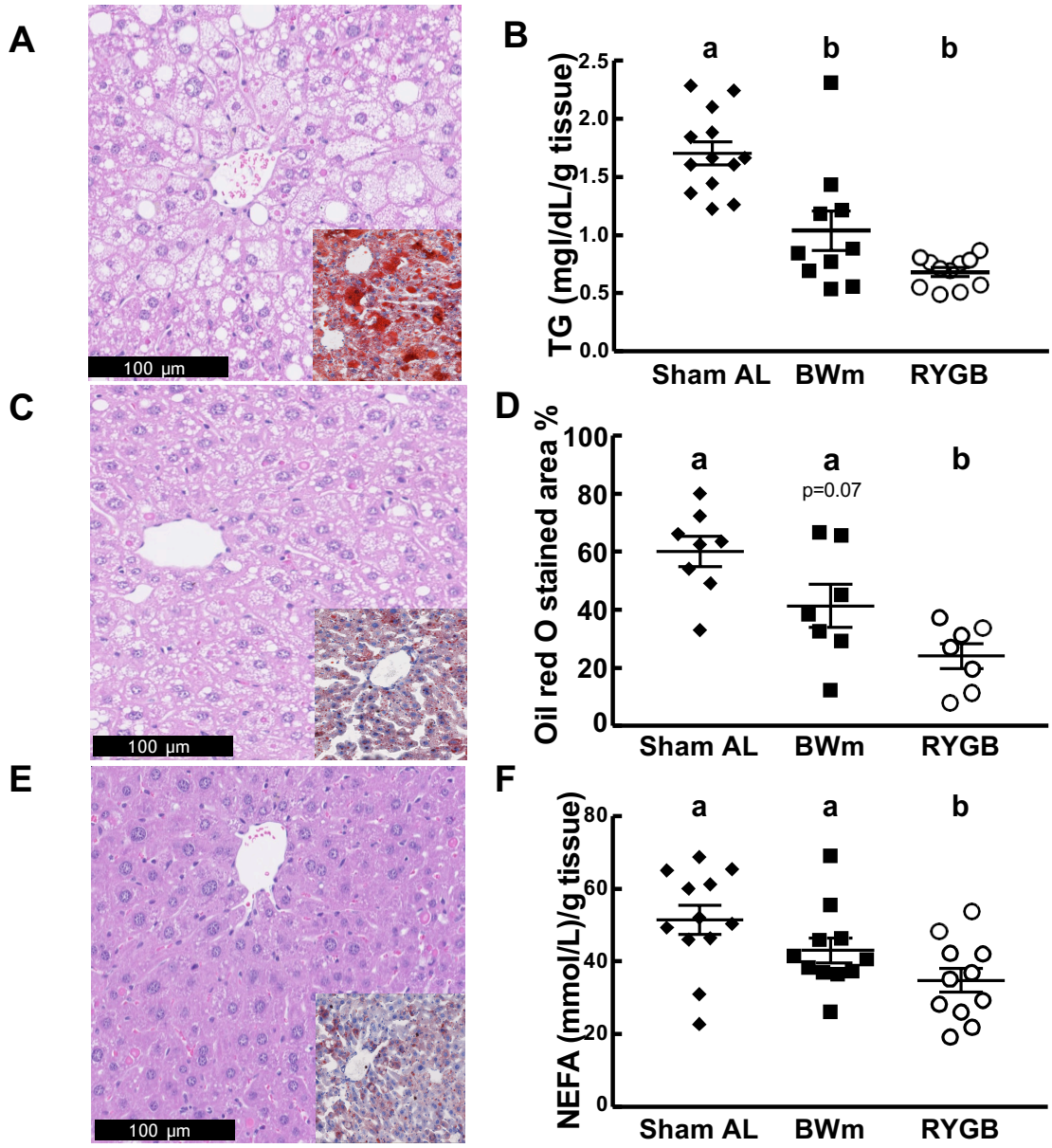
A
100 µm
B
a
b
b
TG (mgl/dL/g tissue)
2.5
2.0
1.5
1.0
0.5
0.0
Sham AL
BWm
RYGB
C
100 µm
D
a
a
b
p=0.07
Oil red O stained area %
100
80
60
40
20
0
Sham AL
BWm
RYGB
E
100 µm
F
a
a
b
NEFA (mmol/L)/g tissue
80
60
40
20
0
Sham AL
BWm
RYGB

Figure 3

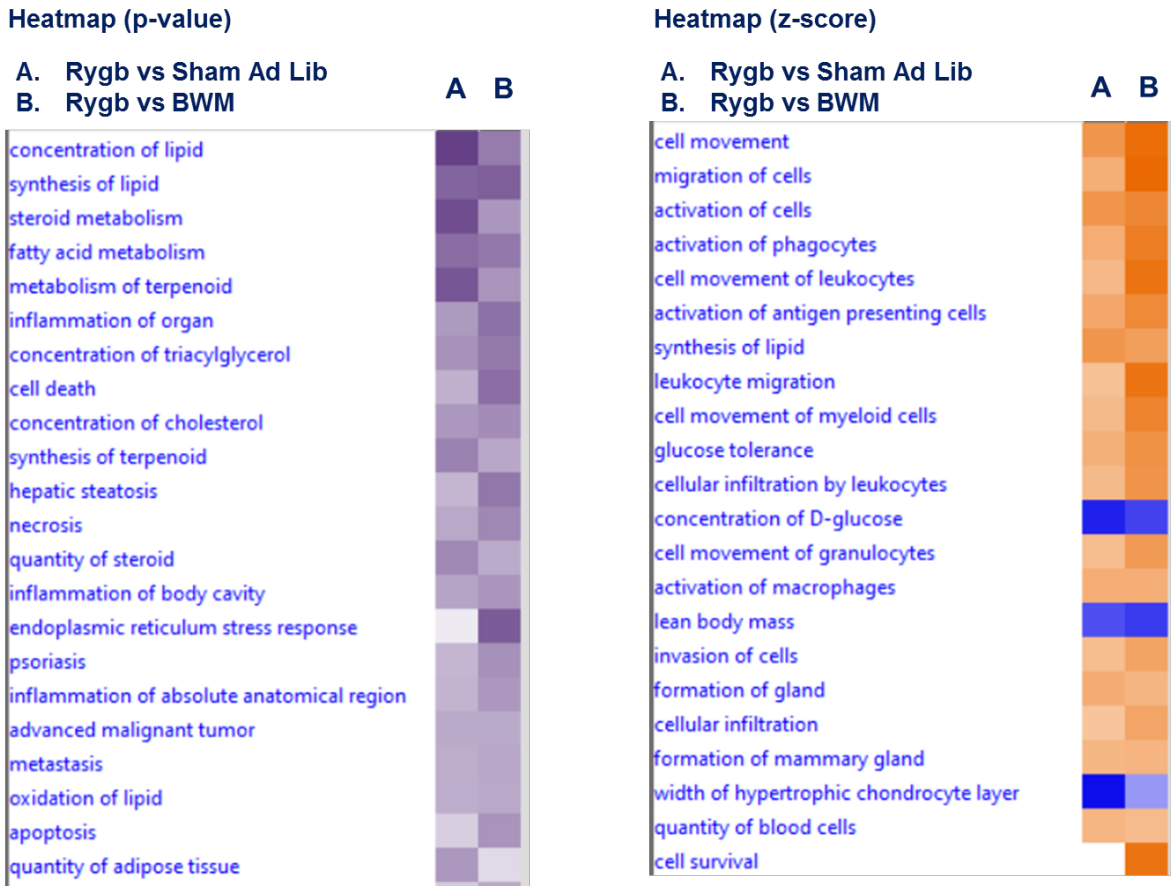
Heatmap (p-value)
A. Rygb vs Sham Ad Lib
B. Rygb vs BWM
A
B
concentration of lipid
synthesis of lipid
steroid metabolism
fatty acid metabolism
metabolism of terpenoid
inflammation of organ
concentration of triacylglycerol
cell death
concentration of cholesterol
synthesis of terpenoid
hepatic steatosis
necrosis
quantity of steroid
inflammation of body cavity
endoplasmic reticulum stress response
psoriasis
inflammation of absolute anatomical region
advanced malignant tumor
metastasis
oxidation of lipid
apoptosis
quantity of adipose tissue
Heatmap (z-score)
A. Rygb vs Sham Ad Lib
B. Rygb vs BWM
A
B
cell movement
migration of cells
activation of cells
activation of phagocytes
cell movement of leukocytes
activation of antigen presenting cells
synthesis of lipid
leukocyte migration
cell movement of myeloid cells
glucose tolerance
cellular infiltration by leukocytes
concentration of D-glucose
cell movement of granulocytes
activation of macrophages
lean body mass
invasion of cells
formation of gland
cellular infiltration
formation of mammary gland
width of hypertrophic chondrocyte layer
quantity of blood cells
cell survival

SUPPLEMENTARY DATA

Supplementary Material and Methods

Sphingolipids measurements

Analysis were performed via MS-LC system at the Institute of Clinical Chemistry, University of Zurich and University Hospital Zurich, Switzerland. 20 µL of heparin plasma were extracted following the MMC (Methanol:methyl-tert-butyl ether:chloroform method) protocol from Pellegrino et al [60] and analyzed. 1mL of Methanol / MTBE / Chloroform (MMC 1.33/1/1 v/v/v) mixture containing internal standards (D7-Sphinganine, D7-Sphingosine, Ceramide d18:0 / 12:0, Ceramide d18:1 / 12:0, deoxy ceramide (doxCer) m18:0 / 12:0, doxCer m18:1 / 12:0, Sphingomyelin (SM) d18:1 / 12:0, Glucosylceramide (GluCer) d18:1 / 8:0, D7-Sphingosine-1-Posphate (S1P), Posphates (PA) 17:0 / 17:0, Phosphoethanolamine (PE) 14:0 / 14:0, Lyso-phosphoethanolamine (LPE) 17:1, Phosphoglycerols (PG) 17:0 / 17:0, Phosphocolines (PC) 14:0 / 14:0, PC 24:0 / 24:0, Lyso-phosphocolines (LPC) 17:0) was added to the plasma and vortexed for 20 seconds. Then, the mixture was shaken for 20 min in an Eppendorf Thermo shaker at 37°C at 1400 rpm. Protein precipitate was pelleted by centrifuging for 5 min at 16000 rpm at 24°C, and 1mL of the supernatant was transferred to a new tube. The solvent was dried under a stream of N_2. For LC-MS analysis, the sample was re-suspended in 100 µL methanol and transferred to MS vial. For one run, 25 µL was injected into the LC system.

For quality control, a pooled sample was made, taking additional 5 µL of each sample and combined with a pool. From the pool, 2.5 µL, 5 µL, 10 µL, and 20 µL were aliquoted to a new tube and filled with PBS to 20 µL. These control samples were treated the same as the rest of the samples for extraction.

For chromatographic separation, a C18 Uptispere (120 Å, 5 µm, 125 × 2 mm) column (Interchim, Montluçon, France) was used. The following mobile phases were used: Eluting A: Water / Acetonitrile 80/20 v/v with 10mM ammonium Acetate and 0.1% formic acid and Eluting B: Isopropanol / Acetonitrile 80/20 v/v with 10mM ammonium Acetate and 0.1% formic acid. The gradient was started with 70% A and 30% B for 1.5 min and is increased to 100% B within

the next 17min. After the column is washed with 100% B for 7 min and re-equilibrated to starting condition within the next 5 min. Conditions were adopted from Basit et al [61]. Samples were analyzed on a Q Exactive (Thermo, Reinach, BL, Switzerland) using a heated electrospray ionization (HESI) interface. For mass spectral detection in positive mode, the following parameters were set on the HESI source: spray voltage 3.5kV, a vaporizer temperature of 300°C, sheath gas pressure 20 AU, aux gas 8 AU and a capillary temperature of 320°C. The detector is set to an MS^2 method using a top^{10} approach with a 140k resolution for full spectrum and 17.5k for MS^2, where a full scan is followed by fragmentation spectra of the ten most intense ions per full scan with stepped collision energy between 25 and 30. For the selection of ions to be fragmented, a dynamic exclusion filter was applied which will exclude ions after fragmentation for 20 seconds.

Liver and Pancreas histology

All animals were euthanized by cardiac puncture 20 days after surgery and a complete necropsy was performed on each mouse. Organ of interest (liver and pancreas) were removed and fixed in 10% neutral-buffered formalin (Formafox, Hittmau, Switzerland) or snap-frozen. Formalin-fixed samples were trimmed according to guidelines[28] , dehydrated through graded alcohols and routinely paraffin wax embedded. Consecutive sections (3–5 µm) were prepared, mounted on glass slides and routinely stained with hematoxylin eosin (HE) or subjected to immunohistochemical staining. Immunohistochemistry was employed on pancreas slices to semi-quantify insulin (A0564 DAKO, Agilent, Switzerland) and glucagon (A0565 DAKO, Agilent, Switzerland).

Microscopic findings in the HE-stained livers slides were classified with standard pathological nomenclature and severities of findings were graded on a scale of 0 to 4 (no finding present 0, minimal 1, mild 2, moderate 3, or severe 4). Grades of severity for microscopic findings were subjective; minimal was the least extent discernible and severe was the greatest extent possible [29]. Oil red O (ORO) staining was performed on snap-frozen cryomold-embedded

livers. Liver sections were cut at 6 µm, mounted on glass slides and allowed to dry at room temperature. They were then rinsed briefly in 50% ethanol, incubated in a 60% aqueous ORO solution (375 mg Oil Red O [Merck KGaA, Darmstadt, Germany] in isopropanol) at room temperature for 20 min, rinsed again in 50% ethanol and counterstained with hematoxylin for 2 min. ORO stained slides were scanned using a digital slide scanner (NanoZoomer-XR C12000, Hamamatsu Photonics K.K., Japan) and the fat content was calculated in the digital slides using the Visiopharm Integrator System (VIS, version 4.5.1.324, Visiopharm, Hørsholm, Denmark). Briefly, a threshold classification allowed recognition of positive (red) hepatocellular cytoplasm and negative hepatic parenchyma, and the results were expressed as positive area versus total area in the whole liver section. Data are presented as average (± SEM) percentage of lipid-containing parenchyma in the group.

Islets isolation and Glucose-Stimulated insulin secretion

After sacrifice, pancreas of few randomly selected mice was digested and islets were isolated following an islet isolation procedure adapted from Nordmann et al [62]. Islets were let recover for 24h in a cell culture incubator (37°C, 20%O_2 and 5%CO_2) then hand picked and plated 10 islets/well into a 24 well ECM plate (Novamed, Jerusalem, Israle) before performing glucose-stimulated insulin secretion (GSIS) test following a modified procedure from Rütti et al [63]. Krebs-Ringer phosphate solution supplemented with 0.1% BSA and 1M Hepes (KRH) were used. Islets were preincubated for 30 min with KRH with 2.8 mM glucose at 37°C to let islets adapt to KRH solution before starting to collect the supernatant to measure insulin secretion. To measure basal insulin release, islets were incubated for 1h with fresh KRH + 2.8 mM glucose followed by 1h with KRH + 13.7 mM glucose in order to measure stimulated insulin release. At each incubation, supernatant was collected, immediately frozen and used to measure insulin. To quantify insulin content after the two incubations, islets were lysed with 0.18M HCl in 70% EtOH at 4°C overnight. Insulin was measured with the Mouse Insulin ELISA

(Mercodia AB, Uppsala, Sweden) and insulin secretion was calculated as percentage of total insulin content.

Supplementary result

Pancreas

Pancreas histological analysis did not show any differences among groups, e.g. for islets size, number of islets or quantity of glucagon/insulin in the islets. This is in agreement with our findings during static glucose stimulation in isolated islets from RYGB, BWm and sham AL mice at time of sacrifice. Static high glucose stimulation (13.7mM) increased insulin secretion in pancreatic islets isolated from all groups. Pancreatic islets isolated from sham AL mice showed the highest insulin secretion of 1.5 ± 0.2% compared to 0.5 ± 0.1% of RYGB and 1.2 ± 0.3 of BWM, despite similar levels of basal insulin secretion at 2.8 mM glucose.

Figure 1S

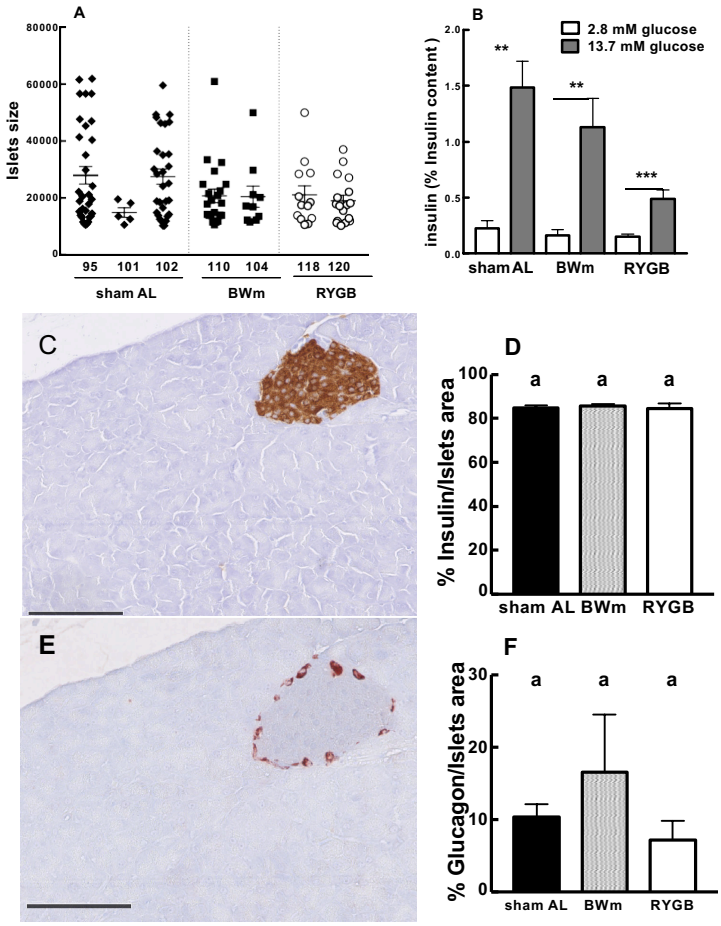

Fig 1S: (A) Islets quantification by size from Sham *ad libitum* (Sham AL=3), body weight-matched (BWm=2) and Roux-en-Y (RYGB=2) male ApoEL.CETP operated mice. Islets above 15000 μm^2 were considered for this quantification. No difference was found among groups. (B) Insulin concentration relative to insulin content in islets from Sham AL, BWm and RYGB operated mice 3 weeks after surgery. After isolation, islets were let to recover for 24h then stimulated for 60 min with low (2.8 mM) and high (13.7mM) glucose solution, resp., to measure insulin secretion. Sham AL secreted more insulin compared to BWm and RYGB isolated islets. (C -D) Insulin staining and quantification in Sham AL, BWm and RYGB operated mice, scale bars = 100 µm.

(E-F) Glucagon staining and quantification in Sham AL, BWm and RYGB operated mice, scale bars = 100 µm.

Data are represented as mean ± SEM. **, *** P<0.01 or 0.001, Sham AL vs BWm and RYGB, resp., after Paired Student's T test (B) or after post hoc Bonferroni adjustment significant intergroup differences were found by one-way ANOVA multiple comparison (D-F); different letters indicate significant differences.

6 Discussion

This dissertation project was part of RESOLVE, a consortium of 12 multidisciplinary teams of computational modellers, engineers, biomedical researchers and clinicians whose goal was to elucidate the underlying mechanisms that connect the main pathophysiological hallmarks of the MetS: low HDL-C, high triglycerides and loss of glycaemic control. Particularly, RESOLVE wanted to develop a computational modelling system able to combine outcome from pre-clinical and clinical research with network analyses to potentially identify new targets for the MetS, e.g. to develop new strategies or drugs to treat the MetS.

As a matter of fact, the mathematical model is still under validation since it is quite difficult to translate animal model research directly to human research and to clinical applications; nevertheless, some aspects of the MetS could be validated with the computational model: for example, a new method to quantify the interaction between glucose and NEFA had been proposed [164], or a computational model to describe T2DM [165]. Another aspect that has been developped in this physiology-based dynamic model is a way to analyse postprandial glucose and insulin profiles, e.g. in situations of impaired glucose tolerance and insulin resistance (personal communication).

RESOLVE in general and, particularly, in our part where we carried our pre-clinical studies using a humanized murine model, the ApoE3L.CETP mice, aimed to clarify the complex polygenic and multifactorial setting of the MetS as well as the pathogenic sequence in the development of insulin resistance and the high triglyceride/low HDL-C phenotype as well as their relationships.

My contribution in the RESOLVE project aimed to investigate the physiological effects of RYGB in ApoE3L.CETP mice in order to produce computational model predictions that could eventually be verified in parallel studies conducted in MetS patients who underwent RYGB surgery by another partner of RESOLVE.

To provide these data, firstly, we characterized the effect of long-term access to a HFHC diet in the ApoE*3Leiden.CETP mice on feeding behaviour, glucose and lipid metabolism, highlighting the presence of two different phenotypes: responder and non-responder mice. Secondly, we deciphered the effects of RYGB surgery in obese male responder ApoE*3Leiden.CETP mice on glucose and lipid metabolism. Hence, we highlighted the relevance of surgery-specific effects compared to the pure body weight loss and caloric restriction mediated effects.

Considering that individual studies have been discussed in detail in the respective sections, for this discussion part, I will briefly summarize the general conclusion and focus on potential future perspectives.

It is well established that the obesity epidemic is increasing worldwide and that it is one of the main factors that contributes to and drives hypertension, elevated plasma insulin concentrations and insulin resistance (IR), and, eventually, T2DM, hypertriglyceridaemia and low HDL-C levels. All these mentioned factors are components of the MetS [14, 15].
Moreover, these symptoms are not only indicating some features of the MetS alone, but it has been shown that they are interconnected. For example, data in the literature indicated that T2DM patients might show features of dyslipidaemia [166], or that patients treated with statins showed increased T2DM incidence [167] or that elevated HDL-C may improve function and survival of pancreatic β-cells [168]. Even if this interconnection has been proven in many studies [166-169], up to now it is not known whether high triglycerides/low HDL-C causes IR or if it is the opposite, or even if they are both appear simultaneously.

Compared to all the animal model used in obesity and MetS research [170], our ApoE3L.CETP mouse model is known to better describe the MetS in terms of both glucose and lipid metabolism in response to a Western type diet [30, 32, 46] than other available rodent models.

Furthermore, some degree of phenotypic heterogeneity was reported among age-matched ApoE3L.CETP mice kept under similar experimental conditions [46], and we clarified it by showing the presence of two different phenotypes: responder (R) mice and non-responder (NR) mice. Because the human population is highly heterogeneous, we consider the same feature in ApoE3L.CETP mice useful for its role in pre-clinical research.

We highlighted in detail a distinction between R mice and NR mice responses to a HFHC diet. Mice classified as R mice, indeed, exhibited the features of the MetS: increased body weight, increased subcutaneous and intra-abdominal adipose tissues, increased plasma total cholesterol, triglycerides and HDL-C [30, 32, 46, 171], and reduced glucose sensitivity [172, 173] compared to NR mice. Particularly, we confirmed that the separation between R mice and NR mice at an early stage based on triglycerides levels seemed to be generally predictive of the final phenotype, even though we observed also a certain degree of heterogeneity within our NR and R populations, respectively, and in our analysis in comparing NR mice and R mice; in other words, we pointed out a partial overlap between the two groups.

A limitation in the use of NR mice in MetS studies found its explanation in liver histology: not only did NR mice exhibit reduced levels of lipidosis, but also showed prominent hepatic inflammatory and proliferative changes. These findings suggested that the hepatic pathology seen in NR mice may have a detrimental effect on hepatic function, making them unhealthy controls to the R mice; this needs to be considered when using these mice in studies of the MetS.

Some aspects in the heterogeneity in this model, related to the responder mice, are also representative for the human situation with a very heterogenous patient population; in the first part of these studies using the ApoE3L.CETP mice we studied some reasons leading to this heterogeneity and are propose the introduction of other parameters such as liver histology for the final classification of these mice, in addition to circulating metabolites.

We therefore suggest that it is important to identify NR mice and to use them with caution; when assessing aspects of the MetS with R mice, appropriate controls should also be R mice, with potentially an additional control with NR mice, keeping the mentioned limitations in mind. It may also be suggested the use different controls such as chow fed R mice, huCETP mice, ApoE-/- chow and HFHC diet; other diet induced obese (DIO) mice [174] could also be used as an established model to define some aspect of the MetS.

The second part of my dissertation aimed at clarifying the effects of RYGB in ApoE3L.CETP responder mice. Our findings confirmed the use of RYGB as a “golden standard” procedure in treating the MetS [119]. Particularly, we used the body-weight matched (BWm) mice as one of our control to be able to discriminate between pure body weight loss dependent effect from surgical effects.

In our experimental setup, RYGB mice lost weight without altering their food intake, while the BWm mice had to be highly food restricted to maintain the same body weight as RYGB mice; the difference may be due to the increased energy expenditure in RYGB mice [132, 175]. This aspect is different from what has been shown in rats and in humans. In fact, RYGB operated rats had reduced food intake compared to Sham AL rats despite an increase in their energy expenditure [133, 176, 177]; in humans increased energy expenditure has been reported in some [178, 179], but not in all studies.

In rodents or in humans, body weight loss also indicates a loss in fat mass [126, 180]. Typically, body weight and fat loss occurs immediately after surgery until a plateau is reached 14 days after the surgery for rodents and around one year after surgery for humans [181].

Our results highlighted specific RYGB effects that appeared to be body weight loss dependent [97, 132, 136] and some other effects independent from body weight loss [135, 182].

In agreement with other studies, our results showed improvement in liver lipidosis [183], lipid metabolism [184, 185] and glucose metabolism [132, 186, 187], and these effects were dependent to body weight loss since they were also found in BWm mice.

Nonetheless, specific greater reduction in some lipid parameters such as total cholesterol and non HDL-C, in RYGB mice indicated a direct surgical effect independently from body weight loss [136]. We hypothesized that physiological changes in the gut, mainly in lipid absorption, i.e. reduced cholesterol uptake, could explain why RYGB operated mice may have had lower total cholesterol and non-HDL-C levels [142, 143].

Moreover, some sphingolipids, e.g. ceramide were highly reduced in RYGB mice similarly to what has been shown in human studies [155, 182, 188]. To us, this aspect was interesting because not only it has been shown that increased sphingolipids, especially ceramide, were correlated with obesity [155] and atherosclerosis [189, 190], but also that ceramide decreases after RYGB in humans [155, 182, 188]. Hence, this specific result underlined how important data can be translated from animal models to humans. Particularly, we believe that this is an important goal in the context of modelling metabolic data from a humanized animal model such as ApoE3L.CETP mice that can be used to predict human outcomes.

Therefore, our data will help in the development of the computational model in RESOLVE and we could provide evidence confirming the importance of bariatric surgery in defeating the MetS.

Based on our preliminary results and the consideration that RYGB improves insulin secretion [132, 191] and that HDL may also directly modulate glucose metabolism by influencing pancreatic β-cells [192, 193], further experiments could investigate how RYGB ameliorates functionality and viability of β-cells via HDL's anti-apoptotic effect. This could perhaps include tests of whether islets function and viability are improved after RYGB, and on the other hand investigations whether HDL function is improved after RYGB.

These future investigations will help to understand the effect of bariatric surgery on the function of pancreatic islets in general, and on the functionality of HDL lipoprotein in respect to HDL's

role in modulating pancreatic islet cell viability. Hence, these experiments will provide a crucial missing piece that connects dyslipidemia and diabetes in obesity.

7 Abbreviations

ApoE – apolipoprotein E

BPD-DS – Biliopancreatic Diversion with Duodenal Switch

CAD – Cardiovascular Disease

CETP – Cholesterol Ester Transfer Protein

GB – Gastric Banding

HDL-C – High Density Lipoprotein Cholesterol

HFHC – High Fat High Cholesterol

IR – Insulin Resistance

IST – Insulin Sensitivity Test

LDL-C – Low Density Lipoprotein Cholesterol

MetS – Metabolic syndrome

NAFLD – Non-Alcoholic Fatty Liver Disease

OGTT – Oral Glucose Tolerance Test

RYGB – Roux-en-Y Gastric Bypass

SG – Sleeve Gastrectomy

T2DM – Type 2 Diabetes Mellitus

TC - Total Cholesterol

TG – Triglycerides

VLDL – Very Low Density Lipoprotein

8 References

1. Collaboration NCDRF: **Worldwide trends in body-mass index, underweight, overweight, and obesity from 1975 to 2016: a pooled analysis of 2416 population-based measurement studies in 128.9 million children, adolescents, and adults**. *Lancet* 2017, **390**(10113):2627-2642.
2. Bleich SN, Vercammen KA, Zatz LY, Frelier JM, Ebbeling CB, Peeters A: **Interventions to prevent global childhood overweight and obesity: a systematic review**. *Lancet Diabetes Endocrinol* 2017.
3. Hruby A, Hu FB: **The Epidemiology of Obesity: A Big Picture**. *Pharmacoeconomics* 2015, **33**(7):673-689.
4. Ravussin E, Valencia ME, Esparza J, Bennett PH, Schulz LO: **Effects of a traditional lifestyle on obesity in Pima Indians**. *Diabetes Care* 1994, **17**(9):1067-1074.
5. Bouchard C, Tremblay A, Despres JP, Nadeau A, Lupien PJ, Theriault G, Dussault J, Moorjani S, Pinault S, Fournier G: **The response to long-term overfeeding in identical twins**. *N Engl J Med* 1990, **322**(21):1477-1482.
6. Loos RJ: **The genetics of adiposity**. *Curr Opin Genet Dev* 2018, **50**:86-95.
7. den Hoed M, Smeets AJ, Veldhorst MA, Nieuwenhuizen AG, Bouwman FG, Heidema AG, Mariman EC, Westerterp-Plantenga MS, Westerterp KR: **SNP analyses of postprandial responses in (an)orexigenic hormones and feelings of hunger reveal long-term physiological adaptations to facilitate homeostasis**. *Int J Obes (Lond)* 2008, **32**(12):1790-1798.
8. Speliotes EK, Willer CJ, Berndt SI, Monda KL, Thorleifsson G, Jackson AU, Lango Allen H, Lindgren CM, Luan J, Magi R *et al*: **Association analyses of 249,796 individuals reveal 18 new loci associated with body mass index**. *Nat Genet* 2010, **42**(11):937-948.
9. Heitmann BL, Westerterp KR, Loos RJ, Sorensen TI, O'Dea K, McLean P, Jensen TK, Eisenmann J, Speakman JR, Simpson SJ *et al*: **Obesity: lessons from evolution and the environment**. *Obes Rev* 2012, **13**(10):910-922.
10. Qasim A, Turcotte M, de Souza RJ, Samaan MC, Champredon D, Dushoff J, Speakman JR, Meyre D: **On the origin of obesity: identifying the biological, environmental and cultural drivers of genetic risk among human populations**. *Obes Rev* 2018, **19**(2):121-149.
11. Barlow SE, Expert C: **Expert committee recommendations regarding the prevention, assessment, and treatment of child and adolescent overweight and obesity: summary report**. *Pediatrics* 2007, **120 Suppl 4**:S164-192.
12. Kitahara CM, Flint AJ, Berrington de Gonzalez A, Bernstein L, Brotzman M, MacInnis RJ, Moore SC, Robien K, Rosenberg PS, Singh PN *et al*: **Association between class III obesity (BMI of 40-59 kg/m2) and mortality: a pooled analysis of 20 prospective studies**. *PLoS Med* 2014, **11**(7):e1001673.
13. Singh AS, Mulder C, Twisk JW, van Mechelen W, Chinapaw MJ: **Tracking of childhood overweight into adulthood: a systematic review of the literature**. *Obes Rev* 2008, **9**(5):474-488.
14. Grundy SM: **Metabolic syndrome pandemic**. *Arterioscler Thromb Vasc Biol* 2008, **28**(4):629-636.
15. Kopelman PG: **Obesity as a medical problem**. *Nature* 2000, **404**(6778):635-643.
16. Aguilar M, Bhuket T, Torres S, Liu B, Wong RJ: **Prevalence of the metabolic syndrome in the United States, 2003-2012**. *JAMA* 2015, **313**(19):1973-1974.
17. Kennedy AJ, Ellacott KL, King VL, Hasty AH: **Mouse models of the metabolic syndrome**. *Dis Model Mech* 2010, **3**(3-4):156-166.
18. Zhang Y, Proenca R, Maffei M, Barone M, Leopold L, Friedman JM: **Positional cloning of the mouse obese gene and its human homologue**. *Nature* 1994, **372**(6505):425-432.

19. Coleman DL, Hummel KP: **The influence of genetic background on the expression of the obese (Ob) gene in the mouse**. *Diabetologia* 1973, **9**(4):287-293.
20. Tschop M, Heiman ML: **Rodent obesity models: an overview**. *Exp Clin Endocrinol Diabetes* 2001, **109**(6):307-319.
21. Semenkovich CF: **Insulin resistance and atherosclerosis**. *J Clin Invest* 2006, **116**(7):1813-1822.
22. Ishibashi S, Brown MS, Goldstein JL, Gerard RD, Hammer RE, Herz J: **Hypercholesterolemia in low density lipoprotein receptor knockout mice and its reversal by adenovirus-mediated gene delivery**. *J Clin Invest* 1993, **92**(2):883-893.
23. Plump AS, Smith JD, Hayek T, Aalto-Setala K, Walsh A, Verstuyft JG, Rubin EM, Breslow JL: **Severe hypercholesterolemia and atherosclerosis in apolipoprotein E-deficient mice created by homologous recombination in ES cells**. *Cell* 1992, **71**(2):343-353.
24. Coenen KR, Gruen ML, Hasty AH: **Obesity causes very low density lipoprotein clearance defects in low-density lipoprotein receptor-deficient mice**. *J Nutr Biochem* 2007, **18**(11):727-735.
25. Coenen KR, Hasty AH: **Obesity potentiates development of fatty liver and insulin resistance, but not atherosclerosis, in high-fat diet-fed agouti LDLR-deficient mice**. *Am J Physiol Endocrinol Metab* 2007, **293**(2):E492-499.
26. Gruen ML, Saraswathi V, Nuotio-Antar AM, Plummer MR, Coenen KR, Hasty AH: **Plasma insulin levels predict atherosclerotic lesion burden in obese hyperlipidemic mice**. *Atherosclerosis* 2006, **186**(1):54-64.
27. Gao J, Katagiri H, Ishigaki Y, Yamada T, Ogihara T, Imai J, Uno K, Hasegawa Y, Kanzaki M, Yamamoto TT *et al*: **Involvement of apolipoprotein E in excess fat accumulation and insulin resistance**. *Diabetes* 2007, **56**(1):24-33.
28. Hofmann SM, Perez-Tilve D, Greer TM, Coburn BA, Grant E, Basford JE, Tschop MH, Hui DY: **Defective lipid delivery modulates glucose tolerance and metabolic response to diet in apolipoprotein E-deficient mice**. *Diabetes* 2008, **57**(1):5-12.
29. King VL, Hatch NW, Chan HW, de Beer MC, de Beer FC, Tannock LR: **A murine model of obesity with accelerated atherosclerosis**. *Obesity (Silver Spring)* 2010, **18**(1):35-41.
30. van den Hoek AM, van der Hoorn JW, Maas AC, van den Hoogen RM, van Nieuwkoop A, Droog S, Offerman EH, Pieterman EJ, Havekes LM, Princen HM: **APOE*3Leiden.CETP transgenic mice as model for pharmaceutical treatment of the metabolic syndrome**. *Diabetes Obes Metab* 2014, **16**(6):537-544.
31. van der Hoorn JW, de Haan W, Berbee JF, Havekes LM, Jukema JW, Rensen PC, Princen HM: **Niacin increases HDL by reducing hepatic expression and plasma levels of cholesteryl ester transfer protein in APOE*3Leiden.CETP mice**. *Arterioscler Thromb Vasc Biol* 2008, **28**(11):2016-2022.
32. Westerterp M, van der Hoogt CC, de Haan W, Offerman EH, Dallinga-Thie GM, Jukema JW, Havekes LM, Rensen PC: **Cholesteryl ester transfer protein decreases high-density lipoprotein and severely aggravates atherosclerosis in APOE*3-Leiden mice**. *Arterioscler Thromb Vasc Biol* 2006, **26**(11):2552-2559.
33. Irace C, Cortese C, Fiaschi E, Carallo C, Sesti G, Farinaro E, Gnasso A: **Components of the metabolic syndrome and carotid atherosclerosis: role of elevated blood pressure**. *Hypertension* 2005, **45**(4):597-601.
34. Gupte M, Boustany-Kari CM, Bharadwaj K, Police S, Thatcher S, Gong MC, English VL, Cassis LA: **ACE2 is expressed in mouse adipocytes and regulated by a high-fat diet**. *Am J Physiol Regul Integr Comp Physiol* 2008, **295**(3):R781-788.

35. Kouyama R, Suganami T, Nishida J, Tanaka M, Toyoda T, Kiso M, Chiwata T, Miyamoto Y, Yoshimasa Y, Fukamizu A *et al*: **Attenuation of diet-induced weight gain and adiposity through increased energy expenditure in mice lacking angiotensin II type 1a receptor**. *Endocrinology* 2005, **146**(8):3481-3489.
36. Police SB, Thatcher SE, Charnigo R, Daugherty A, Cassis LA: **Obesity promotes inflammation in periaortic adipose tissue and angiotensin II-induced abdominal aortic aneurysm formation**. *Arterioscler Thromb Vasc Biol* 2009, **29**(10):1458-1464.
37. Symons JD, McMillin SL, Riehle C, Tanner J, Palionyte M, Hillas E, Jones D, Cooksey RC, Birnbaum MJ, McClain DA *et al*: **Contribution of insulin and Akt1 signaling to endothelial nitric oxide synthase in the regulation of endothelial function and blood pressure**. *Circ Res* 2009, **104**(9):1085-1094.
38. Mark AL, Shaffer RA, Correia ML, Morgan DA, Sigmund CD, Haynes WG: **Contrasting blood pressure effects of obesity in leptin-deficient ob/ob mice and agouti yellow obese mice**. *J Hypertens* 1999, **17**(12 Pt 2):1949-1953.
39. Bodary PF, Shen Y, Ohman M, Bahrou KL, Vargas FB, Cudney SS, Wickenheiser KJ, Myers MG, Jr., Eitzman DT: **Leptin regulates neointima formation after arterial injury through mechanisms independent of blood pressure and the leptin receptor/STAT3 signaling pathways involved in energy balance**. *Arterioscler Thromb Vasc Biol* 2007, **27**(1):70-76.
40. Kintscher U, Bramlage P, Paar WD, Thoenes M, Unger T: **Irbesartan for the treatment of hypertension in patients with the metabolic syndrome: a sub analysis of the Treat to Target post authorization survey. Prospective observational, two armed study in 14,200 patients**. *Cardiovasc Diabetol* 2007, **6**:12.
41. Masuo K, Mikami H, Ogihara T, Tuck ML: **Weight reduction and pharmacologic treatment in obese hypertensives**. *Am J Hypertens* 2001, **14**(6 Pt 1):530-538.
42. Delsing DJ, Offerman EH, van Duyvenvoorde W, van Der Boom H, de Wit EC, Gijbels MJ, van Der Laarse A, Jukema JW, Havekes LM, Princen HM: **Acyl-CoA:cholesterol acyltransferase inhibitor avasimibe reduces atherosclerosis in addition to its cholesterol-lowering effect in ApoE*3-Leiden mice**. *Circulation* 2001, **103**(13):1778-1786.
43. Kleemann R, Princen HM, Emeis JJ, Jukema JW, Fontijn RD, Horrevoets AJ, Kooistra T, Havekes LM: **Rosuvastatin reduces atherosclerosis development beyond and independent of its plasma cholesterol-lowering effect in APOE*3-Leiden transgenic mice: evidence for anti-inflammatory effects of rosuvastatin**. *Circulation* 2003, **108**(11):1368-1374.
44. Kooistra T, Verschuren L, de Vries-van der Weij J, Koenig W, Toet K, Princen HM, Kleemann R: **Fenofibrate reduces atherogenesis in ApoE*3Leiden mice: evidence for multiple antiatherogenic effects besides lowering plasma cholesterol**. *Arterioscler Thromb Vasc Biol* 2006, **26**(10):2322-2330.
45. van der Hoorn JW, Kleemann R, Havekes LM, Kooistra T, Princen HM, Jukema JW: **Olmesartan and pravastatin additively reduce development of atherosclerosis in APOE*3Leiden transgenic mice**. *J Hypertens* 2007, **25**(12):2454-2462.
46. Paalvast Y, Gerding A, Wang Y, Bloks VW, van Dijk TH, Havinga R, Willems van Dijk K, Rensen PCN, Bakker BM, Kuivenhoven JA *et al*: **Male apoE*3-Leiden.CETP mice on high-fat high-cholesterol diet exhibit a biphasic dyslipidemic response, mimicking the changes in plasma lipids observed through life in men**. *Physiol Rep* 2017, **5**(19).
47. Shah PK, Kaul S, Nilsson J, Cercek B: **Exploiting the vascular protective effects of high-density lipoprotein and its apolipoproteins: an idea whose time for testing is coming, part I**. *Circulation* 2001, **104**(19):2376-2383.

48. Kontush A, Lindahl M, Lhomme M, Calabresi L, Chapman MJ, Davidson WS: **Structure of HDL: particle subclasses and molecular components**. *Handb Exp Pharmacol* 2015, **224**:3-51.
49. De Lalla OF, Gofman JW: **Ultracentrifugal analysis of serum lipoproteins**. *Methods Biochem Anal* 1954, **1**:459-478.
50. Nichols AV, Krauss RM, Musliner TA: **Nondenaturing polyacrylamide gradient gel electrophoresis**. *Methods Enzymol* 1986, **128**:417-431.
51. Zannis VI, Fotakis P, Koukos G, Kardassis D, Ehnholm C, Jauhiainen M, Chroni A: **HDL biogenesis, remodeling, and catabolism**. *Handb Exp Pharmacol* 2015, **224**:53-111.
52. Zannis VI, Chroni A, Krieger M: **Role of apoA-I, ABCA1, LCAT, and SR-BI in the biogenesis of HDL**. *J Mol Med (Berl)* 2006, **84**(4):276-294.
53. Duka A, Fotakis P, Georgiadou D, Kateifides A, Tzavlaki K, von Eckardstein L, Stratikos E, Kardassis D, Zannis VI: **ApoA-IV promotes the biogenesis of apoA-IV-containing HDL particles with the participation of ABCA1 and LCAT**. *J Lipid Res* 2013, **54**(1):107-115.
54. Kypreos KE, Zannis VI: **Pathway of biogenesis of apolipoprotein E-containing HDL in vivo with the participation of ABCA1 and LCAT**. *Biochem J* 2007, **403**(2):359-367.
55. Oram JF, Yokoyama S: **Apolipoprotein-mediated removal of cellular cholesterol and phospholipids**. *J Lipid Res* 1996, **37**(12):2473-2491.
56. Murakami T, Michelagnoli S, Longhi R, Gianfranceschi G, Pazzucconi F, Calabresi L, Sirtori CR, Franceschini G: **Triglycerides are major determinants of cholesterol esterification/transfer and HDL remodeling in human plasma**. *Arterioscler Thromb Vasc Biol* 1995, **15**(11):1819-1828.
57. Rashid S, Genest J: **Effect of obesity on high-density lipoprotein metabolism**. *Obesity (Silver Spring)* 2007, **15**(12):2875-2888.
58. Albrecht C, Baynes K, Sardini A, Schepelmann S, Eden ER, Davies SW, Higgins CF, Feher MD, Owen JS, Soutar AK: **Two novel missense mutations in ABCA1 result in altered trafficking and cause severe autosomal recessive HDL deficiency**. *Biochim Biophys Acta* 2004, **1689**(1):47-57.
59. Chroni A, Duka A, Kan HY, Liu T, Zannis VI: **Point mutations in apolipoprotein A-I mimic the phenotype observed in patients with classical lecithin:cholesterol acyltransferase deficiency**. *Biochemistry* 2005, **44**(43):14353-14366.
60. Williams PT, Haskell WL, Vranizan KM, Krauss RM: **The associations of high-density lipoprotein subclasses with insulin and glucose levels, physical activity, resting heart rate, and regional adiposity in men with coronary artery disease: the Stanford Coronary Risk Intervention Project baseline survey**. *Metabolism* 1995, **44**(1):106-114.
61. Smith JD: **Dysfunctional HDL as a diagnostic and therapeutic target**. *Arterioscler Thromb Vasc Biol* 2010, **30**(2):151-155.
62. Sorrentino SA, Besler C, Rohrer L, Meyer M, Heinrich K, Bahlmann FH, Mueller M, Horvath T, Doerries C, Heinemann M *et al*: **Endothelial-vasoprotective effects of high-density lipoprotein are impaired in patients with type 2 diabetes mellitus but are improved after extended-release niacin therapy**. *Circulation* 2010, **121**(1):110-122.
63. Khera AV, Cuchel M, de la Llera-Moya M, Rodrigues A, Burke MF, Jafri K, French BC, Phillips JA, Mucksavage ML, Wilensky RL *et al*: **Cholesterol efflux capacity, high-density lipoprotein function, and atherosclerosis**. *N Engl J Med* 2011, **364**(2):127-135.
64. Bertiere MC, Fumeron F, Rigaud D, Malon D, Apfelbaum M, Girard-Globa A: **Low high density lipoprotein-2 concentrations in obese male subjects**. *Atherosclerosis* 1988, **73**(1):57-61.

65. Ginsberg HN: **Insulin resistance and cardiovascular disease**. *J Clin Invest* 2000, **106**(4):453-458.
66. Kaur N, Pandey A, Negi H, Shafiq N, Reddy S, Kaur H, Chadha N, Malhotra S: **Effect of HDL-raising drugs on cardiovascular outcomes: a systematic review and meta-regression**. *PLoS One* 2014, **9**(4):e94585.
67. Incalcaterra E, Caruso M, Balistreri CR, Candore G, Lo Presti R, Hoffmann E, Caimi G: **Role of genetic polymorphisms in myocardial infarction at young age**. *Clin Hemorheol Microcirc* 2010, **46**(4):291-298.
68. Gutstein DE, Krishna R, Johns D, Surks HK, Dansky HM, Shah S, Mitchel YB, Arena J, Wagner JA: **Anacetrapib, a novel CETP inhibitor: pursuing a new approach to cardiovascular risk reduction**. *Clin Pharmacol Ther* 2012, **91**(1):109-122.
69. Colditz GA, Willett WC, Rotnitzky A, Manson JE: **Weight gain as a risk factor for clinical diabetes mellitus in women**. *Ann Intern Med* 1995, **122**(7):481-486.
70. Tabak AG, Jokela M, Akbaraly TN, Brunner EJ, Kivimaki M, Witte DR: **Trajectories of glycaemia, insulin sensitivity, and insulin secretion before diagnosis of type 2 diabetes: an analysis from the Whitehall II study**. *Lancet* 2009, **373**(9682):2215-2221.
71. Vollenweider P, von Eckardstein A, Widmann C: **HDLs, diabetes, and metabolic syndrome**. *Handb Exp Pharmacol* 2015, **224**:405-421.
72. Qi Y, Xu Z, Zhu Q, Thomas C, Kumar R, Feng H, Dostal DE, White MF, Baker KM, Guo S: **Myocardial loss of IRS1 and IRS2 causes heart failure and is controlled by p38alpha MAPK during insulin resistance**. *Diabetes* 2013, **62**(11):3887-3900.
73. Guo S: **Insulin signaling, resistance, and the metabolic syndrome: insights from mouse models into disease mechanisms**. *J Endocrinol* 2014, **220**(2):T1-T23.
74. Janghorbani M, Soltanian N, Sirous M, Amini M, Iraj B: **Risk of diabetes in combined metabolic abnormalities and body mass index categories**. *Diabetes Metab Syndr* 2016, **10**(1 Suppl 1):S71-78.
75. Townsend DK, McGregor K, Wu E, Cialkowski K, Haub MD, Barstow TJ: **Insulin resistance and metabolic syndrome criteria in lean, normoglycemic college-age subjects**. *Diabetes Metab Syndr* 2018.
76. Martin KA, Mani MV, Mani A: **New targets to treat obesity and the metabolic syndrome**. *Eur J Pharmacol* 2015, **763**(Pt A):64-74.
77. Haslam DW, James WP: **Obesity**. *Lancet* 2005, **366**(9492):1197-1209.
78. Patel DK, Stanford FC: **Safety and tolerability of new-generation anti-obesity medications: a narrative review**. *Postgrad Med* 2018, **130**(2):173-182.
79. Bijani B, Pahlevan AA, Qasemi-Barqi R, Jahanihashemi H: **Metabolic syndrome as an independent risk factor of hypoxaemia in influenza A (H1N1) 2009 pandemic**. *Infez Med* 2016, **24**(2):123-130.
80. Kaur J: **A comprehensive review on metabolic syndrome**. *Cardiol Res Pract* 2014, **2014**:943162.
81. Saunders KH, Umashanker D, Igel LI, Kumar RB, Aronne LJ: **Obesity Pharmacotherapy**. *Med Clin North Am* 2018, **102**(1):135-148.
82. Nguyen NT, Varela JE: **Bariatric surgery for obesity and metabolic disorders: state of the art**. *Nat Rev Gastroenterol Hepatol* 2017, **14**(3):160-169.
83. Simonson DC, Halperin F, Foster K, Vernon A, Goldfine AB: **Clinical and Patient-Centered Outcomes in Obese Patients With Type 2 Diabetes 3 Years After Randomization to Roux-en-Y Gastric Bypass Surgery Versus Intensive Lifestyle Management: The SLIMM-T2D Study**. *Diabetes Care* 2018, **41**(4):670-679.
84. Handelsman Y, Bloomgarden ZT, Grunberger G, Umpierrez G, Zimmerman RS, Bailey TS, Blonde L, Bray GA, Cohen AJ, Dagogo-Jack S *et al*: **American association of clinical endocrinologists and american college of endocrinology**

- clinical practice guidelines for developing a diabetes mellitus comprehensive care plan - 2015. *Endocr Pract* 2015, **21 Suppl 1**:1-87.
85. Nguyen NT, Ho HS, Palmer LS, Wolfe BM: **A comparison study of laparoscopic versus open gastric bypass for morbid obesity**. *J Am Coll Surg* 2000, **191**(2):149-155; discussion 155-147.
86. Puzziferri N, Austrheim-Smith IT, Wolfe BM, Wilson SE, Nguyen NT: **Three-year follow-up of a prospective randomized trial comparing laparoscopic versus open gastric bypass**. *Ann Surg* 2006, **243**(2):181-188.
87. Chang SH, Stoll CR, Song J, Varela JE, Eagon CJ, Colditz GA: **The effectiveness and risks of bariatric surgery: an updated systematic review and meta-analysis, 2003-2012**. *JAMA Surg* 2014, **149**(3):275-287.
88. Nguyen NT, Vu S, Kim E, Bodunova N, Phelan MJ: **Trends in utilization of bariatric surgery, 2009-2012**. *Surg Endosc* 2016, **30**(7):2723-2727.
89. Nguyen NT, Goldman C, Rosenquist CJ, Arango A, Cole CJ, Lee SJ, Wolfe BM: **Laparoscopic versus open gastric bypass: a randomized study of outcomes, quality of life, and costs**. *Ann Surg* 2001, **234**(3):279-289; discussion 289-291.
90. Ponce J, Nguyen NT, Hutter M, Sudan R, Morton JM: **American Society for Metabolic and Bariatric Surgery estimation of bariatric surgery procedures in the United States, 2011-2014**. *Surg Obes Relat Dis* 2015, **11**(6):1199-1200.
91. Angrisani L, Santonicola A, Iovino P, Formisano G, Buchwald H, Scopinaro N: **Bariatric Surgery Worldwide 2013**. *Obes Surg* 2015, **25**(10):1822-1832.
92. Mason EE, Ito C: **Gastric bypass in obesity**. *Surg Clin North Am* 1967, **47**(6):1345-1351.
93. Marceau P, Hould FS, Simard S, Lebel S, Bourque RA, Potvin M, Biron S: **Biliopancreatic diversion with duodenal switch**. *World J Surg* 1998, **22**(9):947-954.
94. Regan JP, Inabnet WB, Gagner M, Pomp A: **Early experience with two-stage laparoscopic Roux-en-Y gastric bypass as an alternative in the super-super obese patient**. *Obes Surg* 2003, **13**(6):861-864.
95. Sarr MG, Billington CJ, Brancatisano R, Brancatisano A, Toouli J, Kow L, Nguyen NT, Blackstone R, Maher JW, Shikora S *et al*: **The EMPOWER study: randomized, prospective, double-blind, multicenter trial of vagal blockade to induce weight loss in morbid obesity**. *Obes Surg* 2012, **22**(11):1771-1782.
96. Ponce J, Woodman G, Swain J, Wilson E, English W, Ikramuddin S, Bour E, Edmundowicz S, Snyder B, Soto F *et al*: **The REDUCE pivotal trial: a prospective, randomized controlled pivotal trial of a dual intragastric balloon for the treatment of obesity**. *Surg Obes Relat Dis* 2015, **11**(4):874-881.
97. Kraljevic M, Delko T, Kostler T, Osto E, Lutz T, Thommen S, Droeser RA, Rothwell L, Oertli D, Zingg U: **Laparoscopic Roux-en-Y gastric bypass versus laparoscopic mini gastric bypass in the treatment of obesity: study protocol for a randomized controlled trial**. *Trials* 2017, **18**(1):226.
98. Altieri MS, Wright B, Peredo A, Pryor AD: **Common weight loss procedures and their complications**. *Am J Emerg Med* 2018, **36**(3):475-479.
99. Altieri MS, Yang J, Telem DA, Meng Z, Frenkel C, Halbert C, Talamini M, Pryor AD: **Lap band outcomes from 19,221 patients across centers and over a decade within the state of New York**. *Surg Endosc* 2016, **30**(5):1725-1732.
100. Tice JA, Karliner L, Walsh J, Petersen AJ, Feldman MD: **Gastric banding or bypass? A systematic review comparing the two most popular bariatric procedures**. *Am J Med* 2008, **121**(10):885-893.
101. Mistry P, Currie V, Super P, le Roux CW, Tahrani AA, Singhal R: **Changes in glycaemic control, blood pressure and lipids 5 years following laparoscopic adjustable gastric banding combined with medical care in patients with type 2 diabetes: a longitudinal analysis**. *Clin Obes* 2018.

102. Singhal R, Kitchen M, Ndirika S, Hunt K, Bridgwater S, Super P: **The "Birmingham stitch"--avoiding slippage in laparoscopic gastric banding**. *Obes Surg* 2008, **18**(4):359-363.
103. Ding SA, Simonson DC, Wewalka M, Halperin F, Foster K, Goebel-Fabbri A, Hamdy O, Clancy K, Lautz D, Vernon A *et al*: **Adjustable Gastric Band Surgery or Medical Management in Patients With Type 2 Diabetes: A Randomized Clinical Trial**. *J Clin Endocrinol Metab* 2015, **100**(7):2546-2556.
104. D'Hondt M, Vanneste S, Pottel H, Devriendt D, Van Rooy F, Vansteenkiste F: **Laparoscopic sleeve gastrectomy as a single-stage procedure for the treatment of morbid obesity and the resulting quality of life, resolution of comorbidities, food tolerance, and 6-year weight loss**. *Surg Endosc* 2011, **25**(8):2498-2504.
105. Hutter MM, Schirmer BD, Jones DB, Ko CY, Cohen ME, Merkow RP, Nguyen NT: **First report from the American College of Surgeons Bariatric Surgery Center Network: laparoscopic sleeve gastrectomy has morbidity and effectiveness positioned between the band and the bypass**. *Ann Surg* 2011, **254**(3):410-420; discussion 420-412.
106. Hady HR, Olszewska M, Czerniawski M, Groth D, Diemieszczyk I, Pawluszewicz P, Kretowski A, Ladny JR, Dadan J: **Different surgical approaches in laparoscopic sleeve gastrectomy and their influence on metabolic syndrome: A retrospective study**. *Medicine (Baltimore)* 2018, **97**(4):e9699.
107. Shi X, Karmali S, Sharma AM, Birch DW: **A review of laparoscopic sleeve gastrectomy for morbid obesity**. *Obes Surg* 2010, **20**(8):1171-1177.
108. Coluzzi I, Raparelli L, Guarnacci L, Paone E, Del Genio G, le Roux CW, Silecchia G: **Food Intake and Changes in Eating Behavior After Laparoscopic Sleeve Gastrectomy**. *Obes Surg* 2016, **26**(9):2059-2067.
109. Clapp B, Wynn M, Martyn C, Foster C, O'Dell M, Tyroch A: **Long term (7 or more years) outcomes of the sleeve gastrectomy: a meta-analysis**. *Surg Obes Relat Dis* 2018.
110. Schauer PR, Kashyap SR, Wolski K, Brethauer SA, Kirwan JP, Pothier CE, Thomas S, Abood B, Nissen SE, Bhatt DL: **Bariatric surgery versus intensive medical therapy in obese patients with diabetes**. *N Engl J Med* 2012, **366**(17):1567-1576.
111. Cohen R: **Sleeve gastrectomy: the ideal option for metabolic surgery?** *Nat Rev Endocrinol* 2013, **9**(10):623.
112. Kafali ME, Sahin M, Ece I, Acar F, Yilmaz H, Alptekin H, Ates L: **The effects of bariatric surgical procedures on the improvement of metabolic syndrome in morbidly obese patients: Comparison of laparoscopic sleeve gastrectomy versus laparoscopic Roux-en-Y gastric bypass**. *Turk J Surg* 2017, **33**(3):142-146.
113. Cottam D, Qureshi FG, Mattar SG, Sharma S, Holover S, Bonanomi G, Ramanathan R, Schauer P: **Laparoscopic sleeve gastrectomy as an initial weight-loss procedure for high-risk patients with morbid obesity**. *Surg Endosc* 2006, **20**(6):859-863.
114. Rubino F, Forgione A, Cummings DE, Vix M, Gnuli D, Mingrone G, Castagneto M, Marescaux J: **The mechanism of diabetes control after gastrointestinal bypass surgery reveals a role of the proximal small intestine in the pathophysiology of type 2 diabetes**. *Ann Surg* 2006, **244**(5):741-749.
115. Gagner M: **Sleeve gastrectomy: an ideal choice for T2DM**. *Nat Rev Endocrinol* 2013, **9**(10):623.
116. Buchwald H, Avidor Y, Braunwald E, Jensen MD, Pories W, Fahrbach K, Schoelles K: **Bariatric surgery: a systematic review and meta-analysis**. *JAMA* 2004, **292**(14):1724-1737.
117. Rutledge R: **Naming the mini-gastric bypass**. *Obes Surg* 2014, **24**(12):2173.

118. Rutledge R: **The mini-gastric bypass: experience with the first 1,274 cases**. *Obes Surg* 2001, **11**(3):276-280.
119. Miras AD, le Roux CW: **Surgery: The new gold-standard - medical gastric bypass**. *Nat Rev Endocrinol* 2018, **14**(5):257-258.
120. Miras AD, le Roux CW: **Mechanisms underlying weight loss after bariatric surgery**. *Nat Rev Gastroenterol Hepatol* 2013, **10**(10):575-584.
121. Poirier P, Cornier MA, Mazzone T, Stiles S, Cummings S, Klein S, McCullough PA, Ren Fielding C, Franklin BA, American Heart Association Obesity Committee of the Council on Nutrition PA *et al*: **Bariatric surgery and cardiovascular risk factors: a scientific statement from the American Heart Association**. *Circulation* 2011, **123**(15):1683-1701.
122. Ballesta C, Berindoague R, Cabrera M, Palau M, Gonzales M: **Management of anastomotic leaks after laparoscopic Roux-en-Y gastric bypass**. *Obes Surg* 2008, **18**(6):623-630.
123. Higa K, Ho T, Tercero F, Yunus T, Boone KB: **Laparoscopic Roux-en-Y gastric bypass: 10-year follow-up**. *Surg Obes Relat Dis* 2011, **7**(4):516-525.
124. Steele KE, Prokopowicz GP, Magnuson T, Lidor A, Schweitzer M: **Laparoscopic antecolic Roux-en-Y gastric bypass with closure of internal defects leads to fewer internal hernias than the retrocolic approach**. *Surg Endosc* 2008, **22**(9):2056-2061.
125. Capella JF, Capella RF: **Gastro-gastric fistulas and marginal ulcers in gastric bypass procedures for weight reduction**. *Obes Surg* 1999, **9**(1):22-27; discussion 28.
126. Lutz TA, Bueter M: **The Use of Rat and Mouse Models in Bariatric Surgery Experiments**. *Front Nutr* 2016, **3**:25.
127. Stefater MA, Wilson-Perez HE, Chambers AP, Sandoval DA, Seeley RJ: **All bariatric surgeries are not created equal: insights from mechanistic comparisons**. *Endocr Rev* 2012, **33**(4):595-622.
128. Bloomston M, Zervos EE, Camps MA, Goode SE, Rosemurgy AS: **Outcome following bariatric surgery in super versus morbidly obese patients: does weight matter?** *Obes Surg* 1997, **7**(5):414-419.
129. Shah SS, Todkar JS, Shah PS, Cummings DE: **Diabetes remission and reduced cardiovascular risk after gastric bypass in Asian Indians with body mass index <35 kg/m(2)**. *Surg Obes Relat Dis* 2010, **6**(4):332-338.
130. Papamargaritis D, Panteliou E, Miras AD, le Roux CW: **Mechanisms of weight loss, diabetes control and changes in food choices after gastrointestinal surgery**. *Curr Atheroscler Rep* 2012, **14**(6):616-623.
131. Tadross JA, le Roux CW: **The mechanisms of weight loss after bariatric surgery**. *Int J Obes (Lond)* 2009, **33 Suppl 1**:S28-32.
132. Hao Z, Townsend RL, Mumphrey MB, Morrison CD, Munzberg H, Berthoud HR: **RYGB Produces more Sustained Body Weight Loss and Improvement of Glycemic Control Compared with VSG in the Diet-Induced Obese Mouse Model**. *Obes Surg* 2017, **27**(9):2424-2433.
133. Stylopoulos N, Hoppin AG, Kaplan LM: **Roux-en-Y gastric bypass enhances energy expenditure and extends lifespan in diet-induced obese rats**. *Obesity (Silver Spring)* 2009, **17**(10):1839-1847.
134. Flancbaum L, Choban PS, Bradley LR, Burge JC: **Changes in measured resting energy expenditure after Roux-en-Y gastric bypass for clinically severe obesity**. *Surgery* 1997, **122**(5):943-949.
135. Osto E, Doytcheva P, Corteville C, Bueter M, Dorig C, Stivala S, Buhmann H, Colin S, Rohrer L, Hasballa R *et al*: **Rapid and body weight-independent improvement of endothelial and high-density lipoprotein function after Roux-en-Y gastric bypass: role of glucagon-like peptide-1**. *Circulation* 2015, **131**(10):871-881.

136. Carswell KA, Belgaumkar AP, Amiel SA, Patel AG: **A Systematic Review and Meta-analysis of the Effect of Gastric Bypass Surgery on Plasma Lipid Levels**. *Obes Surg* 2016, **26**(4):843-855.
137. Kruseman M, Leimgruber A, Zumbach F, Golay A: **Dietary, weight, and psychological changes among patients with obesity, 8 years after gastric bypass**. *J Am Diet Assoc* 2010, **110**(4):527-534.
138. Odstrcil EA, Martinez JG, Santa Ana CA, Xue B, Schneider RE, Steffer KJ, Porter JL, Asplin J, Kuhn JA, Fordtran JS: **The contribution of malabsorption to the reduction in net energy absorption after long-limb Roux-en-Y gastric bypass**. *Am J Clin Nutr* 2010, **92**(4):704-713.
139. Thirlby RC, Bahiraei F, Randall J, Drewnoski A: **Effect of Roux-en-Y gastric bypass on satiety and food likes: the role of genetics**. *J Gastrointest Surg* 2006, **10**(2):270-277.
140. Pihlajamaki J, Gronlund S, Simonen M, Kakela P, Moilanen L, Paakkonen M, Pirinen E, Kolehmainen M, Karja V, Kainulainen S *et al*: **Cholesterol absorption decreases after Roux-en-Y gastric bypass but not after gastric banding**. *Metabolism* 2010, **59**(6):866-872.
141. Kong LC, Tap J, Aron-Wisnewsky J, Pelloux V, Basdevant A, Bouillot JL, Zucker JD, Dore J, Clement K: **Gut microbiota after gastric bypass in human obesity: increased richness and associations of bacterial genera with adipose tissue genes**. *Am J Clin Nutr* 2013, **98**(1):16-24.
142. Carswell KA, Vincent RP, Belgaumkar AP, Sherwood RA, Amiel SA, Patel AG, le Roux CW: **The effect of bariatric surgery on intestinal absorption and transit time**. *Obes Surg* 2014, **24**(5):796-805.
143. Kumar R, Lieske JC, Collazo-Clavell ML, Sarr MG, Olson ER, Vrtiska TJ, Bergstralh EJ, Li X: **Fat malabsorption and increased intestinal oxalate absorption are common after Roux-en-Y gastric bypass surgery**. *Surgery* 2011, **149**(5):654-661.
144. Gonlachanvit S, Coleski R, Owyang C, Hasler W: **Inhibitory actions of a high fibre diet on intestinal gas transit in healthy volunteers**. *Gut* 2004, **53**(11):1577-1582.
145. Sancho V, Trigo MV, Martin-Duce A, Gonz Lez N, Acitores A, Arnes L, Valverde I, Malaisse WJ, Villanueva-Penacarrillo ML: **Effect of GLP-1 on D-glucose transport, lipolysis and lipogenesis in adipocytes of obese subjects**. *Int J Mol Med* 2006, **17**(6):1133-1137.
146. Giorgino F, Laviola L, Eriksson JW: **Regional differences of insulin action in adipose tissue: insights from in vivo and in vitro studies**. *Acta Physiol Scand* 2005, **183**(1):13-30.
147. Korner J, Bessler M, Cirilo LJ, Conwell IM, Daud A, Restuccia NL, Wardlaw SL: **Effects of Roux-en-Y gastric bypass surgery on fasting and postprandial concentrations of plasma ghrelin, peptide YY, and insulin**. *J Clin Endocrinol Metab* 2005, **90**(1):359-365.
148. Mingrone G, Panunzi S, De Gaetano A, Guidone C, Iaconelli A, Leccesi L, Nanni G, Pomp A, Castagneto M, Ghirlanda G *et al*: **Bariatric surgery versus conventional medical therapy for type 2 diabetes**. *N Engl J Med* 2012, **366**(17):1577-1585.
149. Sjostrom L, Lindroos AK, Peltonen M, Torgerson J, Bouchard C, Carlsson B, Dahlgren S, Larsson B, Narbro K, Sjostrom CD *et al*: **Lifestyle, diabetes, and cardiovascular risk factors 10 years after bariatric surgery**. *N Engl J Med* 2004, **351**(26):2683-2693.
150. Johansson LE, Danielsson AP, Parikh H, Klintenberg M, Norstrom F, Groop L, Ridderstrale M: **Differential gene expression in adipose tissue from obese human subjects during weight loss and weight maintenance**. *Am J Clin Nutr* 2012, **96**(1):196-207.
151. Asztalos BF, Swarbrick MM, Schaefer EJ, Dallal GE, Horvath KV, Ai M, Stanhope KL, Austrheim-Smith I, Wolfe BM, Ali M *et al*: **Effects of weight loss, induced by**

gastric bypass surgery, on HDL remodeling in obese women. *J Lipid Res* 2010, **51**(8):2405-2412.
152. Zvintzou E, Skroubis G, Chroni A, Petropoulou PI, Gkolfinopoulou C, Sakellaropoulos G, Gantz D, Mihou I, Kalfarentzos F, Kypreos KE: **Effects of bariatric surgery on HDL structure and functionality: results from a prospective trial**. *J Clin Lipidol* 2014, **8**(4):408-417.
153. Culnan DM, Cooney RN, Stanley B, Lynch CJ: **Apolipoprotein A-IV, a putative satiety/antiatherogenic factor, rises after gastric bypass**. *Obesity (Silver Spring)* 2009, **17**(1):46-52.
154. Pardina E, Lopez-Tejero MD, Llamas R, Catalan R, Galard R, Allende H, Vargas V, Lecube A, Fort JM, Baena-Fustegueras JA *et al*: **Ghrelin and apolipoprotein AIV levels show opposite trends to leptin levels during weight loss in morbidly obese patients**. *Obes Surg* 2009, **19**(10):1414-1423.
155. Heneghan HM, Huang H, Kashyap SR, Gornik HL, McCullough AJ, Schauer PR, Brethauer SA, Kirwan JP, Kasumov T: **Reduced cardiovascular risk after bariatric surgery is linked to plasma ceramides, apolipoprotein-B100, and ApoB100/A1 ratio**. *Surg Obes Relat Dis* 2013, **9**(1):100-107.
156. Schauer PR, Burguera B, Ikramuddin S, Cottam D, Gourash W, Hamad G, Eid GM, Mattar S, Ramanathan R, Barinas-Mitchel E *et al*: **Effect of laparoscopic Roux-en Y gastric bypass on type 2 diabetes mellitus**. *Ann Surg* 2003, **238**(4):467-484; discussion 484-465.
157. Isbell JM, Tamboli RA, Hansen EN, Saliba J, Dunn JP, Phillips SE, Marks-Shulman PA, Abumrad NN: **The importance of caloric restriction in the early improvements in insulin sensitivity after Roux-en-Y gastric bypass surgery**. *Diabetes Care* 2010, **33**(7):1438-1442.
158. Jorgensen NB, Jacobsen SH, Dirksen C, Bojsen-Moller KN, Naver L, Hvolris L, Clausen TR, Wulff BS, Worm D, Lindqvist Hansen D *et al*: **Acute and long-term effects of Roux-en-Y gastric bypass on glucose metabolism in subjects with Type 2 diabetes and normal glucose tolerance**. *Am J Physiol Endocrinol Metab* 2012, **303**(1):E122-131.
159. Patriti A, Facchiano E, Sanna A, Gulla N, Donini A: **The enteroinsular axis and the recovery from type 2 diabetes after bariatric surgery**. *Obes Surg* 2004, **14**(6):840-848.
160. Drucker DJ: **Glucagon-like peptide-1 and the islet beta-cell: augmentation of cell proliferation and inhibition of apoptosis**. *Endocrinology* 2003, **144**(12):5145-5148.
161. Pories WJ, Albrecht RJ: **Etiology of type II diabetes mellitus: role of the foregut**. *World J Surg* 2001, **25**(4):527-531.
162. Gorst C, Kwok CS, Aslam S, Buchan I, Kontopantelis E, Myint PK, Heatlie G, Loke Y, Rutter MK, Mamas MA: **Long-term Glycemic Variability and Risk of Adverse Outcomes: A Systematic Review and Meta-analysis**. *Diabetes Care* 2015, **38**(12):2354-2369.
163. Nosso G, Lupoli R, Saldalamacchia G, Griffo E, Cotugno M, Costabile G, Riccardi G, Capaldo B: **Diabetes remission after bariatric surgery is characterized by high glycemic variability and high oxidative stress**. *Nutr Metab Cardiovasc Dis* 2017, **27**(11):949-955.
164. Sips FL, Nyman E, Adiels M, Hilbers PA, Stralfors P, van Riel NA, Cedersund G: **Model-Based Quantification of the Systemic Interplay between Glucose and Fatty Acids in the Postprandial State**. *PLoS One* 2015, **10**(9):e0135665.
165. Nyman E, Rozendaal YJ, Helmlinger G, Hamren B, Kjellsson MC, Stralfors P, van Riel NA, Gennemark P, Cedersund G: **Requirements for multi-level systems pharmacology models to reach end-usage: the case of type 2 diabetes**. *Interface Focus* 2016, **6**(2):20150075.

166. Parhofer KG: **Interaction between Glucose and Lipid Metabolism: More than Diabetic Dyslipidemia**. *Diabetes Metab J* 2015, **39**(5):353-362.
167. Sattar N, Preiss D, Murray HM, Welsh P, Buckley BM, de Craen AJ, Seshasai SR, McMurray JJ, Freeman DJ, Jukema JW *et al*: **Statins and risk of incident diabetes: a collaborative meta-analysis of randomised statin trials**. *Lancet* 2010, **375**(9716):735-742.
168. Drew BG, Rye KA, Duffy SJ, Barter P, Kingwell BA: **The emerging role of HDL in glucose metabolism**. *Nat Rev Endocrinol* 2012, **8**(4):237-245.
169. Wali JA, Thomas HE, Sutherland AP: **Linking obesity with type 2 diabetes: the role of T-bet**. *Diabetes Metab Syndr Obes* 2014, **7**:331-340.
170. Lutz TA: **Considering our methods: Methodological issues with rodent models of appetite and obesity research**. *Physiol Behav* 2018.
171. Gierman LM, Kuhnast S, Koudijs A, Pieterman EJ, Kloppenburg M, van Osch GJ, Stojanovic-Susulic V, Huizinga TW, Princen HM, Zuurmond AM: **Osteoarthritis development is induced by increased dietary cholesterol and can be inhibited by atorvastatin in APOE*3Leiden.CETP mice--a translational model for atherosclerosis**. *Ann Rheum Dis* 2014, **73**(5):921-927.
172. Montgomery MK, Hallahan NL, Brown SH, Liu M, Mitchell TW, Cooney GJ, Turner N: **Mouse strain-dependent variation in obesity and glucose homeostasis in response to high-fat feeding**. *Diabetologia* 2013, **56**(5):1129-1139.
173. Yang Y, Smith DL, Jr., Keating KD, Allison DB, Nagy TR: **Variations in body weight, food intake and body composition after long-term high-fat diet feeding in C57BL/6J mice**. *Obesity (Silver Spring)* 2014, **22**(10):2147-2155.
174. Wang CY, Liao JK: **A mouse model of diet-induced obesity and insulin resistance**. *Methods Mol Biol* 2012, **821**:421-433.
175. Nestoridi E, Kvas S, Kucharczyk J, Stylopoulos N: **Resting energy expenditure and energetic cost of feeding are augmented after Roux-en-Y gastric bypass in obese mice**. *Endocrinology* 2012, **153**(5):2234-2244.
176. Bueter M, Lowenstein C, Olbers T, Wang M, Cluny NL, Bloom SR, Sharkey KA, Lutz TA, le Roux CW: **Gastric bypass increases energy expenditure in rats**. *Gastroenterology* 2010, **138**(5):1845-1853.
177. Shin AC, Zheng H, Townsend RL, Patterson LM, Holmes GM, Berthoud HR: **Longitudinal assessment of food intake, fecal energy loss, and energy expenditure after Roux-en-Y gastric bypass surgery in high-fat-fed obese rats**. *Obes Surg* 2013, **23**(4):531-540.
178. Thivel D, Brakonieki K, Duche P, Morio B, Boirie Y, Laferrere B: **Surgical weight loss: impact on energy expenditure**. *Obes Surg* 2013, **23**(2):255-266.
179. Werling M, Olbers T, Fandriks L, Bueter M, Lonroth H, Stenlof K, le Roux CW: **Increased postprandial energy expenditure may explain superior long term weight loss after Roux-en-Y gastric bypass compared to vertical banded gastroplasty**. *PLoS One* 2013, **8**(4):e60280.
180. Barres R, Kirchner H, Rasmussen M, Yan J, Kantor FR, Krook A, Naslund E, Zierath JR: **Weight loss after gastric bypass surgery in human obesity remodels promoter methylation**. *Cell Rep* 2013, **3**(4):1020-1027.
181. Schauer PR, Mingrone G, Ikramuddin S, Wolfe B: **Clinical Outcomes of Metabolic Surgery: Efficacy of Glycemic Control, Weight Loss, and Remission of Diabetes**. *Diabetes Care* 2016, **39**(6):902-911.
182. Kayser BD, Lhomme M, Dao MC, Ichou F, Bouillot JL, Prifti E, Kontush A, Chevallier JM, Aron-Wisnewsky J, Dugail I *et al*: **Serum lipidomics reveals early differential effects of gastric bypass compared with banding on phospholipids and sphingolipids independent of differences in weight loss**. *Int J Obes (Lond)* 2017.
183. Alli V, Rogers AM: **Gastric Bypass and Influence on Improvement of NAFLD**. *Curr Gastroenterol Rep* 2017, **19**(6):25.

184. Blanchard C, Moreau F, Ayer A, Toque L, Garcon D, Arnaud L, Borel F, Aguesse A, Croyal M, Krempf M *et al*: **Roux-en-Y gastric bypass reduces plasma cholesterol in diet-induced obese mice by affecting trans-intestinal cholesterol excretion and intestinal cholesterol absorption**. *Int J Obes (Lond)* 2018, **42**(3):552-560.
185. Heffron SP, Lin BX, Parikh M, Scolaro B, Adelman SJ, Collins HL, Berger JS, Fisher EA: **Changes in High-Density Lipoprotein Cholesterol Efflux Capacity After Bariatric Surgery Are Procedure Dependent**. *Arterioscler Thromb Vasc Biol* 2018, **38**(1):245-254.
186. Jackness C, Karmally W, Febres G, Conwell IM, Ahmed L, Bessler M, McMahon DJ, Korner J: **Very low-calorie diet mimics the early beneficial effect of Roux-en-Y gastric bypass on insulin sensitivity and beta-cell Function in type 2 diabetic patients**. *Diabetes* 2013, **62**(9):3027-3032.
187. Rubino F, Gagner M, Gentileschi P, Kini S, Fukuyama S, Feng J, Diamond E: **The early effect of the Roux-en-Y gastric bypass on hormones involved in body weight regulation and glucose metabolism**. *Ann Surg* 2004, **240**(2):236-242.
188. Huang H, Kasumov T, Gatmaitan P, Heneghan HM, Kashyap SR, Schauer PR, Brethauer SA, Kirwan JP: **Gastric bypass surgery reduces plasma ceramide subspecies and improves insulin sensitivity in severely obese patients**. *Obesity (Silver Spring)* 2011, **19**(11):2235-2240.
189. Holewijn S, den Heijer M, Swinkels DW, Stalenhoef AF, de Graaf J: **Apolipoprotein B, non-HDL cholesterol and LDL cholesterol for identifying individuals at increased cardiovascular risk**. *J Intern Med* 2010, **268**(6):567-577.
190. Jiang XC, Paultre F, Pearson TA, Reed RG, Francis CK, Lin M, Berglund L, Tall AR: **Plasma sphingomyelin level as a risk factor for coronary artery disease**. *Arterioscler Thromb Vasc Biol* 2000, **20**(12):2614-2618.
191. Mokadem M, Zechner JF, Margolskee RF, Drucker DJ, Aguirre V: **Effects of Roux-en-Y gastric bypass on energy and glucose homeostasis are preserved in two mouse models of functional glucagon-like peptide-1 deficiency**. *Mol Metab* 2014, **3**(2):191-201.
192. Petremand J, Puyal J, Chatton JY, Duprez J, Allagnat F, Frias M, James RW, Waeber G, Jonas JC, Widmann C: **HDLs protect pancreatic beta-cells against ER stress by restoring protein folding and trafficking**. *Diabetes* 2012, **61**(5):1100-1111.
193. von Eckardstein A, Hersberger M, Rohrer L: **Current understanding of the metabolism and biological actions of HDL**. *Curr Opin Clin Nutr Metab Care* 2005, **8**(2):147-152.

9 Ackowledgements

First of all, I would like to thank you my supervisor Prof. Thomas Lutz for giving me the opportunity to be part of in his lab for four years working not only on my very interesting PhD project but also in several other side projects. Thank you to be always present and for pushing me beyond my limits and to make me giving always my best.

I would like also to thank all the other members of my PhD Committee: Prof. Thorsten Hornemann, Prof. Christian Wolfrum, and Prof. Max Gassmann for their support, and helpful discussions during PhD committee meetings, making me believe in my results. I also would like to thank you Prof. Arnold von Eckardstein and Dr. Elena Osto, even if you were not part of my PhD Committee you gave me good suggestions and ideas for my project.

I would like to thank you Dr. Christina N. Boyle and Dr. Christelle le Foll, because even if they were not my direct supervisors, they always took care of me and helped any time I was showing up at their office's door. Christina, thank you for your supervision in my first year in the lab, to make me be able to publish my first author paper and to have performed all the surgeries, without you my project wouldn't had been possible.
Christelle, thank you for all the time spent together in my last 2 years, from the little afternoon coffee break to the more important help in writing and in statistics.
I think we created a good team and I will really miss to work with both of you.

Thanks to Dr. Giovanni Pellegrini, one of the pillar of my project, for the excellent pathological expertise; without him I wouldn't be able to learn a lot in pathology and microscopy and I wouldn't be able to investigate more about the mouse model I was working with.

I would like to thank the present and former member of Lutz's and Gassmann lab for their help, support and great time we had together. A special thank goes to Fabienne, Fufu and Jay, my "PhD buddies", together we shared the good and bad side of being PhD students.
On a personal note, I would like to thank Julia Baumann. You became much more than a working colleague. Thank you because you always listened to my personal and working problems, my little "Italian Dramas". We had and we will have a great time together after work, in going out, in organizing our amazing dinners or our small holidays. Thank to be Julia and to make me feel fully integrated in Switzerland.

Outside the lab, I would like to thank my Italian and International friends; even if we did not see to each other daily, you always had a nice word for me and I knew you were there: Valeria, Daniel, Monica, Laura, Silvia, Roberto and Johan. Especially Valeria, my best friend, we always supported each other and with our "pensiero positivo" we reached every goal we set.

A special thank goes also to my awesome salsa dancing partner Claudio, and my other salsa buddies: Emmi, Lukas and Marc. Thanks to listen to me and to make me feel better after a bad day at work.

Last, but not the least, I would like to thank my family for their support, and constant confidence in me and to teach me to be always ambitious and pushing me to do my best in everything I was doing.

10 Curriculum Vitae
ERIKA TARASCO

Date of birth: 04 August 1988, Genova (Ge), Italy
Nationality: Italian

Education

01/2015 to date	**University of Zürich, Switzerland** PhD in Integrative Molecular Medicine, Faculty of Science, UZH. Title: "Effects of Roux-en Y bariatric surgery on glucose and lipid metabolism in obese male ApoE*3Leiden.CETP mice"
10/2010 – 07/2012	**University of Pavia, Italy** Merit M.Sc. in Experimental and Applied Biology with thesis topic "*Helicobacter pylori* L-asparaginase: mutants selection with directed evolution"
10/2007 – 07/2010	**University of Pavia, Italy** B. Sc. in Biological Sciences with the thesis topic "Oxytocin inflects spontaneous IPSC's frequency and amplitude in mouse hippocampus Pyramidal Neurons"
09/2009 – 07/2007	**Secondary School** Scientific High School (Liceo Scientifico) G.P. Vieusseux, Imperia, Italy

Practical Experience

01/2015 – 03-2018	**University of Zürich, Switzerland** Teaching assistant at the Institute of Veterinary Physiology practical courses for veterinarian students I, II and III year
01/2013 – 06-2013	Teaching assistant in practical courses in Histology and Cell Morphology in "General Pathology" course for III year students

Research and Project Experience

10/2013 – 12-2014	**University of Zürich, Switzerland** Principal investigator in a CTI project with University of Lausanne on the effects of somatostatin analogues in rats Team worker in Collaboration with the Centre of Molecular Cardiology, UZH on the effect of RYGB on endothelial function in obese rats Team worker investigating the role of islet amyloid polypeptide (IAPP) derived deposits in vascular dysfunction in diabetes
01-2013 – 06-2013	**Institute of Molecular Medicine**, **University of Pavia, Italy** Internship for Master thesis "Helicobacter pylori *L-asparaginase:* mutants selection with directed evolution"
10/2009 – 07/2010	**Institute of Physiological and Pharmacological Sciences, University of Pavia, Italy** Internship for Bachelor Degree "Oxytocin inflects spontaneous IPSC's frequency and amplitude in mouse hippocampus Pyramidal Neurons"

Skills and Achievements

Languages:	**Italian:** native speaker	**English**: fluent
	French: working knowledge	**German:** basic

Conferences: May 2018: Oral presentation RESOLVE final meeting, EAS, Lisbon, Portugal
October 2017: Poster presentation LS2 meeting, Lausanne, Switzerland

October 2017: Poster presentation, ICBL 2017, Zürich, Switzerland
August 2017: Poster presentation ZIHP, symposium, Zürich, Switzerland
May 2017: Poster presentation at Gastrointestinal Control of Metabolism, Keystone, Copenhagen
February 2017: Oral and poster presentation, LS2 meeting, Zürich, Switzerland

Publications:

Tarasco E, Seebeck P, Pfundstein S, Daly AF, Eugster PJ, Harris AG *et al.* Effect of AP102, a subtype 2 and 5 specific somatostatin analog, on glucose metabolism in rats. *Endocrine* 2017; 58(1): 124-133.

Doytcheva P, Bachler T, Tarasco E, Marzolla V, Engeli M, Pellegrini G *et al.* Inhibition of Vascular c-Jun N-Terminal Kinase 2 Improves Obesity-Induced Endothelial Dysfunction After Roux-en-Y Gastric Bypass. *J Am Heart Assoc* 2017; 6(11).

Eugster PJ, Boyle CN, Prod'hom S, Tarasco E, Buclin T, Lutz TA *et al.* Sensitive quantification of the somatostatin analog AP102 in plasma by ultra-high pressure liquid chromatography-tandem mass spectrometry and application to a pharmacokinetic study in rats. *Drug Test Anal* 2018

Parmentier JH, Maggi M, Tarasco E, Scotti C, Avramis VI, Mittelman SD. Glutaminase activity determines cytotoxicity of L-asparaginases on most leukemia cell lines. *Leuk Res* 2015; 39(7): 757-62.

Grants:

Forschungskredit 2017, Best poster award LS2 Zürich 2017